

The Quaternion-Based Spatial Coordinate and Orientation Frame Alignment Problems

Andrew J. Hanson

Luddy School of Informatics, Computing, and Engineering
Indiana University, Bloomington, Indiana, 47405, USA

Abstract

We review the general problem of finding a global rotation that transforms a given set of points and/or coordinate frames (the “test” data) into the best possible alignment with a corresponding set (the “reference” data). For 3D point data, this “orthogonal Procrustes problem” is often phrased in terms of minimizing a root-mean-square deviation or RMSD corresponding to a Euclidean distance measure relating the two sets of matched coordinates. We focus on quaternion eigensystem methods that have been exploited to solve this problem for at least five decades in several different bodies of scientific literature where they were discovered independently. While numerical methods for the eigenvalue solutions dominate much of this literature, it has long been realized that the quaternion-based RMSD optimization problem can also be solved using exact algebraic expressions based on the form of the quartic equation solution published by Cardano in 1545; we focus on these exact solutions to expose the structure of the entire eigensystem for the traditional 3D spatial alignment problem. We then explore the structure of the less-studied orientation data context, investigating how quaternion methods can be extended to solve the corresponding 3D quaternion orientation frame alignment (QFA) problem, noting the interesting equivalence of this problem to the rotation-averaging problem, which also has been the subject of independent literature threads. We conclude with a brief discussion of the combined 3D translation-orientation data alignment problem. Appendices are devoted to a tutorial on quaternion frames, a related quaternion technique for extracting quaternions from rotation matrices, and a review of quaternion rotation-averaging methods relevant to the orientation-frame alignment problem. Supplementary Material sections cover novel extensions of quaternion methods to the 4D Euclidean point alignment and 4D orientation-frame alignment problems, some miscellaneous topics, and additional details of the quartic algebraic eigenvalue problem.

1 Context

Aligning matched sets of spatial point data is a universal problem that occurs in a wide variety of applications. In addition, generic objects such as protein residues, parts of composite object models, satellites, cameras, or camera-calibrating reference objects are not only located at points in three-dimensional space, but may also need 3D orientation frames to describe them effectively for certain applications. We are therefore led to consider both the Euclidean translation alignment problem and the orientation-frame alignment problem on the same footing.

Our purpose in this article is to review, and in some cases to refine, clarify, and extend, the

possible quaternion-based approaches to the optimal alignment problem for matched sets of translated and/or rotated objects in 3D space, which could be referred to in its most generic sense as the "Generalized Orthogonal Procrustes Problem" [Golub and van Loan, 1983]. We also devote some attention to identifying the surprising breadth of domains and literature where the various approaches, including particularly quaternion-based methods, have appeared; in fact the number of times in which quaternion-related methods have been described independently without cross-disciplinary references is rather interesting, and exposes some challenging issues that scientists, including the author, have faced in coping with the wide dispersion of both historical and modern scientific literature relevant to these subjects.

We present our study on two levels. The first level, the present main article, is devoted to a description of the 3D spatial and orientation alignment problems, emphasizing quaternion methods, with an historical perspective and a moderate level of technical detail that strives to be accessible. The second level, comprising the Supplementary Material, treats novel extensions of the quaternion method to the 4D spatial and orientation alignment problems, along with many other technical topics, including analysis of algebraic quartic eigenvalue solutions and numerical studies of the applicability of certain common approximations and methods.

In the following, we first review the diverse bodies of literature regarding the extraction of 3D rotations that optimally align matched pairs of Euclidean point data sets. It is important for us to remark that we have repeatedly become aware of additional literature in the course of this work, and it is entirely possible that other worthy references have been overlooked: if so, we apologize for any oversights, and hope that the literature that we have found to review will provide an adequate context for the interested reader. We then introduce our own preferred version of the quaternion approach to the spatial alignment problem, often described as the root mean square deviation (RMSD) minimization problem, and we will adopt that terminology when convenient; our intent is to consolidate a range of distinct variants in the literature into one uniform treatment, and, given the wide variations in symbolic notation and terminology, here we will adopt terms and conventions that work well for us personally. Following a technical introduction to quaternions, we treat the quaternion-based 3D spatial alignment problem itself. Next we introduce the quaternion approach to the 3D orientation frame alignment (QFA) problem in a way that parallels the 3D spatial problem, and note its equivalence to quaternion frame averaging methods. We conclude with a brief analysis of the 6-degree-of-freedom problem, combining the 3D spatial and 3D orientation-frame measures. Appendices include treatments of the basics of quaternion orientation frames, an elegant method that extracts a quaternion from a numerical 3D rotation matrix, and the generalization of that method to compute averages of rotations.

2 Summary of Spatial Alignment Problems, Known Solutions, and Historical Contexts

The Problem, Standard Solutions, and the Quaternion Method. The fundamental problem we will be concerned with arises when we are given a well-behaved $D \times D$ matrix E and we wish to find the optimal D -dimensional proper orthogonal matrix R_{opt} that maximizes the measure $\text{tr}(R \cdot E)$. This is equivalent to the RMSD problem, which seeks a global rotation R that rotates an ordered set of point test data X in such a way as to minimize the squared Euclidean differences relative to a matched reference set Y . We will find below that E corresponds to the cross-covariance matrix of the pair (X, Y) of N columns of D -dimensional vectors, namely $E = X \cdot Y^t$, though we

will look at cases where E could have almost any origin.

One solution to this problem in any dimension D uses the decomposition of the general matrix E into an orthogonal matrix U and a symmetric matrix S that takes the form $E = U \cdot S = U \cdot (E^t \cdot E)^{1/2}$, giving $R_{\text{opt}} = U^{-1} = (E^t \cdot E)^{1/2} \cdot E^{-1}$; note that there exist several equivalent forms (see, e.g., [Green, 1952, Horn et al., 1988]). General solutions may also be found using singular-value-decomposition (SVD) methods, starting with the decomposition $E = U \cdot S \cdot V^t$, where S is now diagonal and U and V are orthogonal matrices, to give the result $R_{\text{opt}} = V \cdot D \cdot U^t$, where D is the identity matrix up to a possible sign in one element (see, e.g., [Kabsch, 1976, Kabsch, 1978, Golub and van Loan, 1983, Markley, 1988]).

In addition to these general methods based on traditional linear algebra approaches, a significant literature exists for three dimensions that exploits the relationship between 3D rotation matrices and quaternions, and rephrases the task of finding R_{opt} as a *quaternion eigensystem* problem. This approach notes that, using the quadratic quaternion form $R(q)$ for the rotation matrix, one can rewrite $\text{tr}(R \cdot E) \rightarrow q \cdot M(E) \cdot q$, where the *profile matrix* $M(E)$ is a traceless, symmetric 4×4 matrix consisting of linear combinations of the elements of the 3×3 matrix E . Finding the largest eigenvalue ϵ_{opt} of $M(E)$ determines the optimal quaternion eigenvector q_{opt} and thus the solution $R_{\text{opt}} = R(q_{\text{opt}})$. The quaternion framework will be our main topic here.

Historical Literature Overview. Although our focus is the quaternion eigensystem context, we first note that one of the original approaches to the RMSD task exploited the singular-value-decomposition directly to obtain an optimal rotation matrix. This solution appears to date at least from 1966 in Schönemann’s thesis [Schönemann, 1966] and possibly [Cliff, 1966] later in the same journal issue; Schönemann’s work is chosen for citation, for example, in the earliest editions of Golub and van Loan [Golub and van Loan, 1983]. Applications of the SVD to alignment in the aerospace literature appear, for example, in the context of Wahba’s problem [Wikipedia:Wahba, 2018, Wahba, 1965], and are used explicitly, e.g., in [Markley, 1988], while the introduction of the SVD for the alignment problem in molecular chemistry generally is attributed to Kabsch [Wikipedia:Kabsch, 2018, Kabsch, 1976].

We believe that the quaternion eigenvalue approach itself was first noticed around 1968 by Davenport [Davenport, 1968] in the context of Wahba’s problem, rediscovered in 1983 by Hebert and Faugeras [Hebert, 1983, Faugeras and Hebert, 1983, Faugeras and Hebert, 1986] in the context of machine vision, and then found independently a third time in 1986 by Horn [Horn, 1987].

An alternative quaternion-free approach by [Horn et al., 1988] with the optimal rotation of the form $R_{\text{opt}} = (E^t \cdot E)^{1/2} \cdot E^{-1}$ appeared in 1988, but this basic form was apparently known elsewhere as early as 1952 [Green, 1952, Gibson, 1960].

Much of the recent activity has occurred in the context of the molecular alignment problem, starting from a basic framework put forth by Kabsch [Kabsch, 1976, Kabsch, 1978]. So far as we can determine, the matrix eigenvalue approach to molecular alignment was introduced in 1988 without actually mentioning quaternions by name in Diamond [Diamond, 1988], and refined to specifically incorporate quaternion methods in 1989 by Kearsley [Kearsley, 1989]. In 1991 Kneller [Kneller, 1991] independently described a version of the quaternion-eigenvalue-based approach that is widely cited as well. A concise and useful review can be found in Flower [Flower, 1999], in which the contributions of Schönemann, Faugeras and Hebert, Horn, Diamond, and Kearsley are acknowledged and all cited in the same place. A graphical summary of the discovery chronology in various domains is given in Fig. (1). Most of these treatments mention using numerical methods to find the optimal eigenvalue, though several references, starting with [Horn, 1987], point out

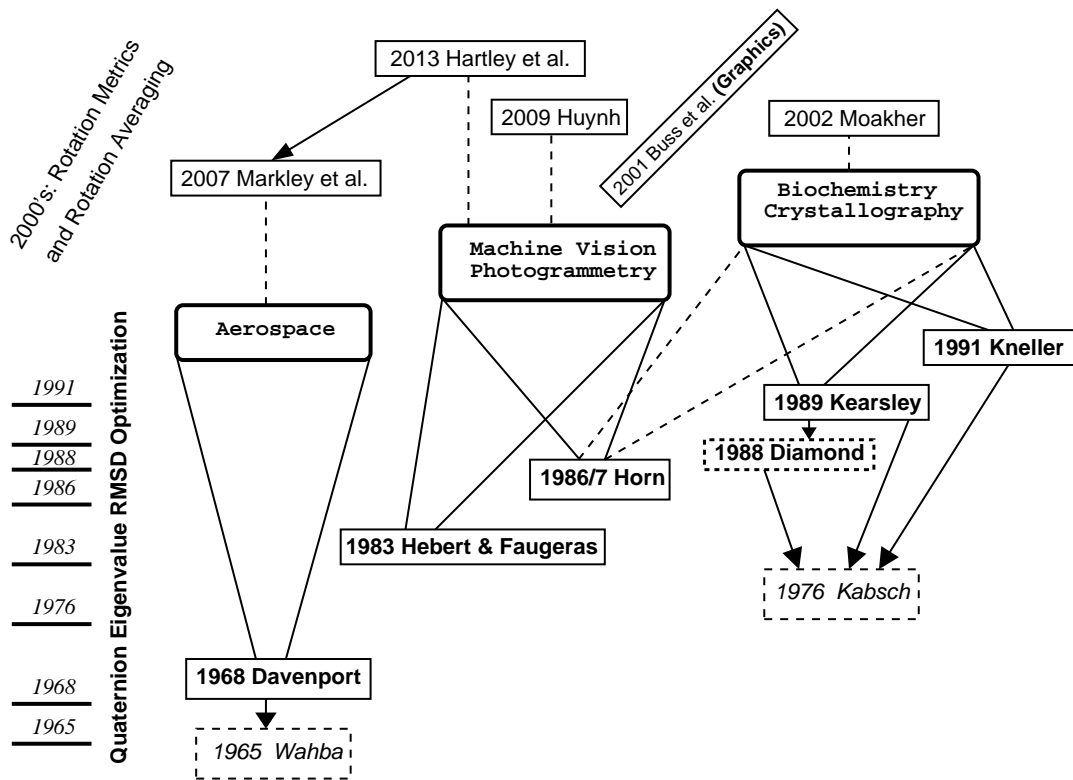


Figure 1: The quaternion eigensystem method for computing the optimal rotation matching two spatial data sets was discovered independently and published without cross-references in at least three distinct literatures. Downward arrows point to the introduction of the abstract problem, and upward rays indicate domains of publications specifically citing the quaternion method. Horn eventually appeared routinely in the crystallography citations, and reviews such as [Flower, 1999] introduced multiple cross-field citations. Several fields have included activity on quaternion-related rotation metrics and rotation averaging with varying degrees of cross-field awareness.

that 16th century algebraic methods for solving the quartic polynomial characteristic equation, discussed in the next paragraph, could also be used to determine the eigenvalues. In our treatment we will study the explicit form of these algebraic solutions for the 3D problem (and also for 4D in the Supplementary Material), taking advantage of several threads of the literature.

Historical Notes on the Quartic. The actual solution to the quartic equation, and thus the solution of the characteristic polynomial of the 4D eigensystem of interest to us, was first published in 1545 by Gerolamo Cardano [Wikipedia:Cardano, 2019] in his book *Ars Magna*. The intellectual history of this fact is controversial and narrated with varying emphasis in diverse sources. It seems generally agreed upon that Cardano’s student Lodovico Ferrari was the first to discover the basic method for solving the quartic in 1540, but his technique was incomplete as it only reduced the problem to the cubic equation, for which no solution was publicly known at that time, and that apparently prevented him from publishing it. The complication appears to be that Cardano had actually learned of a method for solving the cubic already in 1539 from Niccolò Fontana Tartaglia (legendarily in the form of a poem), but had been sworn to secrecy, and so could not reveal the final explicit step needed to complete Ferrari’s implicit solution. Where it gets controversial is that at some point between 1539 and 1545, Cardano learned that Scipione del Ferro had found the same cubic solution as the one of Tartaglia that he had sworn not to reveal, and furthermore that del Ferro had discovered his solution before Tartaglia did. Cardano interpreted that fact as releasing him from his oath of secrecy (which Tartaglia did not appreciate), allowing him to publish the complete solution to the quartic, incorporating the cubic solution into Ferrari’s result. Sources claiming that Cardano “stole” Ferrari’s solution may perhaps be exaggerated, since Ferrari did not have access to the cubic equations, and Cardano did not conceal his sources; exactly who “solved” the quartic is thus philosophically complicated, but Cardano does seem to be the one who combined the multiple threads needed to express the equations as a single complete formula.

Other interesting observations were made later, for example, by Descartes in 1637 [Descartes, 1954], and in 1733 by Euler [Euler, 1733, Bell, 2008]. For further descriptions, one may consult, e.g., [Abramowitz and Stegun, 1970] and [Boyer and Merzbach, 1991], as well as the narratives in Weisstein [Weisstein, 2019a, Weisstein, 2019b]. Additional amusing pedagogical investigations of the historical solutions may be found in several expositions by Nickalls [Nickalls, 1993, Nickalls, 2009].

Further Literature. A very informative treatment of the features of the quaternion eigenvalue solutions has been given by Coutsias, Seok, and Dill in 2004, and expanded in 2019 [Coutsias et al., 2004, Coutsias and Wester, 2019]. Coutsias et al. not only take on a thorough review of the quaternion RMSD method, but also derive the complete relationship between the linear algebra of the SVD method and the quaternion eigenvalue system; furthermore, they exhaustively enumerate the special cases involving mirror geometries and degenerate eigenvalues that may appear rarely, but must be dealt with on occasion. Efficiency is also an area of potential interest, and Theobald et al. in [Theobald, 2005, Liu et al., 2010] argue that among the many variants of numerical methods that have been used to compute the optimal quaternion eigenvalues, Horn’s original proposal to use Newton’s method directly on the characteristic equations of the relevant eigenvalue systems may well be the best approach.

There is also a rich literature dealing with distance measures among representations of rotation frames themselves, some dealing directly with the properties of distances computed with rotation matrices or quaternions, e.g., Huynh [Huynh, 2009], and others combining discussion of the distance measures with associated applications such as rotation averaging or finding “rotational

centers of mass,” e.g., [Brown and Worsey, 1992, Park and Ravani, 1997, Buss and Fillmore, 2001, Moakher, 2002, Markley et al., 2007, Hartley et al., 2013]. The specific computations explored in our section on optimal alignment of matched pairs of orientation frames make extensive use of the quaternion-based and rotation-based measures discussed in these treatments. In the Appendices, we review the details of some of these orientation-frame-based applications.

3 Introduction

We explore the problem of finding global rotations that optimally align pairs of corresponding lists of spatial and/or orientation data. This issue is significant in diverse application domains. Among these are aligning spacecraft (see, e.g., [Wahba, 1965, Davenport, 1968, Markley, 1988, Markley and Mortari, 2000]), obtaining correspondence of registration points in 3D model matching (see, e.g., [Faugeras and Hebert, 1983, Faugeras and Hebert, 1986]), matching structures in aerial imagery (see, e.g., [Horn, 1987, Horn et al., 1988, Huang et al., 1986, Arun et al., 1987, Umeyama, 1991, Zhang, 2000]), and alignment of matched molecular and biochemical structures (see, e.g., [Kabsch, 1976, Kabsch, 1978, MacLachlan, 1982, Lesk, 1986, Diamond, 1988, Kearsley, 1989], [Kearsley, 1990, Kneller, 1991, Coutsias et al., 2004, Theobald, 2005, Liu et al., 2010], [Coutsias and Wester, 2019]). There are several alternative approaches that in principle produce the same optimal global rotation to solve a given alignment problem, and the SVD and $(E^t \cdot E)^{1/2} \cdot E^{-1}$ methods apply to any dimension. Here we critically examine the quaternion eigensystem decomposition approach to studying the rotation matrices appearing in the RMSD optimization formulas for the 3D and 4D spatial alignment problems, along with the extensions to the 3D and 4D orientation-frame alignment problems. Starting from the exact quartic algebraic solutions to the eigensystems arising in these optimization problems, we direct attention to the elegant algebraic forms of the eigenvalue solutions appropriate for these applications. (For brevity, the more complicated 4D treatment is deferred to the Supplementary Material.)

Our extension of the quaternion approach to *orientation data* exploits the fact that 3D orientation frames can *themselves* be expressed as quaternions, e.g., amino acid 3D orientation frames written as quaternions (see [Hanson and Thakur, 2012]), and we will refer to the corresponding “quaternion frame alignment” task as the QFA problem. Various proximity measures for such orientation data have been explored in the literature (see, e.g., [Park and Ravani, 1997, Moakher, 2002, Huynh, 2009, Huggins, 2014a]), and the general consensus is that the most rigorous measure minimizes the sums of squares of geodesic arc-lengths between pairs of quaternions. This ideal QFA proximity measure is highly nonlinear compared to the analogous spatial RMSD measure, but fortunately there is an often-justifiable linearization, the chord angular distance measure; we present several alternative solutions exploiting this approximation that closely parallel our spatial RMSD formulation. In addition, we analyze the problem of optimally aligning *combined* 3D spatial and quaternion 3D-frame-triad data, e.g., for molecules with composite structure. Such rotational-translational measures have appeared mainly in the molecular entropy literature [Huggins, 2014b, Fogolari et al., 2016], where, after some confusion, it was recognized that the spatial and rotational measures are dimensionally incompatible, and either they must be optimized independently, or an arbitrary context-dependent dimensional constant must appear in any combined measure for the RMSD+QFA problem.

In the following, we organize our thoughts by first summarizing the fundamentals of quaternions, which will be our main computational tool. We next introduce the spatial measures that underlie

the alignment problem, then examine the quaternion approach to the 3D problem, together with a class of exact algebraic solutions that can be used as an alternative to the traditional numerical methods. Our quaternion approach to the 3D orientation-frame triad alignment problem is presented next, along with a discussion of the combined spatial-rotational problem. Appendices provide a tutorial on the quaternion orientation-frame methodology, an alternative formulation of the RMSD optimization equations, and a summary of Bar-Itzhack’s method [Bar-Itzhack, 2000] for obtaining the corresponding quaternion from a numerical 3D rotation matrix, along with a treatment of the closely related quaternion-based rotation averaging problem.

In the Supplementary Material, we extend all of our 3D results to 4D space, including 4D spatial RMSD alignment and 4D orientation-based QFA methods employing double quaternions and their relationship to the singular value decomposition, and also a Bar-Itzhack method for finding a pair of quaternions corresponding to a numerical 4D rotation matrix. Other Sections of the Supplementary Material explore properties of the RMSD problem for 2D data and evaluate the accuracy of our 3D orientation frame alignment approximations, as well as studying and evaluating the properties of combined measures for spatial and orientation-frame data in 3D. An appendix is devoted to further details of the quartic equations and forms of the algebraic solutions related to our eigenvalue problems.

4 Foundations of Quaternions

For the purposes of this paper, we take a quaternion to be a point $q = (q_0, q_1, q_2, q_3) = (q_0, \mathbf{q})$ in 4D Euclidean space with unit norm, $q \cdot q = 1$, and so geometrically it is a point on the unit 3-sphere \mathbf{S}^3 (see, e.g., [Hanson, 2006] for further details about quaternions). The first term, q_0 , plays the role of a real number, and the last three terms, denoted as a 3D vector \mathbf{q} , play the role of a generalized imaginary number, and so are treated differently from the first: in particular the conjugation operation is taken to be $\bar{q} = (q_0, -\mathbf{q})$. Quaternions possess a multiplication operation denoted by \star and defined as follows:

$$q \star p = Q(q) \cdot p = \begin{bmatrix} q_0 & -q_1 & -q_2 & -q_3 \\ q_1 & q_0 & -q_3 & q_2 \\ q_2 & q_3 & q_0 & -q_1 \\ q_3 & -q_2 & q_1 & q_0 \end{bmatrix} \cdot \begin{bmatrix} p_0 \\ p_1 \\ p_2 \\ p_3 \end{bmatrix} = (q_0 p_0 - \mathbf{q} \cdot \mathbf{p}, q_0 \mathbf{p} + p_0 \mathbf{q} + \mathbf{q} \times \mathbf{p}), \quad (1)$$

where the orthonormal matrix $Q(q)$ expresses a form of quaternion multiplication that can be useful. Note that the orthonormality of $Q(q)$ means that quaternion multiplication of p by q *literally* produces a rotation of p in 4D Euclidean space.

Choosing exactly one of the three imaginary components in both q and p to be nonzero gives back the classic complex algebra $(q_0 + iq_1)(p_0 + ip_1) = (q_0 p_0 - q_1 p_1) + i(q_0 p_1 + p_0 q_1)$, so there are three copies of the complex numbers embedded in the quaternion algebra; the difference is that in general the final term $\mathbf{q} \times \mathbf{p}$ changes sign if one reverses the order, making the quaternion product order-dependent, unlike the complex product. Nevertheless, like complex numbers, the quaternion algebra satisfies the nontrivial “multiplicative norm” relation

$$\|q\| \|p\| = \|q \star p\|, \quad (2)$$

where $\|q\|^2 = q \cdot q = \Re(q \star \bar{q})$, i.e., quaternions are one of the four possible Hurwitz algebras (real, complex, quaternion, and octonion).

Quaternion triple products obey generalizations of the 3D vector identities $A \cdot (B \times C) = B \cdot (C \times A) = C \cdot (A \times B)$, along with $A \times B = -B \times A$. The corresponding quaternion identities, which we will need in Section 7, are

$$r \cdot (q \star p) = q \cdot (r \star \bar{p}) = \bar{r} \cdot (\bar{p} \star \bar{q}) , \quad (3)$$

where the complex conjugate entries are the natural consequences of the sign changes occurring only in the 3D part.

It can be shown that quadratically conjugating a vector $\mathbf{x} = (x, y, z)$, written as a purely “imaginary” quaternion $(0, \mathbf{x})$ (with only a 3D part), by quaternion multiplication is isomorphic to the construction of a 3D Euclidean rotation $R(q)$ generating all possible elements of the special orthogonal group $\mathbf{SO}(3)$. If we compute

$$q \star (c, x, y, z) \star \bar{q} = (c, R(q) \cdot \mathbf{x}) , \quad (4)$$

we see that only the purely imaginary part is affected, whether or not the arbitrary real constant $c = 0$. The result of collecting coefficients of the vector term is a *proper* orthonormal 3D rotation matrix quadratic in the quaternion elements that takes the form

$$R_{ij}(q) = \left. \begin{aligned} & \delta_{ij} (q_0^2 - \mathbf{q}^2) + 2q_i q_j - 2\epsilon_{ijk} q_0 q_k \\ R(q) = & \left[\begin{array}{ccc} q_0^2 + q_1^2 - q_2^2 - q_3^2 & 2q_1 q_2 - 2q_0 q_3 & 2q_1 q_3 + 2q_0 q_2 \\ 2q_1 q_2 + 2q_0 q_3 & q_0^2 - q_1^2 + q_2^2 - q_3^2 & 2q_2 q_3 - 2q_0 q_1 \\ 2q_1 q_3 - 2q_0 q_2 & 2q_2 q_3 + 2q_0 q_1 & q_0^2 - q_1^2 - q_2^2 + q_3^2 \end{array} \right] \end{aligned} \right\} , \quad (5)$$

with determinant $\det R(q) = (q \cdot q)^3 = +1$. The formula for $R(q)$ is technically a two-to-one mapping from quaternion space to the 3D rotation group because $R(q) = R(-q)$; changing the sign of the quaternion preserves the rotation matrix. Note also that the identity quaternion $q_{\text{ID}} = (1, 0, 0, 0) \equiv q \star \bar{q}$ corresponds to the identity rotation matrix, as does $-q_{\text{ID}} = (-1, 0, 0, 0)$. The 3×3 matrix $R(q)$ is fundamental not only to the quaternion formulation of the spatial RMSD alignment problem, but will also be essential to the QFA orientation-frame problem because the *columns* of $R(q)$ are exactly the needed quaternion representation of the *frame triad* describing the orientation of a body in 3D space, i.e., the columns are the vectors of the frame’s local x , y , and z axes relative to an initial identity frame.

Multiplying a quaternion p by the quaternion q to get a new quaternion $p' = q \star p$ simply *rotates* the 3D frame corresponding to p by the matrix Eq. (5) written in terms of q . This has non-trivial implications for 3D rotation matrices, for which quaternion multiplication corresponds exactly to multiplication of two *independent* 3×3 orthogonal rotation matrices, and we find that

$$R(q \star p) = R(q) \cdot R(p) . \quad (6)$$

This collapse of repeated rotation matrices to a single rotation matrix with multiplied quaternion arguments can be continued indefinitely.

If we choose the following specific 3-variable parameterization of the quaternion q preserving $q \cdot q = 1$,

$$q = (\cos(\theta/2), \hat{n}_1 \sin(\theta/2), \hat{n}_2 \sin(\theta/2), \hat{n}_3 \sin(\theta/2)) \quad (7)$$

(with $\hat{\mathbf{n}} \cdot \hat{\mathbf{n}} = 1$), then $R(q) = R(\theta, \hat{\mathbf{n}})$ is precisely the “axis-angle” 3D spatial rotation by an angle θ leaving the direction $\hat{\mathbf{n}}$ fixed, so $\hat{\mathbf{n}}$ is the lone real eigenvector of $R(q)$.

The Slerp. Relationships among quaternions can be studied using the *slerp*, or “spherical linear interpolation” [Shoemake, 1985, Jupp and Kent, 1987], that smoothly parameterizes the points on the shortest geodesic quaternion path between two constant (unit) quaternions, q_0 and q_1 , as

$$\text{slerp}(q_0, q_1, s) \equiv q(s)[q_0, q_1] = q_0 \frac{\sin((1-s)\phi)}{\sin\phi} + q_1 \frac{\sin(s\phi)}{\sin\phi}. \quad (8)$$

Here $\cos\phi = q_0 \cdot q_1$ defines the angle ϕ between the two given quaternions, while $q(s=0) = q_0$ and $q(s=1) = q_1$. The “long” geodesic can be obtained for $1 \leq s \leq 2\pi/\phi$. For small ϕ , this reduces to the standard linear interpolation $(1-s)q_0 + sq_1$. The unit norm is preserved, $q(s) \cdot q(s) = 1$ for all s , so $q(s)$ is always a valid quaternion and $R(q(s))$ defined by Eq. (5) is always a valid 3D rotation matrix. We note that one can formally write Eq. (8) as an exponential of the form $q_0 \star (\bar{q}_0 \star q_1)^s$, but since this requires computing a logarithm and an exponential whose most efficient reduction to a practical computer program is Eq. (8), this is mostly of pedagogical interest.

In the following we will make little further use of the quaternion’s algebraic properties, but we will extensively exploit Eq. (5) to formulate elegant approaches to RMSD problems, along with employing Eq. (8) to study the behavior of our data under smooth variations of rotation matrices.

Remark on 4D. Our fundamental formula Eq. (5) can be extended to four Euclidean dimensions by choosing two *distinct* quaternions in Eq. (4), producing a 4D Euclidean rotation matrix. Analogously to 3D, the columns of this matrix correspond to the axes of a 4D Euclidean orientation frame. The nontrivial details of the quaternion approach to aligning both 4D spatial and 4D orientation-frame data are given in the Supplementary Material.

5 Reviewing the 3D Spatial Alignment RMSD Problem

We now review the basic ideas of spatial data alignment, and then specialize to 3D (see, e.g., [Wahba, 1965, Davenport, 1968, Markley, 1988, Markley and Mortari, 2000, Kabsch, 1976, Kabsch, 1978, MacLachlan, 1982, Lesk, 1986, Faugeras and Hebert, 1983, Horn, 1987, Huang et al., 1986, Arun et al., 1987, Diamond, 1988, Kearsley, 1989, Kearsley, 1990, Umeyama, 1991, Kneller, 1991, Coutsias et al., 2004, Theobald, 2005]). We will then employ quaternion methods to reduce the 3D spatial alignment problem to the task of finding the optimal quaternion eigenvalue of a certain 4×4 matrix. This is the approach we have discussed in the introduction, and it can be solved using numerical or algebraic eigensystem methods. In a subsequent section, we will explore in particular the classical quartic equation solutions for the exact algebraic form of the entire four-part eigensystem, whose optimal eigenvalue and its quaternion eigenvector produce the optimal global rotation solving the 3D spatial alignment problem.

Aligning Matched Data Sets in Euclidean Space. We begin with the general least-squares form of the RMSD problem, which is solved by minimizing the optimization measure over the space of rotations, which we will convert to an optimization over the space of unit quaternions. We take as input one data array with N columns of D -dimensional points $\{y_k\}$ as the *reference* structure, and a second array of N columns of *matched* points $\{x_k\}$ as the *test* structure. Our task is to rotate the latter in space by a global $\mathbf{SO}(D)$ rotation matrix R_D to achieve the minimum value of the

cumulative quadratic distance measure

$$\mathbf{S}_D = \sum_{k=1}^N \|R_D \cdot x_k - y_k\|^2. \quad (9)$$

We assume, as is customary, that any overall translational components have been eliminated by displacing both data sets to their centers of mass (see, e.g., [Faugeras and Hebert, 1983, Coutsias et al., 2004]). When this measure is minimized with respect to the rotation R_D , the optimal R_D will rotate the test set $\{x_k\}$ to be as close as possible to the reference set $\{y_k\}$. Here we will focus on 3D data sets (and, in the Supplementary Material, 4D data sets) because those are the dimensions that are easily adaptable to our targeted quaternion approach. In 3D, our least squares measure Eq. (9) can be converted directly into a quaternion optimization problem using the method of Hebert and Faugeras detailed in Appendix A.

Remark: Clifford algebras may support alternative methods as well as other approaches to higher dimensions (see, e.g., [Havel and Najfeld, 1994, Buchholz and Sommer, 2005]).

Converting from Least-Squares Minimization to Cross-Term Maximization. We choose from here onward to focus on an equivalent method based on expanding the measure given in Eq. (9), removing the constant terms, and recasting the RMSD least squares minimization problem as the task of maximizing the surviving cross-term expression. This takes the general form

$$\Delta_D = \sum_{k=1}^N (R_D \cdot x_k) \cdot y_k = \sum_{a=1, b=1}^D [R_D]_{ba} E_{ab} = \text{tr } R_D \cdot E, \quad (10)$$

where

$$E_{ab} = \sum_{k=1}^N [x_k]_a [y_k]_b = [\mathbf{X} \cdot \mathbf{Y}^t]_{ab} \quad (11)$$

is the *cross-covariance matrix* of the data, $[x_k]$ denotes the k th column of \mathbf{X} , and the range of the indices (a, b) is the spatial dimension D .

Quaternion Transformation of the 3D Cross-Term Form. We now restrict our attention to the *3D cross-term form* of Eq. (10) with pairs of 3D point data related by a proper rotation. The key step is to substitute Eq. (5) for $R(q)$ into Eq. (10), and pull out the terms corresponding to pairs of components of the quaternions q . In this way the 3D expression is transformed into the 4×4 matrix $M(E)$ sandwiched between two identical quaternions (not a conjugate pair), of the form

$$\Delta(q) = \text{tr } R(q) \cdot E = (q_0, q_1, q_2, q_3) \cdot M(E) \cdot (q_0, q_1, q_2, q_3)^t \equiv q \cdot M(E) \cdot q. \quad (12)$$

Here $M(E)$ is the traceless, symmetric 4×4 matrix

$$M(E) = \begin{bmatrix} E_{xx} + E_{yy} + E_{zz} & E_{yz} - E_{zy} & E_{zx} - E_{xz} & E_{xy} - E_{yx} \\ E_{yz} - E_{zy} & E_{xx} - E_{yy} - E_{zz} & E_{xy} + E_{yx} & E_{zx} + E_{xz} \\ E_{zx} - E_{xz} & E_{xy} + E_{yx} & -E_{xx} + E_{yy} - E_{zz} & E_{yz} + E_{zy} \\ E_{xy} - E_{yx} & E_{zx} + E_{xz} & E_{yz} + E_{zy} & -E_{xx} - E_{yy} + E_{zz} \end{bmatrix}. \quad (13)$$

built from our original 3×3 cross-covariance matrix E defined by Eq. (11). We will refer to $M(E)$ from here on as the *profile matrix*, as it essentially reveals a different viewpoint of the optimization function and its relationship to the matrix E . Note that in some literature, matrices related to the cross-covariance matrix E may be referred to as “attitude profile matrices,” and one also may see the term “key matrix” referring to $M(E)$.

The bottom line is that if one decomposes Eq. (13) into its eigensystem, the measure Eq. (12) is maximized when the unit-length quaternion vector q is the eigenvector of $M(E)$ ’s largest eigenvalue [Davenport, 1968, Faugeras and Hebert, 1983, Horn, 1987, Diamond, 1988, Kearsley, 1989, Kneller, 1991]. The RMSD optimal-rotation problem thus reduces to finding the maximal eigenvalue ϵ_{opt} of $M(E)$ (which we emphasize depends only on the numerical data). Plugging the corresponding eigenvector q_{opt} into Eq. (5), we obtain the rotation matrix $R(q_{\text{opt}})$ that solves the problem. The resulting proximity measure relating $\{x_k\}$ and $\{y_k\}$ is simply

$$\left. \begin{aligned} \Delta_{\text{opt}} &= q_{\text{opt}} \cdot M(E) \cdot q_{\text{opt}} \\ &= q_{\text{opt}} \cdot (\epsilon_{\text{opt}} q_{\text{opt}}) \\ &= \epsilon_{\text{opt}} \end{aligned} \right\}, \quad (14)$$

and does not require us to actually compute q_{opt} or $R(q_{\text{opt}})$ explicitly if all we want to do is compare various test data sets to a reference structure.

Note. In the interests of conceptual and notational simplicity, we have made a number of assumptions. For one thing, in declaring that Eq. (5) describes our sought-for rotation matrix, we have presumed that the optimal rotation matrix will always be a proper rotation, with $\det R = +1$. Also, as mentioned, we have omitted any general translation problems, assuming that there is a way to translate each data set to an appropriate center, e.g., by subtracting the center of mass. The global translation optimization process is treated in [Faugeras and Hebert, 1986, Coutsias et al., 2004], and discussions of center-of-mass alignment, scaling, and point weighting are given in much of the original literature, see e.g., [Horn, 1987, Coutsias et al., 2004, Theobald, 2005]. Finally, in real problems, structures such as molecules may appear in mirror-image or enantiomer form, and such issues were introduced early on by Kabsch [Kabsch, 1976, Kabsch, 1978]. There can also be particular symmetries, or very close approximations to symmetries, that can make some of our natural assumptions about the good behavior of the profile matrix invalid, and many of these issues, including ways to treat degenerate cases, have been carefully studied, see, e.g., [Coutsias et al., 2004, Coutsias and Wester, 2019]. The latter authors also point out that if a particular data set $M(E)$ produces a negative smallest eigenvalue ϵ_4 such that $|\epsilon_4| > \epsilon_{\text{opt}}$, this can be a sign of a reflected match, and the *negative* rotation matrix $R_{\text{opt}} = -R(q(\epsilon_4))$ may actually produce the best alignment. These considerations may be essential in some applications, and readers are referred to the original literature for details.

Illustrative Example. We can visualize the transition from the initial data $\Delta(q_{\text{ID}}) = \text{tr } E$ to the optimal alignment $\Delta(q_{\text{opt}}) = \epsilon_{\text{opt}}$ by exploiting the geodesic interpolation Eq. (8) from the identity quaternion q_{ID} to q_{opt} given by

$$q(s) = \text{slerp}(q_{\text{ID}}, q_{\text{opt}}, s), \quad (15)$$

and applying the resulting rotation matrix $R(q(s))$ to the test data, ending with $R(q_{\text{opt}})$ showing the best alignment of the two data sets. In Fig. (2), we show a sample reference data set in red, a sample test data set in blue connected to the reference data set by blue lines, an intermediate partial alignment, and finally the optimally aligned pair, respectively. The yellow arrow is the *spatial part of the quaternion solution*, proportional to the eigenvector $\hat{\mathbf{n}}$ (fixed axis) of the optimal 3D rotation matrix $R(q) = R(\theta, \hat{\mathbf{n}})$, and whose length is $\sin(\theta/2)$, sine of half the rotation angle needed to perform the optimal alignment of the test data with the reference data. In Fig. (3), we visualize the optimization process in an alternative way, showing random samples of $q = (q_0, \mathbf{q})$ in \mathbf{S}^3 , separated into the “northern hemisphere” 3D unit-radius ball in (A) with $q_0 \geq 0$, and the “southern hemisphere” 3D unit-radius ball in (B) with $q_0 < 0$. (This is like representing the Earth as two flattened disks, one showing everything above the equator and one showing everything below the equator; the distance from the equatorial plane is implied by the location in the disk, with the maximum at the centers, the north and south poles.) Either solid ball contains one unique quaternion for every possible choice of $R(q)$. The values of $\Delta(q) = \text{tr } R(q) \cdot E$ are shown as scaled dots located at their corresponding spatial (“real”) quaternion points \mathbf{q} in the solid balls. The yellow arrows, equivalent negatives of each other, show the spatial part \mathbf{q}_{opt} of the optimal quaternion q_{opt} , and the tips of the arrows clearly fall in the middle of the mirror pair of clusters of the largest values of $\Delta(q)$. Note that the lower left dots in (A) continue smoothly into the larger lower left dots in (B), which is the center of the optimal quaternion in (B). Further details of such methods of displaying quaternions are provided in Appendix B (see also [Hanson, 2006]).

6 Algebraic Solution of the Eigensystem for 3D Spatial Alignment

At this point, one can simply use the traditional *numerical* methods to solve Eq. (12) for the maximal eigenvalue ϵ_{opt} of $M(E)$ and its eigenvector q_{opt} , thus solving the 3D spatial alignment problem of Eq. (10). Alternatively, we can also exploit *symbolic* methods to study the properties of the eigensystems of 4×4 matrices M algebraically to provide deeper insights into the structure of the problem, and that is the subject of this Section.

Theoretically, the algebraic form of our eigensystem is a textbook problem following from the 16th-century-era solution of the quartic algebraic equation in, e.g., [Abramowitz and Stegun, 1970]. Our objective here is to explore this textbook solution in the specific context of its application to eigensystems of 4×4 matrices and its behavior relative to the properties of such matrices. The real, symmetric, traceless profile matrix $M(E)$ in Eq. (13) appearing in the 3D spatial RMSD optimization problem must necessarily possess only real eigenvalues, and the properties of $M(E)$ permit some particular simplifications in the algebraic solutions that we will discuss. The quaternion RMSD literature varies widely in the details of its treatment of the algebraic solutions, ranging from no discussion at all, to Horn, who mentions the possibility but does not explore it, to the work of Coutsias et al. [Coutsias et al., 2004, Coutsias and Wester, 2019], who present an exhaustive treatment, in addition to working out the exact details of the correspondence between the SVD eigensystem and the quaternion eigensystem, both of which in principle embody the algebraic solution to the RMSD optimization problem. In addition to the treatment of Coutsias et al., other approaches similar to the one we will study are due to Euler [Euler, 1733, Bell, 2008], as well as a series of papers on the quartic by Nickalls [Nickalls, 1993, Nickalls, 2009].

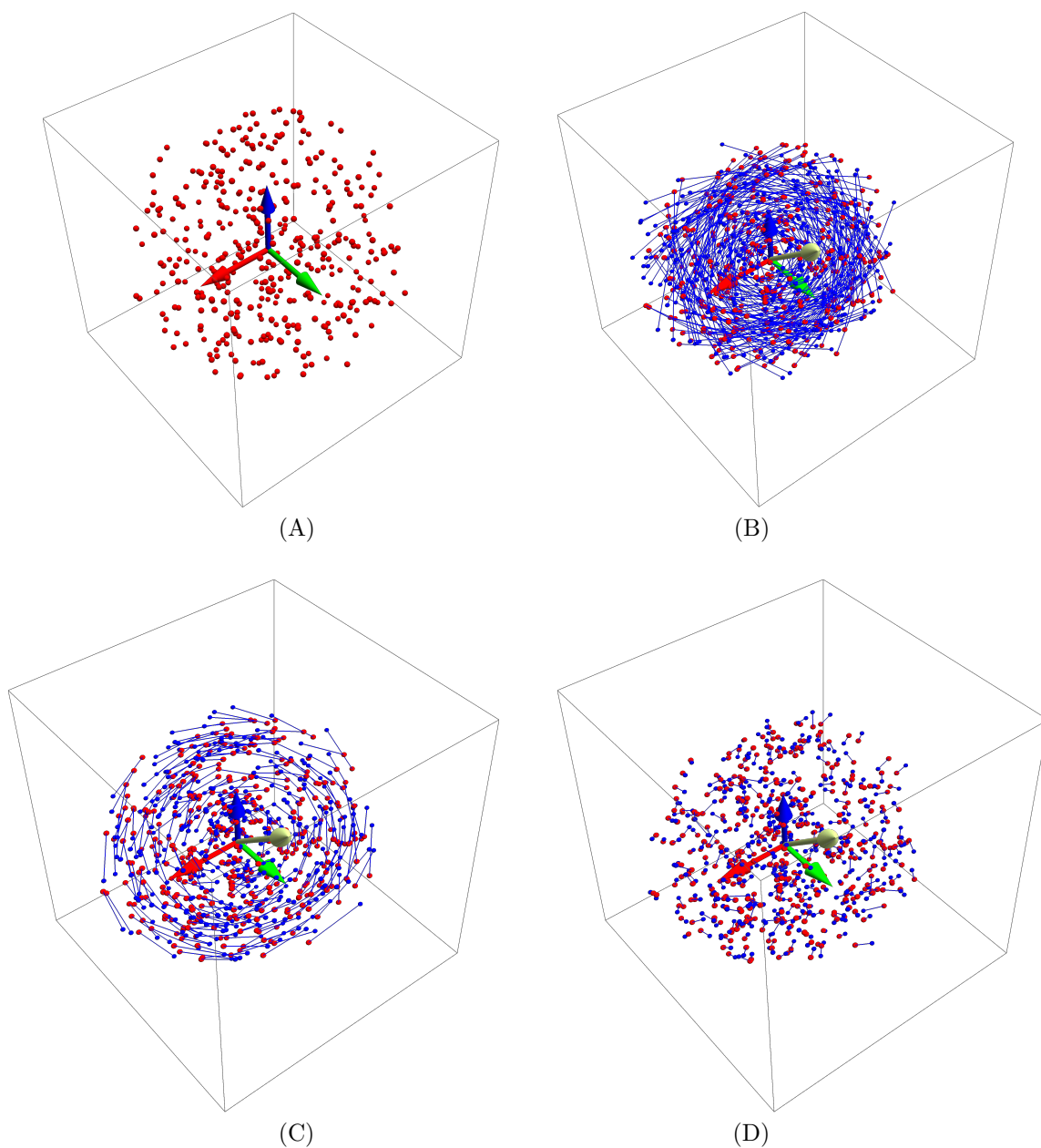


Figure 2: (A) A typical 3D spatial reference data set. (B) The reference data in red alongside the test data in blue, with blue lines representing the Euclidean distances connecting each test data point with its corresponding reference point. (C) The partial alignment at $s = 0.75$. (D) The optimal alignment for this data set at $s = 1.0$. The yellow arrow is the axis of rotation specified by the optimal quaternion's spatial components.

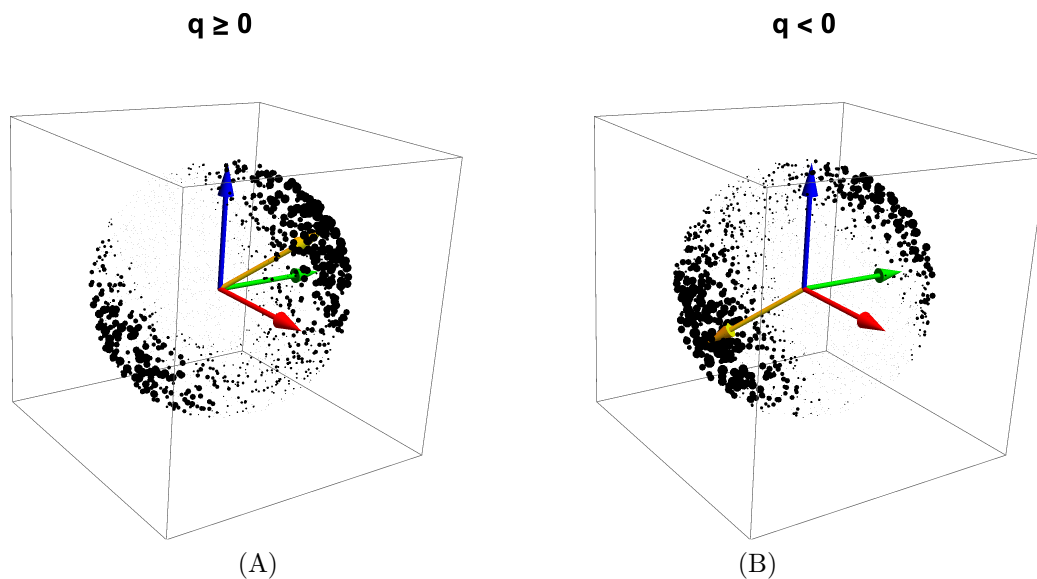


Figure 3: The values of $\Delta(q) = \text{tr } R(q) \cdot E = q \cdot M(E) \cdot q$ represented by the sizes of the dots placed randomly in the "northern" and "southern" 3D solid balls spanning the entire hypersphere \mathbf{S}^3 with (A) containing the $q_0 \geq 0$ sector and B containing the $q_0 < 0$ sector. We display the data dots at the locations of their spatial quaternion components $\mathbf{q} = (q_1, q_2, q_3)$, and we know that $q_0 = \pm\sqrt{1 - \mathbf{q} \cdot \mathbf{q}}$ so the \mathbf{q} data uniquely specify the full quaternion. Since $R(q) = R(-q)$, the points in *each* ball actually represent all possible unique rotation matrices. The spatial component of the maximal eigenvector is shown by the yellow arrows, which clearly end in the middle of the maximum values of $\Delta(q)$. Note that, in the quaternion context, diametrically opposite points on the spherical surface are identical rotations, so the cluster of larger dots at the upper right of (A) is, in the entire sphere, representing the same data as the "diametrically opposite" lower left cluster in (B), both surrounding the tips of their own yellow arrows. The smaller dots at the upper right of (B) are contiguous with the upper right region of (A), forming a single cloud centered on \mathbf{q}_{opt} , and similarly for the lower left of (A) and the lower left of (B). The whole figure contains two distinct clusters of dots (related by $q \rightarrow -q$) centered around $\pm\mathbf{q}_{\text{opt}}$.

Eigenvalue Expressions. We begin by writing down the eigenvalue expansion of the profile matrix,

$$\det[M - eI_4] = e^4 + e^3 p_1 + e^2 p_2 + e p_3 + p_4 = 0 \quad , \quad (16)$$

where e denotes a generic eigenvalue, I_4 is the 4D identity matrix, and the p_k are homogeneous polynomials of degree k in the elements of M . For the special case of a traceless, symmetric profile matrix $M(E)$ defined by Eq. (13), the $p_k(E)$ coefficients simplify and can be expressed numerically as the following functions either of M or of E :

$$p_1(E) = -\text{tr}[M] = 0 \quad (17)$$

$$\begin{aligned} p_2(E) &= -\frac{1}{2} \text{tr}[M \cdot M] = -2 \text{tr}[E \cdot E^\dagger] \\ &= -2 (E_{xx}^2 + E_{xy}^2 + E_{xz}^2 + E_{yx}^2 + E_{yy}^2 + E_{yz}^2 + E_{zx}^2 + E_{zy}^2 + E_{zz}^2) \end{aligned} \quad (18)$$

$$\begin{aligned} p_3(E) &= -\frac{1}{3} \text{tr}[M \cdot M \cdot M] = -8 \det[E] \\ &= 8 (E_{xx} E_{yz} E_{zy} + E_{yy} E_{xz} E_{zx} + E_{zz} E_{xy} E_{yx}) \\ &\quad - 8 (E_{xx} E_{yy} E_{zz} + E_{xy} E_{yz} E_{zx} + E_{xz} E_{zy} E_{yx}) \end{aligned} \quad (19)$$

$$p_4(E) = \det[M] = 2 \text{tr}[E \cdot E^\dagger \cdot E \cdot E^\dagger] - (\text{tr}[E \cdot E^\dagger])^2 \quad . \quad (20)$$

Interestingly, the polynomial $M(E)$ is arranged so that $-p_2(E)/2$ is the (squared) Fröbenius norm of E , and $-p_3(E)/8$ is its determinant. Our task now is to express the four eigenvalues $e = \epsilon_k(p_1, p_2, p_3, p_4)$, $k = 1, \dots, 4$, usefully in terms of the matrix elements, and also to find their eigenvectors; we are of course particularly interested in the maximal eigenvalue ϵ_{opt} .

Approaches to Algebraic Solutions. Equation (16) can be solved directly using the quartic equations published by Cardano in 1545 (see, e.g., [Abramowitz and Stegun, 1970, Weisstein, 2019b, Wikipedia:Cardano, 2019]), which are incorporated into the Mathematica function

$$\text{Solve}[\text{myQuarticEqn}[e] == 0, e, \text{Quartics} \rightarrow \text{True}] \quad (21)$$

that immediately returns a suitable algebraic formula. At this point we defer detailed discussion of the textbook solution to the Supplementary Material, and instead focus on a particularly symmetric version of the solution and the form it takes for the eigenvalue problem for traceless, symmetric 4×4 matrices such as our profile matrices $M(E)$. For this purpose, we look for an alternative solution by considering the following traceless ($p_1 = 0$) Ansatz:

$$\left. \begin{aligned} \epsilon_1(p) &\stackrel{?}{=} \sqrt{X(p)} + \sqrt{Y(p)} + \sqrt{Z(p)} & \epsilon_2(p) &\stackrel{?}{=} \sqrt{X(p)} - \sqrt{Y(p)} - \sqrt{Z(p)} \\ \epsilon_3(p) &\stackrel{?}{=} \sqrt{X(p)} + \sqrt{Y(p)} - \sqrt{Z(p)} & \epsilon_4(p) &\stackrel{?}{=} \sqrt{X(p)} - \sqrt{Y(p)} + \sqrt{Z(p)} \end{aligned} \right\} \quad (22)$$

This form emphasizes some additional explicit symmetry that we will see is connected to the role of cube roots in the quartic algebraic solutions (see, e.g., [Coutsias and Wester, 2019]) . We can turn it into an equation for $\epsilon_k(p)$ to be solved in terms of the matrix parameters $p_k(E)$ as follows: First we eliminate e using $(e - \epsilon_1)(e - \epsilon_2)(e - \epsilon_3)(e - \epsilon_4) = 0$ to express the matrix data

expressions p_k directly in terms of totally symmetric polynomials of the eigenvalues in the form [Abramowitz and Stegun, 1970]

$$\left. \begin{aligned} p_1 &= -\epsilon_1 - \epsilon_2 - \epsilon_3 - \epsilon_4 \\ p_2 &= \epsilon_1\epsilon_2 + \epsilon_1\epsilon_3 + \epsilon_2\epsilon_3 + \epsilon_1\epsilon_4 + \epsilon_2\epsilon_4 + \epsilon_3\epsilon_4 \\ p_3 &= -\epsilon_1\epsilon_2\epsilon_3 - \epsilon_1\epsilon_2\epsilon_4 - \epsilon_1\epsilon_3\epsilon_4 - \epsilon_2\epsilon_3\epsilon_4 \\ p_4 &= \epsilon_1\epsilon_2\epsilon_3\epsilon_4 \end{aligned} \right\}. \quad (23)$$

Next we substitute our expression Eq. (22) for the ϵ_k in terms of the $\{X, Y, Z\}$ functions into Eq. (23), yielding a completely different alternative to Eq. (16) that *also* will solve the 3D RMSD eigenvalue problem if we can invert it to express $\{X(p), Y(p), Z(p)\}$ in terms of the data $p_k(E)$ as presented in Eq. (20):

$$\left. \begin{aligned} p_1 &= 0 \\ p_2 &= -2(X + Y + Z) \\ p_3 &= -8\sqrt{XYZ} \\ p_4 &= X^2 + Y^2 + Z^2 - 2(YZ + ZX + XY) \end{aligned} \right\}. \quad (24)$$

We already see the critical property in p_3 that, while p_3 itself has a deterministic sign from the matrix data, the possibly variable signs of the square roots in Eq. (22) have to be constrained so their product \sqrt{XYZ} agrees with the sign of p_3 . Manipulating the quartic equation solutions that we can obtain by applying the library function Eq. (21) to Eq. (24), and restricting our domain to real traceless, symmetric matrices (and hence real eigenvalues), we find solutions for $X(p)$, $Y(p)$, and $Z(p)$ of the following form:

$$F_f(0, p_2, p_3, p_4) = +\frac{1}{6} \left(r(p) \cos_f(p) - p_2 \right) \quad (25)$$

where the $\cos_f(p)$ terms differ only by a cube root phase:

$$\cos_x(p) = \cos\left(\frac{\arg(a+ib)}{3}\right), \quad \cos_y(p) = \cos\left(\frac{\arg(a+ib)}{3} - \frac{2\pi}{3}\right), \quad \cos_z(p) = \cos\left(\frac{\arg(a+ib)}{3} + \frac{2\pi}{3}\right). \quad (26)$$

Here $\arg(a+ib) = \text{atan2}(b, a)$ in the C mathematics library, or $\text{ArcTan}[a, b]$ in Mathematica, $F_f(p)$ with $f = (x, y, z)$ corresponds to $X(p)$, $Y(p)$, or $Z(p)$, and the utility functions appearing in the equations for our traceless $p_1 = 0$ case are

$$\left. \begin{aligned} r^2(0, p_2, p_3, p_4) &= p_2^2 + 12p_4 = \sqrt[3]{a^2 + b^2} = (a+ib)^{1/3}(a-ib)^{1/3} \\ a(0, p_2, p_3, p_4) &= p_2^3 + \frac{1}{2}(27p_3^2 - 72p_2p_4) \\ b^2(0, p_2, p_3, p_4) &= r^6(p) - a^2(p) \\ &= \frac{27}{4}(16p_4p_2^4 - 4p_3^2p_2^3 - 128p_4^2p_2^2 + 144p_3^2p_4p_2 - 27p_3^4 + 256p_4^3) \end{aligned} \right\}. \quad (27)$$

The function $b^2(p)$ has the essential property that, for real solutions to the cubic, which imply the required real solutions to our eigenvalue equations [Abramowitz and Stegun, 1970], we must have $b^2(p) \geq 0$. That essential property allowed us to convert the bare solution into terms involving

$\{(a + ib)^{1/3}, (a - ib)^{1/3}\}$ whose sums form the manifestly real cube-root-related cosine terms in Eq. (26).

Final Eigenvalue Algorithm. While Eqs. (25) and (26) are well-defined, square-roots must be taken to finish the computation of the eigenvalues postulated in Eq. (22). In our special case of symmetric, traceless matrices such as $M(E)$, we can always choose the signs of the first two square roots to be positive, but the sign of the \sqrt{Z} term is non-trivial, and in fact is the sign of $\det[E]$. The form of the solution in Eqs. (22) and (25) that works specifically for all traceless symmetric matrices such as $M(E)$ is given by our equations for $p_k(E)$ in Eqs. (17–20), along with Eqs. (25), (26), and (27) *provided* we modify Eq. (22) using $\sigma(p) = \text{sign}(\det[E]) = \text{sign}(-p_3)$ as follows:

$$\left. \begin{aligned} \epsilon_1(p) &= \sqrt{X(p)} + \sqrt{Y(p)} + \sigma(p)\sqrt{Z(p)} & \epsilon_2(p) &= \sqrt{X(p)} - \sqrt{Y(p)} - \sigma(p)\sqrt{Z(p)} \\ \epsilon_3(p) &= \sqrt{X(p)} + \sqrt{Y(p)} - \sigma(p)\sqrt{Z(p)} & \epsilon_4(p) &= \sqrt{X(p)} - \sqrt{Y(p)} + \sigma(p)\sqrt{Z(p)} \end{aligned} \right\} \quad (28)$$

The particular order of the numerical eigenvalues in our chosen form of the solution Eq. (28) is found in regular cases to be uniformly nonincreasing in numerical order for our $M(E)$ matrices, so $\epsilon_1(p)$ is always the leading eigenvalue. This is our preferred symbolic version of the solution to the 3D RMSD problem defined by $M(E)$.

Note: We have experimentally confirmed the numerical behavior of Eq. (25) in Eq. (28) with 1,000,000 randomly generated sets of 3D cross-covariance matrices E , along with the corresponding profile matrices $M(E)$, producing numerical values of p_k inserted into the equations for $X(p)$, $Y(p)$, and $Z(p)$. We confirmed that the sign of $\sigma(p)$ varied randomly, and found that the algebraically computed values of $\epsilon_k(p)$ corresponded to the standard numerical eigenvalues of the matrices $M(E)$ in all cases, to within expected variations due to numerical evaluation behavior and expected occasional instabilities. In particular, we found a maximum per-eigenvalue discrepancy of about 10^{-13} for the *algebraic* methods relative to the standard *numerical* eigenvalue methods, and a median difference of 10^{-15} , in the context of machine precision of about 10^{-16} . (Why did we do this? Because we had earlier versions of the algebraic formulas that produced anomalies due to inconsistent phase choices in the roots, and felt it worthwhile to perform a practical check on the numerical behavior of our final version of the solutions.)

Eigenvectors for 3D Data. The eigenvector formulas corresponding to ϵ_k can be generically computed by solving any three rows of

$$[M(E) \cdot v - e v] = [A] = 0 \quad (29)$$

for the elements of v , e.g., $v = (1, v_1, v_2, v_3)$, as a function of some eigenvalue e (of course, one must account for special cases, e.g., if some subspace of $M(E)$ is already diagonal). The desired unit quaternion for the optimization problem can then be obtained from the normalized eigenvector

$$q(e, E) = \frac{v}{\|v\|} \quad (30)$$

Note that this can often have $q_0 < 0$, and that whenever the problem in question depends on the sign of q_0 , such as a *slerp* starting at q_{ID} , one should choose the sign of Eq. (30) appropriately; some applications may also require an element of statistical randomness, in which case one might randomly pick a sign for q_0 .

As noted by Liu et al. [Liu et al., 2010], a very clear way of computing the eigenvectors for a given eigenvalue is to exploit the fact that the determinant of Eq. (29) must vanish, that is $\det[A] = 0$; one simply exploits the fact that the columns of the adjugate matrix α_{ij} (the transpose of the matrix of cofactors of the matrix $[A]$) produce its inverse by means of creating multiple copies of the determinant. That is,

$$\sum_{c=1}^4 A_{ac} \alpha_{cb} = \delta_{ab} \det[A] \equiv 0, \quad (31)$$

so we can just compute *any* column of the adjugate via the appropriate set of subdeterminants and, in the absence of singularities, that will be an eigenvector (since any of the four columns can be eigenvectors, if one fails, just try another).

In the general well-behaved case, the form of v in the eigenvector solution for any eigenvalue $e = \epsilon_k$ may be explicitly computed to give the corresponding quaternion (among several equivalent alternative expressions) as

$$q(e, E) = \frac{1}{\|v\|} \times \begin{bmatrix} 2ABC + A^2 e_x + B^2 e_y + C^2 e_z - e_x e_y e_z \\ A(aA - bB - cC) - cB e_y - bC e_z - a e_y e_z \\ B(bB - cC - aA) - aC e_z - cA e_x - b e_z e_x \\ C(cC - aA - bB) - bA e_x - aB e_y - c e_x e_y \end{bmatrix}, \quad (32)$$

where for convenience we define $\{e_x = (e - x + y + z), e_y = (e + x - y + z), e_z = (e + x + y - z)\}$ with $x = E_{xx}$, cyclic, $a = E_{yz} - E_{zy}$, cyclic, and $A = E_{yz} + E_{zy}$, cyclic. We substitute the maximal eigenvector $q_{\text{opt}} = q(\epsilon_1, E)$ into Eq. (5) to give the sought-for optimal 3D rotation matrix $R(q_{\text{opt}})$ that solves the RMSD problem with $\Delta(q_{\text{opt}}) = \epsilon_1$, as we noted in Eq. (14).

Remark: Yet another approach to computing eigenvectors that, surprisingly, *almost* entirely avoids any reference to the original matrix, but needs only its eigenvalues and minor eigenvalues, has recently been rescued from relative obscurity [Denton et al., 2019]. (The authors uncovered a long list of non-cross-citing literature mentioning the result dating back at least to 1934.) If, for a real, symmetric 4×4 matrix M we label the set of four eigenvectors v_i by the index i and the components of any single such four-vector by a , the squares of each of the sixteen corresponding components take the form

$$([v_i]_a)^2 = \frac{\prod_{j=1}^3 (\lambda_i(M) - \lambda_j(\mu_a))}{\prod_{k=1; k \neq i}^4 (\lambda_i(M) - \lambda_k(M))}. \quad (33)$$

Here the μ_a are the 3×3 minors obtained by removing the a th row and column of M , and the $\lambda_j(\mu_a)$ comprise the list of 3 eigenvalues of each of these minors. Attempting

to obtain the eigenvectors by taking square roots is of course hampered by the non-deterministic sign; however, since the eigenvalues $\lambda_i(M)$ are known, and the overall sign of each eigenvector v_i is arbitrary, one needs to check at most eight sign combinations to find the one for which $M \cdot v_i = \lambda_i(M) v_i$, solving the problem. Note that the general formula extends to Hermitian matrices of any dimension.

7 The 3D Orientation Frame Alignment Problem

We turn next to the orientation-frame problem, assuming that the data are like lists of orientations of roller coaster cars, or lists of residue orientations in a protein, ordered pairwise in some way, but *without* specifically considering any spatial location or nearest-neighbor ordering information. In D -dimensional space, the *columns* of any $\mathbf{SO}(D)$ orthonormal $D \times D$ rotation matrix R_D are what we mean by an orientation frame, since these columns are the directions pointed to by the axes of the identity matrix after rotating something from its defining identity frame to a new attitude; note that no spatial location information whatever is contained in R_D , though one may wish to choose a local center for each frame if the construction involves coordinates such as amino acid atom locations (see, e.g., [Hanson and Thakur, 2012]).

In 2D, 3D, and 4D, there exist two-to-one quadratic maps from the topological spaces \mathbf{S}^1 , \mathbf{S}^3 , and $\mathbf{S}^3 \times \mathbf{S}^3$ to the rotation matrices R_2 , R_3 , and R_4 . These are the quaternion-related objects that we will use to obtain elegant representations of the frame data-alignment problem. In 2D, a frame data element can be expressed as a complex phase, while in 3D the frame is a unit quaternion (see [Hanson, 2006, Hanson and Thakur, 2012]). In 4D (see the Supplementary Material), the frame is described by a *pair* of unit quaternions.

Note. Readers unfamiliar with the use of complex numbers and quaternions to obtain elegant representations of 2D and 3D orientation frames are encouraged to review the tutorial in Appendix B.

Overview. We focus now on the problem of aligning corresponding sets of 3D orientation frames, just as we already studied the alignment of sets of 3D spatial coordinates by performing an optimal rotation. There will be more than one feasible method. We might assume we could just define the quaternion-frame-alignment or “QFA” problem by converting any list of frame orientation matrices to quaternions (see [Hanson, 2006, Hanson and Thakur, 2012] and also Appendix C), and writing down the quaternion equivalents of the RMSD treatment in Eq. (9) and Eq. (10). However, unlike the linear Euclidean problem, the preferred quaternion optimization function technically requires a *non-linear* minimization of the squared sums of geodesic arc-lengths connecting the points on the quaternion hypersphere \mathbf{S}^3 . The task of formulating this ideal problem as well as studying alternative approximations is the subject of its own branch of the literature, often known as the *quaternionic barycenter* problem or the *quaternion averaging* problem (see, e.g., [Brown and Worsey, 1992, Buss and Fillmore, 2001, Moakher, 2002, Markley et al., 2007, Huynh, 2009, Hartley et al., 2013] and also Appendix D). We will focus on L_2 norms (the aforementioned sums of squares of arc-lengths), although alternative approaches to the rotation averaging problem, such as employing L_1 norms and using the Weiszfeld algorithm to find the optimal rotation numerically, have been advocated, e.g., by [Hartley et al., 2011]. The computation of optimally aligning rotations, based on plausible exact or approximate measures relating collections of corresponding pairs of (quaternionic) orientation frames, is now our task.

Choices for the forms of the measures encoding the distance between orientation frames have been widely discussed, see, e.g., [Park and Ravani, 1997, Moakher, 2002, Markley et al., 2007, Huynh, 2009, Hartley et al., 2011, Hartley et al., 2013, Huggins, 2014a]. Since we are dealing primarily with quaternions, we will start with two measures dealing directly with the quaternion geometry, the geodesic arc length and the chord length, and later on examine some advantages of starting with quaternion-sign-independent rotation-matrix forms.

3D Geodesic Arc Length Distance. First, we recall that the matrix Eq. (5) has three orthonormal columns that define a quadratic map from the quaternion three-sphere \mathbf{S}^3 , a smooth connected Riemannian manifold, to a 3D orientation frame. The squared geodesic arc-length distance between two quaternions lying on the three sphere \mathbf{S}^3 is generally agreed upon as the measure of orientation-frame proximity whose properties are the closest in principle to the ordinary squared Euclidean distance measure Eq. (9) between points [Huynh, 2009], and we will adopt this measure as our starting point. We begin by writing down a frame-frame distance measure between two unit quaternions q_1 and q_2 , corresponding precisely to two orientation frames defined by the columns of $R(q_1)$ and $R(q_2)$. We define the geodesic arc length as an angle α on the hypersphere \mathbf{S}^3 computed geometrically from $q_1 \cdot q_2 = \cos \alpha$. As pointed out by [Huynh, 2009, Hartley et al., 2013], the geodesic arc length between a test quaternion q_1 and a data-point quaternion q_2 of ambiguous sign (since $R(+q_2) = R(-q_2)$) can take two values, and we want the minimum value. Furthermore, to work on a spherical manifold instead of a plane, we need basically to cluster the ambiguous points in a deterministic way. Starting with the bare angle between two quaternions on \mathbf{S}^3 , $\alpha = \arccos(q_1 \cdot q_2)$, where we recall that $\alpha \geq 0$, we define a *pseudometric* [Huynh, 2009] for the geodesic arc-length distance as

$$d_{\text{geodesic}}(q_1, q_2) = \min(\alpha, \pi - \alpha) : 0 \leq d_{\text{geodesic}}(q_1, q_2) \leq \frac{\pi}{2}, \quad (34)$$

illustrated in Fig. (4). An efficient implementation of this is to take

$$d_{\text{geodesic}}(q_1, q_2) = \arccos(|q_1 \cdot q_2|). \quad (35)$$

We now seek to define an ideal minimizing L_2 orientation frame measure, comparable to our minimizing Euclidean RMSD measure, but constructed from geodesic arc-lengths on the quaternion hypersphere instead of Euclidean distances in space. Thus to compare a test quaternion-frame data set $\{p_k\}$ to a reference data set $\{r_k\}$, we propose the geodesic-based least squares measure

$$\mathbf{S}_{\text{geodesic}} = \sum_{k=1}^N (\arccos |(q \star p_k) \cdot r_k|)^2 = \sum_{k=1}^N (\arccos |q \cdot (r_k \star \bar{p}_k)|)^2, \quad (36)$$

where we have used the identities of Eq. (3). When $q = q_{\text{ID}}$, the individual measures correspond to Eq. (35), and otherwise “ $q \star p_k$ ” is the exact analog of “ $R(q) \cdot x_k$ ” in Eq. (9), and denotes the quaternion rotation q acting on the entire set $\{p_k\}$ to rotate it to a new orientation that we want to align optimally with the reference frames $\{r_k\}$. Analogously, for points on a sphere, the arccosine of an inner product is equivalent to a distance between points in Euclidean space.

Remark: For improved numerical behavior in the computation of the quaternion inner product angle between two quaternions, one may prefer to convert the arccosine to an arctangent form, $\alpha = \arctan(dx, dy) = \arctan(\cos \alpha, |\sin \alpha|)$ (remember the C math library uses the opposite argument order $\text{atan2}(dy, dx)$), with the parameters

$$\cos(\alpha) = |\Re(q_1 \star q_2^{-1})| = |q_1 \cdot q_2|, \quad |\sin(\alpha)| = \|\Im(q_1 \star q_2^{-1})\| = \|- [q_1]_0 \mathbf{q}_2 + [q_2]_0 \mathbf{q}_1 - \mathbf{q}_1 \times \mathbf{q}_2 \|,$$

which is somewhat more stable.

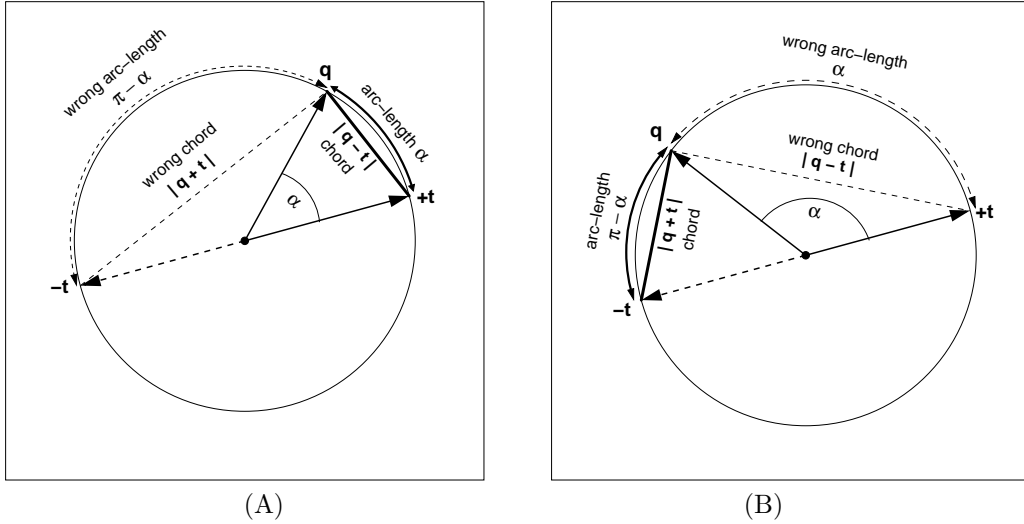


Figure 4: Geometric context involved in choosing a *quaternion distance* that will result in the correct *average rotation matrix* when the quaternion measures are optimized. Because the quaternion vectors represented by t and $-t$ give the same rotation matrix, one must choose $|\cos \alpha|$ or the *minima*, that is $\min(\alpha, \pi - \alpha)$ or $\min(\|q - t\|, \|q + t\|)$, of the alternative distance measures to get the *correct* items in the arc-length or chord measure summations. (A) and (B) represent the cases when the first or second choice should be made, respectively.

Adopting the Solvable Chord Measure. Unfortunately, the geodesic arc-length measure does not fit into the linear algebra approach that we were able to use to obtain exact solutions for the Euclidean data alignment problem treated so far. Thus we are led to investigate instead a very close approximation to $d_{\text{geodesic}}(q_1, q_2)$ that *does* correspond closely to the Euclidean data case and does, with some contingencies, admit exact solutions. This approximate measure is the *chord distance*, whose individual distance terms analogous to Eq. (35) take the form of a closely related pseudometric [Huynh, 2009, Hartley et al., 2013],

$$d_{\text{chord}}(q_1, q_2) = \min(\|q_1 - q_2\|, \|q_1 + q_2\|) : 0 \leq d_{\text{chord}}(q_1, q_2) \leq \sqrt{2}. \quad (37)$$

We compare the geometric origins for Eq. (35) and Eq. (37) in Fig. (4). Note that the crossover point between the two expressions in Eq. (37) is at $\pi/2$, so the hypotenuse of the right isosceles triangle at that point has length $\sqrt{2}$.

The solvable approximate optimization function analogous to $\|R \cdot x - y\|^2$ that we will now explore for the quaternion-frame alignment problem will thus take the form that must be minimized as

$$\mathbf{S}_{\text{chord}} = \sum_{k=1}^N (\min(\|(q \star p_k) - r_k\|, \|(q \star p_k) + r_k\|))^2. \quad (38)$$

We can convert the sign ambiguity in Eq. (38) to a deterministic form like Eq. (35) by observing, with the help of Fig. (4), that

$$\|q_1 - q_2\|^2 = 2 - 2q_1 \cdot q_2, \quad \|q_1 + q_2\|^2 = 2 + 2q_1 \cdot q_2. \quad (39)$$

Clearly $(2 - 2|q_1 \cdot q_2|)$ is always the smallest of the two values. Thus minimizing Eq. (38) amounts to maximizing the now-familiar cross-term form, which we can write as

$$\left. \begin{aligned} \Delta_{\text{chord}}(q) &= \sum_{k=1}^N |(q \star p_k) \cdot r_k| \\ &= \sum_{k=1}^N |q \cdot (r_k \star \bar{p}_k)| \\ &= \sum_{k=1}^N |q \cdot t_k| \end{aligned} \right\}. \quad (40)$$

Here we have used the identity $(q \star p) \cdot r = q \cdot (r \star \bar{p})$ from Eq. (3) and defined the quaternion displacement or "attitude error" [Markley et al., 2007]

$$t_k = r_k \star \bar{p}_k. \quad (41)$$

Note that we could have derived the same result using Eq. (2) to show that $\|q \star p - r\| = \|q \star p - r\| \|p\| = \|q - r \star \bar{p}\|$.

There are several ways to proceed to our final result at this point. The simplest is to pick a neighborhood in which we will choose the samples of q that include our expected optimal quaternion, and adjust the sign of each data value t_k to \tilde{t}_k by the transformation

$$\tilde{t}_k = t_k \text{sign}(q \cdot t_k) \rightarrow |q \cdot t_k| = q \cdot \tilde{t}_k. \quad (42)$$

The neighborhood of q matters because, as argued by [Hartley et al., 2013], even though the allowed range of 3D rotation angles is $\theta \in (-\pi, \pi)$ (or quaternion sphere angles $\alpha \in (-\pi/2, \pi/2)$), convexity of the optimization problem cannot be guaranteed for collections outside local regions centered on some θ_0 of size $\theta_0 \in (-\pi/2, \pi/2)$ (or $\alpha_0 \in (-\pi/4, \pi/4)$): beyond this range, local basins may exist that allow the mapping Eq. (42) to produce distinct local variations in the assignments of the $\{\tilde{t}_k\}$ and in the solutions for q_{opt} . Within considerations of such constraints, Eq. (42) now allows us to take the summation outside the absolute value, and write the quaternion-frame optimization problem in terms of maximizing the cross-term expression

$$\left. \begin{aligned} \Delta_{\text{chord}}(q) &= \sum_{k=1}^N q \cdot \tilde{t}_k \\ &= q \cdot V(t) \end{aligned} \right\} \quad (43)$$

where $V = \sum_{k=1}^N \tilde{t}_k$ is the analog of the Euclidean RMSD profile matrix M . However, since this is *linear* in q , we have the remarkable result that, as noted in the treatment of [Hartley et al., 2013] regarding the quaternion L_2 chordal-distance norm, the solution is immediate, being simply

$$q_{\text{opt}} = \frac{V}{\|V\|}, \quad (44)$$

since that immediately maximizes the value of $\Delta_{\text{chord}}(q)$ in Eq. (43). This gives the maximal value of the measure as

$$\Delta_{\text{chord}}(q_{\text{opt}}) = \|V\|, \quad (45)$$

and thus $\|V\|$ is the exact orientation frame analog of the spatial RMSD maximal eigenvalue ϵ_{opt} , except it is far easier to compute.

Illustrative Example. Using the quaternion display method described in Appendix B and illustrated in Fig. (12), we present in Fig. (5)(A) a representative quaternion frame reference data set, then in (B) the relationship of the arc and chord distances for each point in a set of arc and chord distances (see Fig. (4)) for each point pair in the quaternion space. In Fig. (5)(C,D), we show the results of the quaternion-frame alignment process using conceptually the same *slerp* of Eq. (15) to transition from the raw state at $q(s=0) = q_{\text{TD}}$ to $q(s=0.5)$ for (C) and $q(s=1.0) = q_{\text{opt}}$ for (D). The yellow arrow is the axis of rotation specified by the spatial part of the optimal quaternion.

The rotation-averaging visualization of the optimization process, though it has exactly the same optimal quaternion, is quite different, since all the quaternion data collapse to a list of single small quaternions $t = r \star \bar{p}$. As illustrated in Fig. (6), with compatible sign choices, the \tilde{t}_k 's cluster around the optimal quaternion, which is clearly consistent with being the barycenter of the quaternion differences, intuitively the place to which all the quaternion frames need to be rotated to optimally coincide. As before, the yellow arrow is the axis of rotation specified by the spatial part of the optimal quaternion. Next, Fig. (7) addresses the question of how the rigorous arc-length measure is related to the chord-length measure that can be treated using the same methods as the spatial RMSD optimization. In parallel to Fig. (5)(B), Fig. (7)(A) shows essentially the same comparison for the \tilde{t}_k quaternion-displacement version of the same data. In Fig. (7)(B), we show the histograms of the chord distances to a sample point, the origin in this case, vs the arc-length or geodesic distances. They obviously differ, but in fact for plausible simulations, the arc-length numerical optimal quaternion barycenter differs from the chord-length counterpart by less than one hundredth of a degree. These issues are studied in more detail in the Supplementary Material.

Next, in Fig. (8), we display the values of $\Delta_{\text{chord}} = q \cdot V$ that parallel the RMSD version in Fig. (3). The dots show the size of the cost $\Delta(q)$ at randomly sampled points across the entire \mathbf{S}^3 , with $q_0 \geq 0$ in (A) and $q_0 < 0$ in (B). We have all the signs of the \tilde{t}_k chosen to be centered in an appropriate local neighborhood, and so, unlike the quadratic Euclidean RMSD case, there is only one value for q_{opt} which is in the direction of V . Finally, in Fig. (9) we present an intuitive sketch of the convexity constraints for the QFA optimization related to [Hartley et al., 2013]. We start with a set of data in (A) (with both $(q, -q)$ partners), that consists of three local clouds that can be smoothly deformed from dispersed to coinciding locations. (B) and (C) both contain a uniform sample of quaternion sample points q spread over all of quaternion space, shown as magenta dots, with positive and negative q_0 plotted on top of each other. Then each sample q is used to compute *one* set of mappings $t_k \rightarrow \tilde{t}_k$, and the *one* value of $q_{\text{opt}} = V(\tilde{t})/\|V\|$ that results. The black arrows show the relation of q_{opt} to each original sample q , effectively showing us their *votes* for the best quaternion average. (B) has the clusters positioned far enough apart that we can clearly see that there are several basins of attraction, with no unique solution for q_{opt} , while in (C), we have interpolated the three clusters to lie in the same local neighborhood, roughly in a ball of quaternion radius $\alpha < \pi/4$, and we see that almost all of the black arrows vote for one unique q_{opt} or its equivalent negative. This seems to be a useful exercise to gain intuition about the nature of the basins of attraction for the quaternion averaging problem that is essential for quaternion frame alignment.

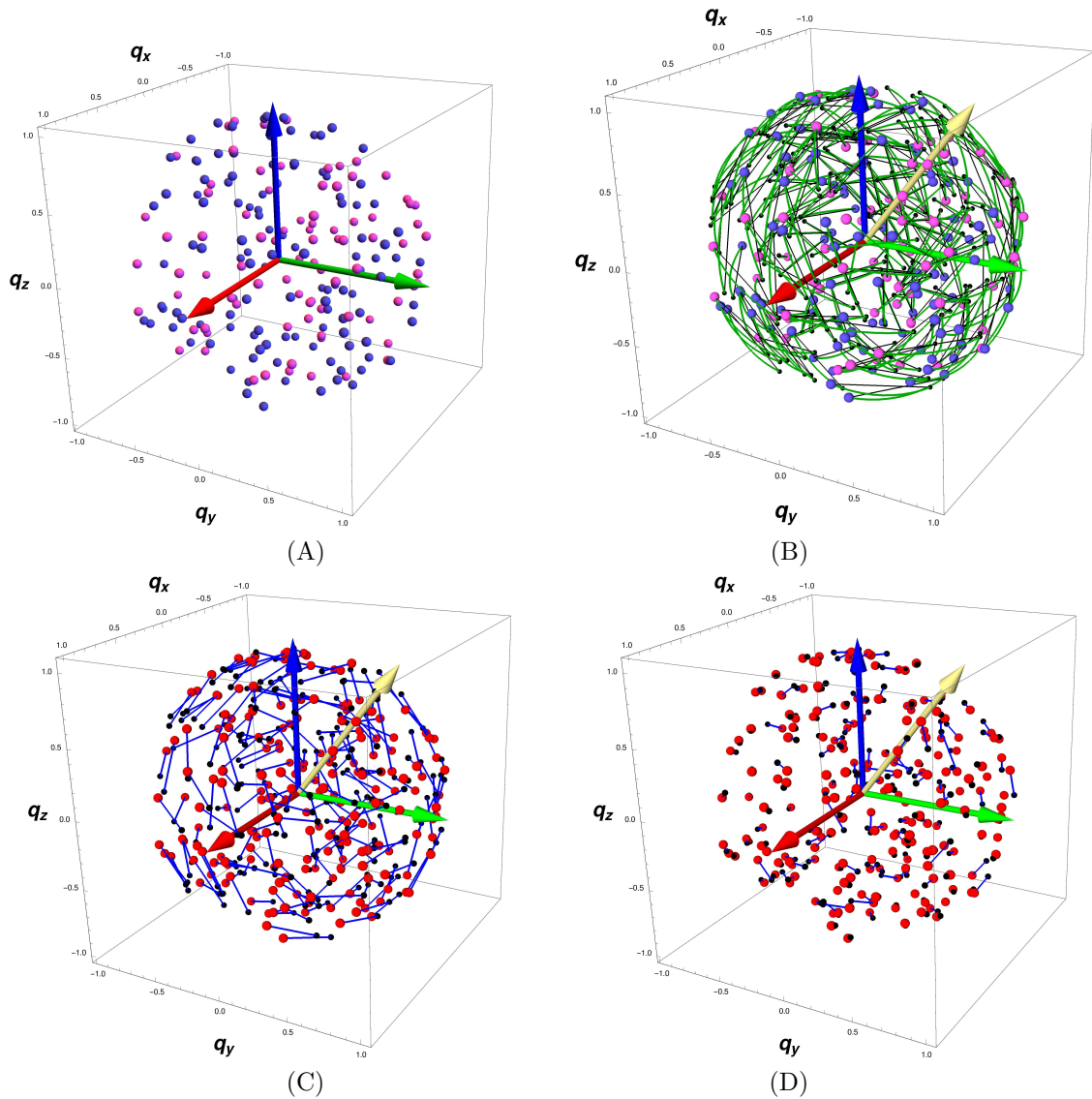


Figure 5: 3D components of a quaternion orientation data set. (A) A quaternion reference set, color coded by the sign of q_0 . (B) *Exact* quaternion arc-length distances (green) vs chord distances (black) between the test and reference points. (C) Part-way from starting state to the aligned state, at $s = 0.5$. (D) The final best alignment at $s = 1.0$. The yellow arrow is the direction of the quaternion eigenvector; when scaled, the length is the sine of half the optimal rotation angle.

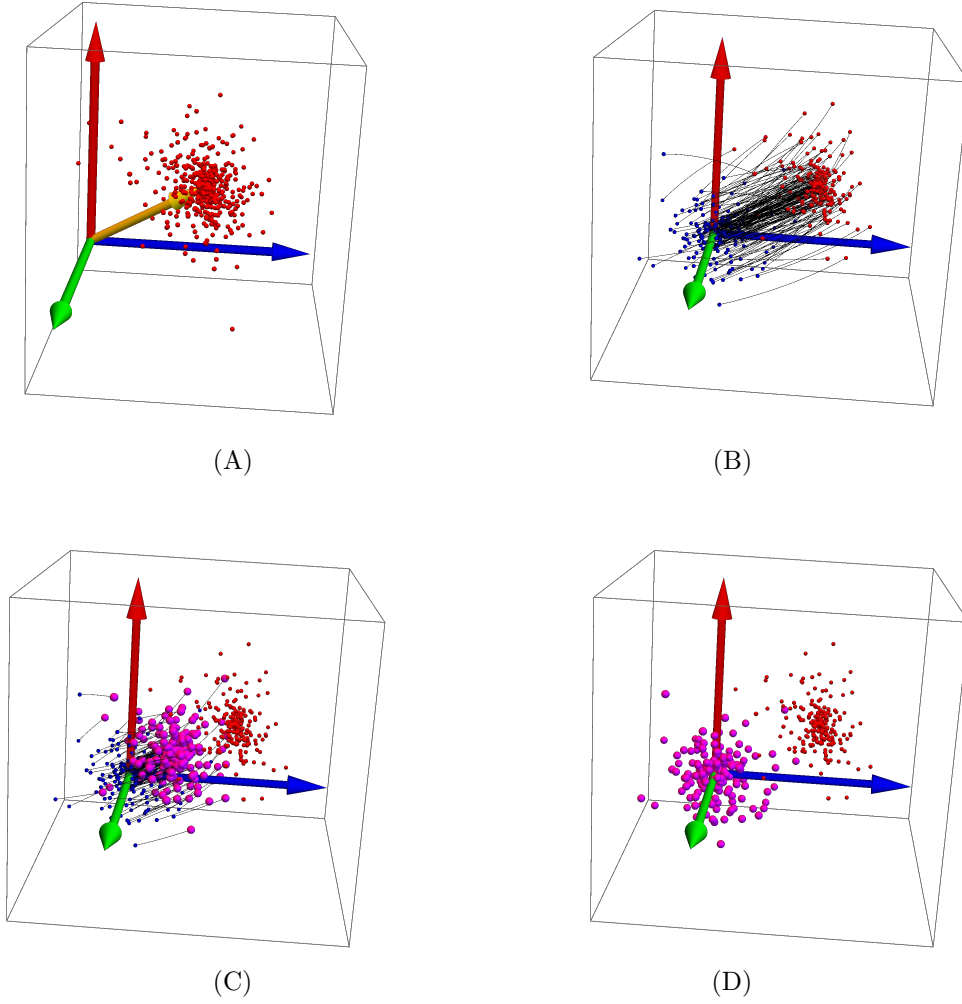


Figure 6: 3D components of the rotation-average transformation of the quaternion orientation data set, with each point denoting the *displacement* between each pair of frames as a single quaternion, corresponding to the rotation taking the test frame to the reference frame. (A) The cluster of points $t_k = r_k \star \bar{p}_k \rightarrow \tilde{t}_k$ derived from the frame matching problem using just the curved arcs in Fig. (5)(B). If there were no alignment errors introduced in the simulation, these would all be a single point. The yellow arrow is the quaternion solution to the chord-distance centroid of this cluster, and is identical to the optimal quaternion rotation transforming the test data to have the minimal chord measure relative to the reference data. (B) Choosing a less cluttered subset of the data in (A), we display the geodesic paths from the initial quaternion displacements \tilde{t}_k to the origin-centered set with minimal chord-measure distance relative to the origin. This is the result of applying the inverse of the quaternion q_{opt} to each \tilde{t}_k . Note that the paths are curved geodesics lying properly within the quaternion sphere. (C,D) Rotating the cluster using a slerp between the quaternion barycenter of the initial misaligned data and the optimally aligned position, which is centered at the origin.

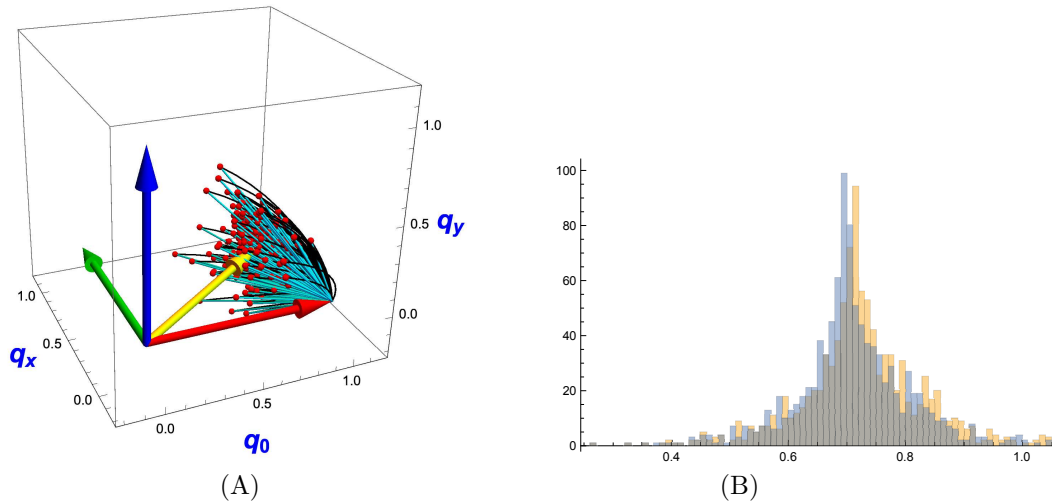


Figure 7: (A) Projecting the geodesic vs chord distances from the origin to sampled points in a set of frame-displacement data $t_k = r_k \star \bar{p}_k \rightarrow \tilde{t}_k$. Since the \mathbf{q} spatial quaternion paths project to a straight line from the origin, we use the (q_0, q_1, q_2) coordinates instead of our standard \mathbf{q} coordinates to expose the curvature in the arc-length distances to the origin. (B) Comparing the distribution of arccosine values of the rigorous geodesic arc-length cost function and vs the chord-length method, sampled with a uniform distribution of random quaternions over \mathbf{S}^3 . The arc-length method has a different distribution, as expected, and produces a very slightly better barycenter. However, the optimal quaternions for the arc-length vs chord-length measure for this simulated data set differ by less than a hundredth of a degree, so drawing the positions of the two distinct optimal quaternions would not reveal any difference in image (A).

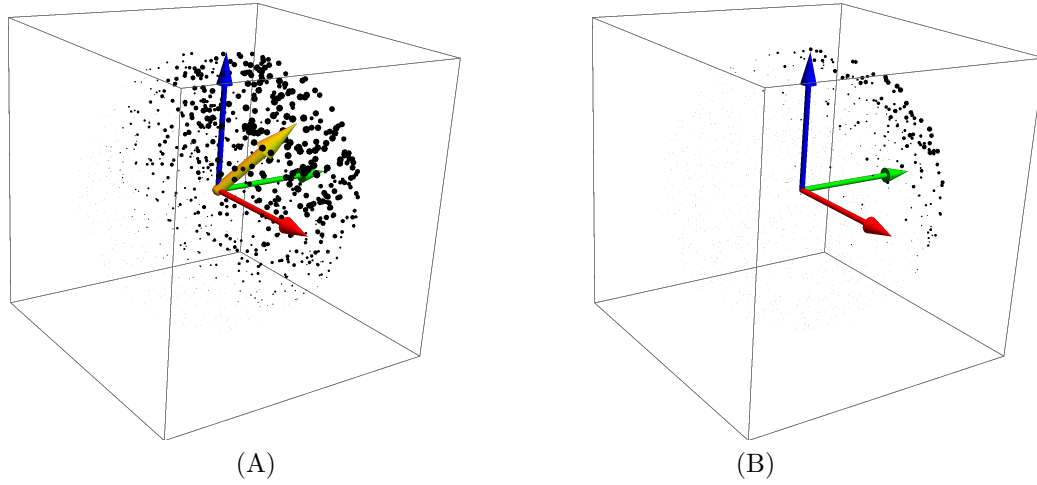
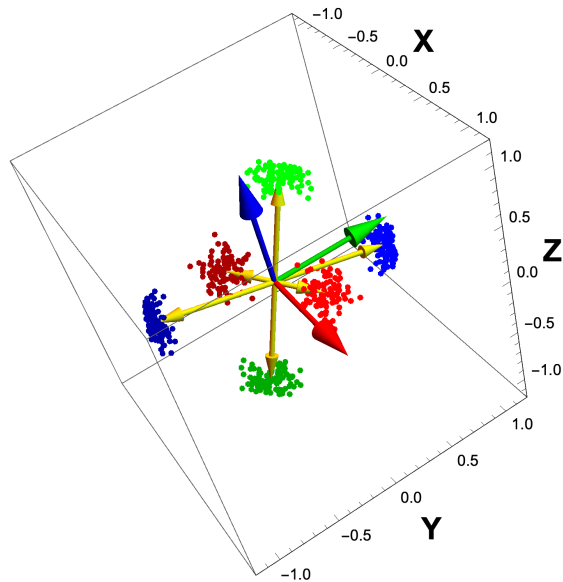
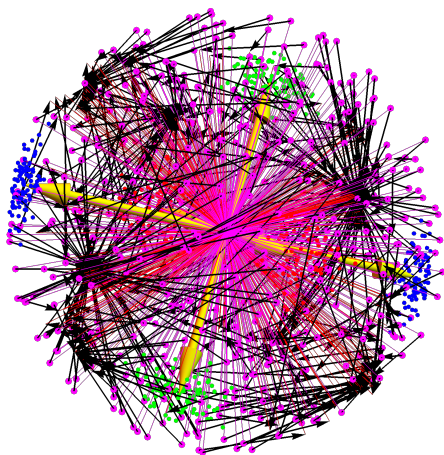


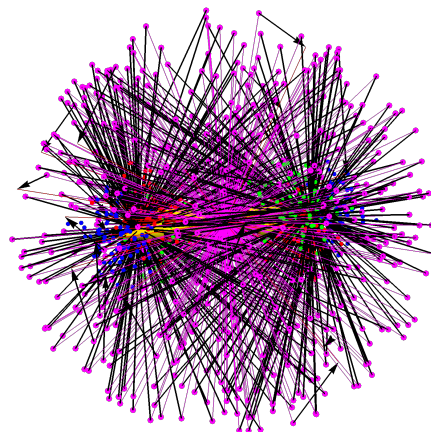
Figure 8: The values of $\Delta = q \cdot V$ represented by the sizes of the dots placed at a random distribution of quaternion points. We display the data dots at the locations of their spatial quaternion components $\mathbf{q} = (q_1, q_2, q_3)$. (A) is the northern hemisphere of \mathbf{S}^3 , with $q_0 \geq 0$, (B) is the southern hemisphere, with $q_0 < 0$, and we implicitly know that the value of q_0 is $\pm\sqrt{1 - q_0^2}$. The points in these two solid balls represent the entire space of quaternions, and it is important to note that, even though $R(q) = R(-q)$ so each ball alone actually represents all possible unique rotation matrices, our cost function covers the *entire* space of quaternions, so q and $-q$ are distinct. The spatial component of the maximal eigenvector is shown by the yellow arrow, which clearly ends in the middle of the maximum values of Δ . The small cloud at the edge of (B) is simply the rest of the complete cloud around the tip of the yellow arrow as q_0 passes through the “equator” at $q_0 = 0$, going from a small positive value at the edge of (A) to a small negative value at the edge of (B).



(A)



(B)



(C)

Figure 9: The behavior of the basins of attraction for the $t_k \rightarrow \tilde{t}_k$ map is shown here, starting in (A) with the $(q, -q)$ pairs for three movable clusters of quaternion frame data, each having a well-defined *local* quaternion average $q_{\text{opt}} = V(\tilde{t})/\|V\|$ shown as the yellow arrows with their $q \rightarrow -q$ equivalents. Next we merge all three samples into one data set that can be smoothly interpolated between the data being outside the $\alpha = \pi/4$ safe zone to all being together within that geometric boundary in quaternion space. (B) shows the results of taking 500 uniform samples of q and computing the set $\{\tilde{t}_k\}$ for *each* sample q , placed at the magenta dots, and *then* computing the resulting q_{opt} ; the black arrows follow the line from the sample point to the resultant q_{opt} . Clearly in (B), where the clusters are in their initial widely dispersed configuration, the black arrows (the “votes” for the best q_{opt}) collect in several different basins of attraction, signifying the absence of a global solution. We then interpolate all the clusters close to each other, and show the new results of the voting in (C). Now almost all of the samplings of the full quaternion space converge to point their arrows densely to the two opposite values of q_{opt} , and there is just one effective basin of attraction.

Alternative Matrix Forms of the Linear Vector Chord Distance. If the signs of the quaternions representing orientation frames are well-behaved, and the frame problem is our only concern, Eqs. (43) and (44) provide a simple solution to finding the optimal global rotation. If we are anticipating wanting to combine a spatial profile matrix $M(E)$ with an orientation problem in a single 4×4 matrix, or we have problems defining a consistent quaternion sign, there are two further choices of orientation frame measure we may consider.

(1) Matrix Form of the Linear Vector Chord Distance. The first option uses the fact that the square of Eq. (43) will yield the same extremal solution, so we can choose a measure of the form

$$\begin{aligned} \Delta_{\text{chord-sq}} &= (q \cdot V)(q \cdot V) \\ &= \sum_{a=0, b=0}^3 q_a V_a V_b q_b \\ &= q \cdot \Omega \cdot q, \end{aligned} \tag{46}$$

where $\Omega_{ab} = V_a V_b$ is a 4×4 rank one symmetric matrix with $\det \Omega = 0$, and $\text{tr} \Omega = \sum_a V_a^2 \neq 0$. The eigensystem of Ω is just defined by the eigenvalue $\|V\|^2$, and combination with the spatial eigensystem can be achieved either numerically or algebraically. The sign issues for the sampled data remain unchanged since they appear inside the sums defining V . This form will acquire more importance in the 4D case.

(2) Fixing Sign Problem with Quadratic Rotation Matrix Chord Distance. Our second approach has a very natural way to *eliminate sign dependence altogether* from the quaternion chord distance method, and has a close relationship to Δ_{chord} . This measure is constructed starting from a minimized Fröbenius norm of the form (this approach is used by [Sarlette and Sepulchre, 2009]; see also, e.g., [Huynh, 2009], as well as [Moakher, 2002, Markley et al., 2007, Hartley et al., 2013])

$$\|R(q) \cdot R(p_k) - R(r_k)\|_{\text{Frob}}^2,$$

and then reducing to the cross-term as usual. The cross-term measure to be maximized, in terms of 3×3 (quaternion-sign-independent) rotation matrices, then becomes

$$\begin{aligned} \Delta_{\text{RRR}} &= \sum_{k=1}^N \text{tr} [R(q) \cdot R(p_k) \cdot R^{-1}(r_k)] = \sum_{k=1}^N \text{tr} [R(q \star p_k \star \bar{r}_k)] \\ &= \sum_{k=1}^N \text{tr} [R(q) \cdot R(p_k \star \bar{r}_k)] = \sum_{k=1}^N \text{tr} [R(q) \cdot R^{-1}(r_k \star \bar{p}_k)], \end{aligned} \tag{47}$$

where \bar{r} denotes the complex conjugate or inverse quaternion. We can verify that this is a chord-distance by noting that each relevant $R \cdot R \cdot R$ term reduces to the square of an individual chord

distance appearing in Δ_{chord} :

$$\left. \begin{aligned} \sum_{k=1}^N \text{tr} [R(q) \cdot R(p_k) \cdot R(\bar{r}_k)] &= \sum_{k=1}^N \left(4((q \star p_k) \cdot r_k)^2 - (q \cdot q)(p_k \cdot p_k)(r_k \cdot r_k) \right) \\ &= \sum_{k=1}^N \left(4(q \cdot (r_k \star \bar{p}_k))^2 - 1 \right) \\ &= 4 \sum_{a,b} q_a \left(\sum_{k=1}^N [t_k]_a [t_k]_b \right) q_b - N \\ &= 4 q \cdot A(t = r \star \bar{p}) \cdot q - N . \end{aligned} \right\} \quad (48)$$

Here the non-conjugated ordinary r on the right-hand side is not a typographical error, and the 4×4 matrix $A(t)$ is the alternative (equivalent) profile matrix that was introduced by [Markley et al., 2007, Hartley et al., 2013] for the chord-based quaternion-averaging problem. We can therefore use either the measure Δ_{RRR} or

$$\Delta_A = q \cdot A(t) \cdot q \quad (49)$$

with $A_{ab} = \sum_{k=1}^N [t_k]_a [t_k]_b$ as our rotation-matrix-based sign-insensitive chord-distance optimization measure. Exactly like our usual spatial measure, these measures must be *maximized* to find the optimal q . It is, however, important to emphasize that the optimal quaternion will *differ* for the Δ_{chord} , $\Delta_{\text{chord-sq}}$, and $\Delta_{\text{RRR}} \sim \Delta_A$ measures, though they will normally be very similar (see discussion in the Supplementary Material).

We now recognize that the sign-insensitive measures are all very closely related to our original spatial RMSD problem, and all can be solved by finding the optimal quaternion eigenvector q_{opt} of a 4×4 matrix. The procedure for $\Delta_{\text{chord-sq}}$ and Δ_A follows immediately, but it is useful to work out the options for Δ_{RRR} in a little more detail. Defining $T_k = R(p_k) \cdot R^{-1}(r_k) = R(p_k \star \bar{r}_k) = R^{-1}(t_k)$, we can write our optimization measure as

$$\Delta_{\text{RRR}} = \sum_{k=1}^N \text{tr} (R(q) \cdot T_k) = \sum_{a=1,b=1}^3 R_{ba}(q) T_{ab} = \sum_{a=0,b=0}^3 q_a \cdot U_{ab}(p, r) \cdot q_b = q \cdot U(p, r) \cdot q , \quad (50)$$

where the frame-based cross-covariance matrix is simply $T_{ab} = \sum_{k=1}^N [T_k]_{ab}$ and $U(p, r) = U(T)$ has the same relation to T as $M(E)$ has to E in Eq. (13).

To compute the necessary 4×4 numerical profile matrix U , one need only substitute the appropriate 3D frame triads or their corresponding quaternions for the k th frame pair and sum over k . Since the orientation-frame profile matrix $U(p, r)$ is symmetric and traceless just like the Euclidean profile matrix M , the same solution methods for the optimal quaternion rotation q_{opt} will work without alteration in this case, which is probably the preferable method for the general problem.

Evaluation. The details of evaluating the properties of our quaternion-frame alignment algorithms, including comparison of the chord approximation to the arc-length measure, are available in the Supplementary Material. The top-level result is that, even for quite large rotational differences, the mean difference between the optimal quaternion using the numerical arc-length measure and the optimal quaternion using the chord approximation for any of the three methods is on the order of small fractions of a degree for the random data distributions that we examined.

8 The 3D Combined Point+Frame Alignment Problem

Since we now have precise alignment procedures for both 3D spatial coordinates and 3D frame triad data (using the exact measure for the former and the approximate chord measure for the latter), we can consider the full 6 degree-of-freedom alignment problem for combined data from a single structure. As always, this problem can be solved either by numerical eigenvalue methods or in closed algebraic form using the eigensystem formulation of the both alignment problems presented in the previous Sections. While there are clearly appropriate domains of this type, e.g., any protein structure in the PDB database can be converted to a list of residue centers and their local frame triads [Hanson and Thakur, 2012], little is known at this time about the potential value of combined alignment. To establish the most complete possible picture, we now proceed to describe the details of our solution to the alignment problem for combined translational and rotational data, but we remark at the outset that the results of the combined system are not obviously very illuminating.

The most straightforward approach to the combined 6DOF measure is to equalize the scales of our spatial $M(E)$ profile matrix and our orientation-frame $U(S)$ profile matrix by imposing a unit-eigenvalue normalization, and then simply to perform a linear interpolation modified by a dimensional constant σ to adjust the relative importance of the orientation-frame portion:

$$\Delta_{xf}(t, \sigma) = q \cdot \left[(1-t) \frac{M(E)}{\epsilon_x} + t \sigma \frac{U(S)}{\epsilon_f} \right] \cdot q . \quad (51)$$

Because of the dimensional incompatibility of Δ_x and Δ_f , we treat the ratio

$$\lambda^2 = \frac{t\sigma}{1-t}$$

as a dimensional weight such as that adopted by Fogolari et al. [Fogolari et al., 2016] in their entropy calculations, so if t is dimensionless, then σ carries the dimensional scale information.

Given the composite profile matrix of Eq. (51), we can now extract our optimal rotation solution by computing the maximal eigenvalue as usual, either numerically or algebraically (though we may need the extension to the non-vanishing trace case examined in the Supplementary Material for some choices of U). The result is a parameterized eigensystem

$$\left. \begin{array}{l} \epsilon_{\text{opt}}(t, \sigma) \\ q_{\text{opt}}(t, \sigma) \end{array} \right\} \quad (52)$$

yielding the optimal values $R(q_{\text{opt}}(t, \sigma))$, $\Delta_{xf} = \epsilon_{\text{opt}}(t, \sigma)$ based on the data $\{E, S\}$ no matter what we take as the values of the two variables (t, σ) .

A Simplified Composite Measure. However, upon inspection of Eq. (51), one wonders what happens if we simply use the *slerp* defined in Eq. (8) to interpolate between the *separate* spatial and orientation-frame optimal quaternions. While the eigenvalues that correspond to the two scaled terms M/ϵ_x and U/ϵ_f in Eq. (51) are both unity, and thus differ from the eigenvalues of M and U , the individual normalized eigenvectors $q_{x:\text{opt}}$ and $q_{f:\text{opt}}$ are the same. Thus, if we are happy with simply using a hand-tuned fraction of the combination of the two corresponding rotations, we can just choose a composite rotation $R(q(t))$ specified by

$$q(t) = \text{slerp}(q_{x:\text{opt}}, q_{f:\text{opt}}, t) . \quad (53)$$

to study the composite 6DOF alignment problem. In fact, as detailed in the Supplementary Material, if we simply plug this $q(t)$ into Eq. (51) for any t (and $\sigma = 1$), we find *negligible differences* between the quaternions $q(t)$ and $q_{\text{opt}}(t, 1)$ as a function of t . We suggest in addition that any particular effect of $\sigma \neq 1$ could be achieved at some value of t in the interpolation. We thus conclude that, for all practical purposes, we might as well use Eq. (53) with the parameter t adjusted to achieve the objective of Eq. (51) to study composite translational and rotational alignment similarities.

9 Conclusion

Our objective has been to explore quaternion-based treatments of the RMSD data-comparison problem as developed in the work of Davenport [Davenport, 1968], Faugeras and Hebert [Faugeras and Hebert, 1983], Horn [Horn, 1987], Diamond [Diamond, 1988], Kearsley [Kearsley, 1989], and Kneller [Kneller, 1991], among others, and to publicize the exact algebraic solutions, as well as extending the method to handle wider problems. We studied the intrinsic properties of the RMSD problem for comparing spatial and orientation-frame data in quaternion-accessible domains, and we examined the nature of the solutions for the eigensystems of the 3D spatial RMSD problem, as well as the corresponding 3D quaternion orientation-frame alignment problem (QFA). Extensions of both the translation and rotation alignment problems and their solutions to 4D are detailed in the Supplementary Material. We also examined solutions for the combined 3D spatial and orientation-frame RMSD problem, arguing that a simple quaternion interpolation between the two individual solutions may well be sufficient for most purposes.

A The 3D Euclidean Space Least Squares Matching Function

This appendix works out the details of the long-form least squares distance measure for the 3D Euclidean alignment problem using the method of Hebert and Faugeras [Faugeras and Hebert, 1983, Hebert, 1983, Faugeras and Hebert, 1986]. Starting with the 3D Euclidean minimizing distance measure Eq. (9), we can exploit Eq. (5) for $R(q)$, along with Eq. (2), to produce an alternative quaternion eigenvalue problem whose *minimal* eigenvalue determines the eigenvector q_{opt} specifying the matrix that rotates the test data into closest correspondence with the reference data.

Adopting the convenient notation $\mathbf{x} = (0, x_1, x_2, x_3)$ for a pure imaginary quaternion, we employ the following steps:

$$\begin{aligned}
 \mathbf{S}_3 &= \sum_{k=1}^N \|R_3(q) \cdot x_k - y_k\|^2 \\
 &= \sum_{k=1}^N \|q \star \mathbf{x}_k \star \bar{q} - \mathbf{y}_k\|^2 = \sum_{k=1}^N \|q \star \mathbf{x}_k \star \bar{q} - \mathbf{y}_k\|^2 \|q\|^2 \\
 &= \sum_{k=1}^N \|q \star \mathbf{x}_k - \mathbf{y}_k \star q\|^2 \quad \text{by Eq. (2)} \\
 &= \sum_{k=1}^N \|A(\mathbf{x}_k, \mathbf{y}_k) \cdot q\|^2 = \sum_{k=1}^N q \cdot A_k^t \cdot A_k \cdot q \\
 &= \sum_{k=1}^N q \cdot B_k \cdot q = q \cdot B \cdot q.
 \end{aligned} \tag{54}$$

Here we may write, for each k , the matrix $A(\mathbf{x}_k, \mathbf{y}_k)$ as

$$A_k = \begin{bmatrix} 0 & -a_1 & -a_2 & -a_3 \\ a_1 & 0 & s_3 & -s_2 \\ a_2 & -s_3 & 0 & s_1 \\ a_3 & s_2 & -s_1 & 0 \end{bmatrix}_k \tag{55}$$

where, with “ a ” for “antisymmetric” and “ s ” for “symmetric,”

$$\begin{aligned}
 a_{\{1,2,3\}} &= \{x_1 - y_1, x_2 - y_2, x_3 - y_3\} \\
 s_{\{1,2,3\}} &= \{x_1 + y_1, x_2 + y_2, x_3 + y_3\}
 \end{aligned}$$

and, again for each k ,

$$B_k = A_k^t \cdot A_k = \begin{bmatrix} a_1^2 + a_2^2 + a_3^2 & a_3 s_2 - a_2 s_3 & a_1 s_3 - a_3 s_1 & a_2 s_1 - a_1 s_2 \\ a_3 s_2 - a_2 s_3 & a_1^2 + s_2^2 + s_3^2 & a_1 a_2 - s_1 s_2 & a_1 a_3 - s_1 s_3 \\ a_1 s_3 - a_3 s_1 & a_1 a_2 - s_1 s_2 & a_2^2 + s_1^2 + s_3^2 & a_2 a_3 - s_2 s_3 \\ a_2 s_1 - a_1 s_2 & a_1 a_3 - s_1 s_3 & a_2 a_3 - s_2 s_3 & a_3^2 + s_1^2 + s_2^2 \end{bmatrix}_k, \tag{56}$$

and $B = \sum_{k=1}^N B_k$. Since, using the full squared-difference minimization measure Eq. (9) requires the global minimal value, the solution for the optimal quaternion in Eq. (54) is the eigenvector of the *minimal* eigenvalue of B in Eq. (56). This is the approach used by Faugeras and Hebert in the earliest application of the quaternion method to scene alignment of which we are aware. While it is important to be aware of this alternative method, in the main text, we have found it more useful, to focus on the alternate form exploiting only the non-constant cross-term appearing in Eq. (9), as does most of the recent molecular structure literature. The cross-term requires the determination of the *maximal* eigenvalue rather than the *minimal* eigenvalue of the corresponding data matrix. Direct numerical calculation verifies that, though the minimal eigenvalue of Eq. (56) differs from

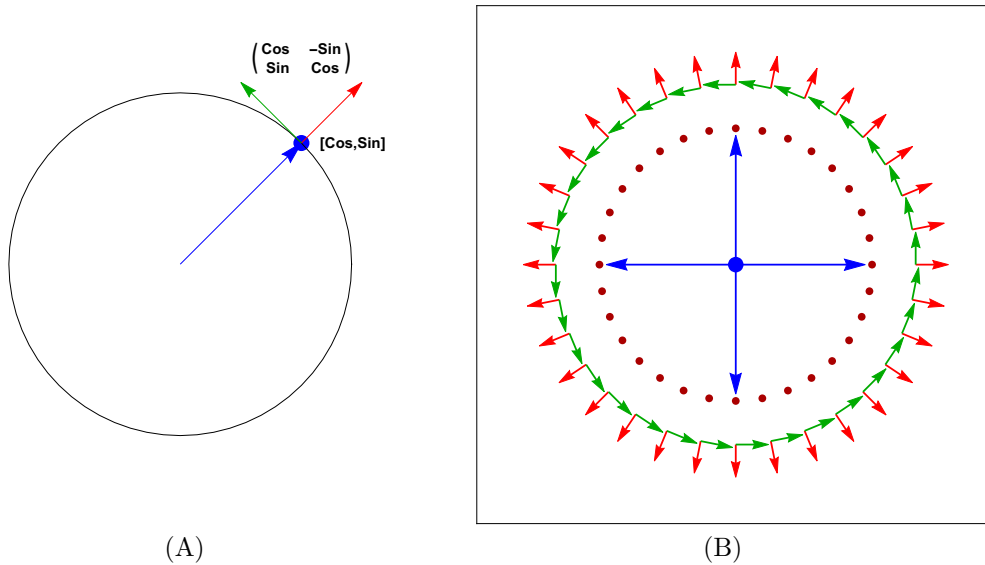


Figure 10: (A) Any standard 2D coordinate frame corresponds to the columns of an ordinary rotation matrix, and is associated to the point $(\cos \theta, \sin \theta)$ on a unit circle. (B) The standard 2D coordinate frames associated with a sampling of the entire circle of points $(\cos \theta, \sin \theta)$.

the maximal eigenvalue of the cross-term approach, the exact same optimal eigenvector is obtained, a result that can presumably be proven algebraically but that we will not need to pursue here.

B Introduction to Quaternion Orientation Frames

What is a Quaternion Frame? We will first present a bit of intuition about coordinate frames that may help some readers with our terminology. If we take the special case of a quaternion representing a rotation in the 2D (x, y) plane, the 3D rotation matrix Eq. (5) reduces to the standard right-handed 2D rotation

$$R_2(\theta) = \begin{bmatrix} \cos \theta & -\sin \theta \\ \sin \theta & \cos \theta \end{bmatrix}. \quad (57)$$

As shown in Fig 10(A), we can use θ to define a unit direction in the complex plane defined by $z = \exp i\theta$, and then the *columns* of the matrix $R_2(\theta)$ naturally correspond to a unique associated 2D coordinate frame diad; an entire collection of points z and their corresponding frame diads are depicted in Fig. 10(B).

Starting from this context, we can get a clear intuitive picture of what we mean by a “quaternion frame” before diving into the quaternion RMSD problem. The essential step is to look again at Eq. (5) for $n_x = 1$, and write the corresponding quaternion as $(a, b, 0, 0)$ with $a^2 + b^2 = 1$, so this is a “2D quaternion,” and is indistinguishable from a complex phase like $z = \exp i\theta$ that we just introduced. There is one significant difference, however, and that is that Eq. (5) shows us that

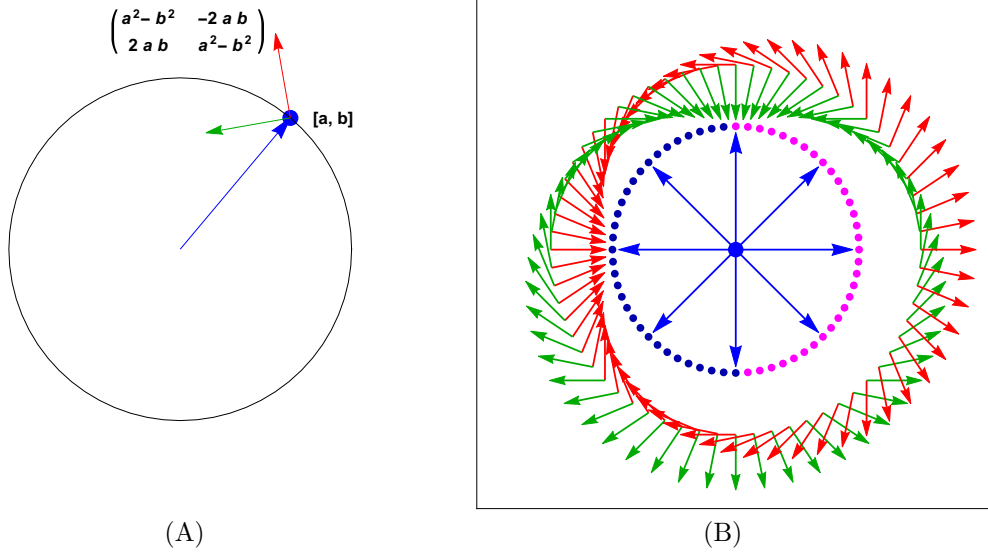


Figure 11: (A) The quaternion point (a, b) , in contrast, corresponds via the double-angle formula to coordinate frames that rotate twice as rapidly as (a, b) progresses around the unit circle that is a simplified version of quaternion space. (B) The set of 2D frames associated with the entire frame of quaternion points (a, b) ; each diametrically opposite point corresponds to an identical frame. For later use in displaying full quaternions, we show how color coding can be used to encode the sign of one of the coordinates on the circle.

$R_2(\theta)$ takes a new form, quadratic in a and b ,

$$R_2(a, b) = \begin{bmatrix} a^2 - b^2 & -2ab \\ 2ab & a^2 - b^2 \end{bmatrix}. \quad (58)$$

Using either the formula Eq. (7) for $q(\theta, \hat{\mathbf{n}})$ or just exploiting the trigonometric double angle formulas, we see that Eq. (57) and Eq. (58) correspond and that

$$(a, b) = (\cos(\theta/2), \sin(\theta/2)) \quad (59)$$

$$u = (a + ib) = \sqrt{z} = e^{i\theta/2}. \quad (60)$$

Our simplified 2D quaternion thus describes the *square root* of the usual Euclidean frame given by the columns of $R_2(\theta)$. Thus the pair (a, b) (the reduced quaternion) itself corresponds to a frame. In Fig. 11(A), we show how a given “quaternion frame,” i.e., the columns of $R_2(a, b)$, corresponds to a point $u = a + ib$ in the complex plane. Diametrically *opposite* points (a, b) and $(-a, -b)$ now correspond to the *same* frame! Fig. 11(B) shows the corresponding frames for a large collection of points (a, b) in the complex plane, and we see the new and unfamiliar feature that the frames make *two* full rotations on the complex circle instead of just one as in Fig. 10(B).

This is what we have to keep in mind as we now pass to using a full quaternion to represent an arbitrary 3D frame triad via Eq. (5). The last step is to notice that in Fig 11(B) we can represent the set of frames in one half of the complex circle, $a \geq 0$ shown in magenta, as distinct from those in the other half, $a < 0$ shown in dark blue; for any value of b , the vertical axis, there is a *pair* of

a 's with opposite signs and colors. In the quaternion case, we can display quaternion frames inside one single sphere, like displaying only the b coordinates in Fig 11(B) projected to the vertical axis, realizing that if we know the sign-correlated coloring, we can determine both the magnitude of the dependent variable $a = \pm\sqrt{1-b^2}$ as well as its sign. The same holds true in the general case: if we display only a quaternion's 3-vector part $\mathbf{q} = (q_x, q_y, q_z)$ along with a color specifying the sign of q_0 , we implicitly know both the magnitude and sign of $q_0 = \pm\sqrt{1-q_x^2-q_y^2-q_z^2}$, and such a 3D plot therefore accurately depicts *any* quaternion. Another alternative employed in the main text is to use *two* solid balls, one a "northern hemisphere" for the $q_0 \geq 0$ components and the other a "southern hemisphere" for the $q_0 < 0$ components. Each may be useful in different contexts.

Example. We illustrate all this in Fig 12(A), which shows a typical collection of quaternion reference-frame data displaying only the \mathbf{q} components of (q_0, \mathbf{q}) ; the $q_0 \geq 0$ data are mixed with the $q_0 < 0$ data, but are distinguished by their color coding. In Fig 12(B), we show the frame triads resulting from applying Eq. (5) to each quaternion point and plotting the result at the associated point \mathbf{q} in the display.

C On Obtaining Quaternions from Rotation Matrices

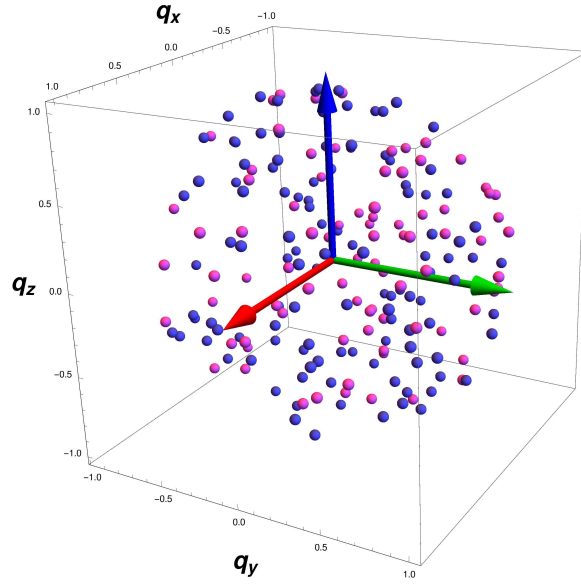
The quaternion RMSD profile matrix method can be used to implement a singularity-free algorithm to obtain the (sign-ambiguous) quaternions corresponding to numerical 3D and 4D rotation matrices. There are many existing approaches to the 3D problem in the literature (see, e.g., [Shepperd, 1978], [Shuster and Natanson, 1993], or Section 16.1 of [Hanson, 2006]). In contrast to these approaches, Bar-Itzhack [Bar-Itzhack, 2000] has observed, in essence, that if we simply replace the data matrix E_{ab} by a numerical 3D orthogonal rotation matrix R , the numeric quaternion q that corresponds to $R_{\text{numeric}} = R(q)$, as defined by Eq. (5), can be found by solving our familiar maximal quaternion eigenvalue problem. The initially unknown optimal matrix (technically its quaternion) computed by maximizing the similarity measure is equivalent to a single-element quaternion barycenter problem, and the construction is designed to yield a best approximation to R itself in quaternion form. To see this, take $S(r)$ to be the sought-for optimal rotation matrix, with its own quaternion r , that must maximize the Bar-Itzhack measure. We start with the Fröbenius measure describing the match of two rotation matrices corresponding to the quaternion r for the unknown quaternion and the numeric matrix R containing the known 3×3 rotation matrix data:

$$\begin{aligned} \mathbf{S}_{\text{BI}} &= \|S(r) - R\|_{\text{Frob}}^2 = \text{tr}([S(r) - R] \cdot [S^{\text{t}}(r) - R^{\text{t}}]) \\ &= \text{tr}(I_3 + I_3 - 2(S(r) \cdot R^{\text{t}})) \\ &= \text{const} - 2 \text{tr} S(r) \cdot R^{\text{t}} . \end{aligned}$$

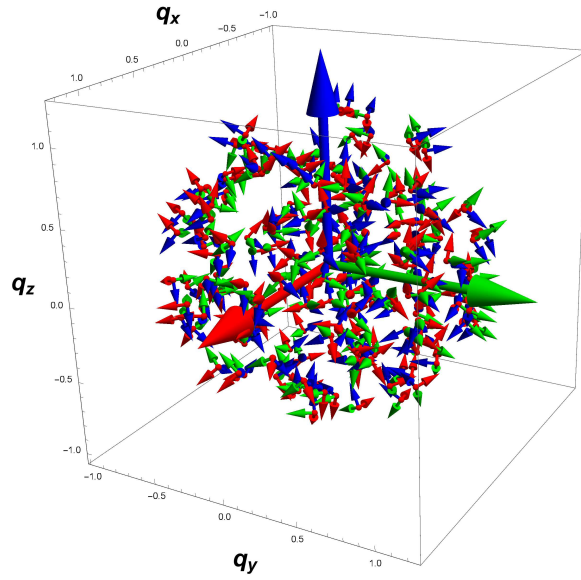
Pulling out the cross-term as usual and converting to a maximization problem over the unknown quaternion r , we arrive at

$$\Delta_{\text{BI}} = \text{tr} S(r) \cdot R^{\text{t}} = r \cdot K(R) \cdot r , \quad (61)$$

where R is (approximately) an orthogonal matrix of numerical data, and $K(R)$ is analogous to the profile matrix $M(E)$. Now S is an abstract rotation matrix, and R is supposed to be a good numerical approximation to a rotation matrix, and thus the product $T = S \cdot R^{\text{t}}$ should also be a good approximation to an $\mathbf{SO}(3)$ rotation matrix; hence that product itself corresponds closely to



(A)



(B)

Figure 12: (A) The 3D portions of the quaternion reference-frame data $q = (q_0, q_x, q_y, q_z)$, using different colors for $q_0 \geq 0$ and $q_0 < 0$ in the unseen direction. Since $|q_0| = \sqrt{q_x^2 + q_y^2 + q_z^2}$, the complete quaternion can in principle be determined from the 3D display. (B) The 3D orientation frame triads for each reference point (q_0, q_x, q_y, q_z) displayed at their associated $\mathbf{q} = (q_x, q_y, q_z)$.

some axis $\hat{\mathbf{n}}$ and angle θ , where (supposing we knew R 's exact quaternion q)

$$\text{tr } S(r) \cdot R^t(q) = \text{tr } T(r \star \bar{q}) = \text{tr } T(\theta, \hat{\mathbf{n}}) = 1 + 2 \cos \theta .$$

The maximum is obviously close to T being the identity matrix, with the ideal value at $\theta = 0$, corresponding to $S \approx R$. Thus if we find the maximal quaternion eigenvalue ϵ_{opt} of the profile matrix $K(R)$ in Eq. (61), our closest solution is well-represented by the corresponding normalized eigenvector r_{opt} ,

$$q = r_{\text{opt}} . \quad (62)$$

This numerical solution for q will correspond to the targeted numerical rotation matrix, solving the problem. To complete the details of the computation, we replace the elements E_{ab} in Eq. (13) by a general orthonormal rotation matrix with columns $\mathbf{X} = (x_1, x_2, x_3)$, \mathbf{Y} , and \mathbf{Z} , scaling by $1/3$, thus obtaining the special 4×4 profile matrix K whose elements in terms of a known numerical matrix $R = [\mathbf{X}|\mathbf{Y}|\mathbf{Z}]$ (transposed in the algebraic expression for K due to the R^t) are

$$K(R) = \frac{1}{3} \begin{bmatrix} x_1 + y_2 + z_3 & y_3 - z_2 & z_1 - x_3 & x_2 - y_1 \\ y_3 - z_2 & x_1 - y_2 - z_3 & x_2 + y_1 & x_3 + z_1 \\ z_1 - x_3 & x_2 + y_1 & -x_1 + y_2 - z_3 & y_3 + z_2 \\ x_2 - y_1 & x_3 + z_1 & y_3 + z_2 & -x_1 - y_2 + z_3 \end{bmatrix} . \quad (63)$$

Determining the algebraic eigensystem of Eq. (63) is a nontrivial task. However, as we know, any orthogonal 3D rotation matrix $R(q)$, or equivalently, $R^t(q) = R(\bar{q})$, can also be ideally expressed in terms of quaternions via Eq. (5), and this yields an alternate useful algebraic form

$$K(q) = \frac{1}{3} \begin{bmatrix} 3q_0^2 - q_1^2 - q_2^2 - q_3^2 & 4q_0q_1 & 4q_0q_2 & 4q_0q_3 \\ 4q_0q_1 & -q_0^2 + 3q_1^2 - q_2^2 - q_3^2 & 4q_1q_2 & 4q_1q_3 \\ 4q_0q_2 & 4q_1q_2 & -q_0^2 - q_1^2 + 3q_2^2 - q_3^2 & 4q_2q_3 \\ 4q_0q_3 & 4q_1q_3 & 4q_2q_3 & -q_0^2 - q_1^2 - q_2^2 + 3q_3^2 \end{bmatrix} \quad (64)$$

This equation then allows us to quickly prove that K has the correct properties to solve for the appropriate quaternion corresponding to R . First we note that the coefficients p_n of the eigensystem are simply constants,

$$p_1 = 0 \quad p_2 = -\frac{2}{3} \quad p_3 = -\frac{8}{27} \quad p_4 = -\frac{1}{27} .$$

Computing the eigenvalues and eigenvectors using the symbolic quaternion form, we see that the eigenvalues are constant, with maximal eigenvalue exactly one, and the eigenvectors are almost trivial, with the maximal eigenvector being the quaternion q that corresponds to the (numerical) rotation matrix:

$$\epsilon = \left\{ 1, -\frac{1}{3}, -\frac{1}{3}, -\frac{1}{3} \right\} \quad (65)$$

$$r = \left\{ \begin{bmatrix} q_0 \\ q_1 \\ q_2 \\ q_3 \end{bmatrix}, \begin{bmatrix} -q_1 \\ q_0 \\ 0 \\ 0 \end{bmatrix}, \begin{bmatrix} -q_2 \\ 0 \\ q_0 \\ 0 \end{bmatrix}, \begin{bmatrix} -q_3 \\ 0 \\ 0 \\ q_0 \end{bmatrix} \right\} . \quad (66)$$

The first column is the quaternion r_{opt} , with $\Delta_{\text{BI}}(r_{\text{opt}}) = 1$. (This would be 3 if we had not divided by 3 in the definition of K .)

Alternate version. From the quaternion barycenter work of Markley et al. [Markley et al., 2007] and the natural form of the quaternion-extraction problem in 4D in the Supplementary Material, we know that Eq. (64) actually has a much simpler form with the same unit eigenvalue and natural quaternion eigenvector. If we simply take Eq. (64) multiplied by 3, add the constant term $I_4 = (q_0^2 + q_1^2 + q_2^2 + q_3^2)I_4$, and divide by 4, we get a more compact quaternion form of the matrix, namely

$$K'(q) = \begin{bmatrix} q_0^2 & q_0q_1 & q_0q_2 & q_0q_3 \\ q_0q_1 & q_1^2 & q_1q_2 & q_1q_3 \\ q_0q_2 & q_1q_2 & q_2^2 & q_2q_3 \\ q_0q_3 & q_1q_3 & q_2q_3 & q_3^2 \end{bmatrix}. \quad (67)$$

This has vanishing determinant and trace $\text{tr } K' = 1 = -p_1$, with all other p_k coefficients vanishing, and leading eigensystem identical to Eq. (64):

$$\epsilon = \{1, 0, 0, 0\} \quad (68)$$

$$r = \left\{ \begin{bmatrix} q_0 \\ q_1 \\ q_2 \\ q_3 \end{bmatrix}, \begin{bmatrix} -q_1 \\ q_0 \\ 0 \\ 0 \end{bmatrix}, \begin{bmatrix} -q_2 \\ 0 \\ q_0 \\ 0 \end{bmatrix}, \begin{bmatrix} -q_3 \\ 0 \\ 0 \\ q_0 \end{bmatrix} \right\}. \quad (69)$$

As elegant as this is, in practice, our numerical input data are from the 3×3 matrix R itself, and not the quaternions, so we will almost always just use those numbers in Eq. (63) to solve the problem.

Completing the solution. In typical applications, *the solution is immediate, requiring only trivial algebra.* The maximal eigenvalue is always known in advance to be unity for any valid rotation matrix, so we need only to compute the eigenvector from the numerical matrix Eq. (63) with unit eigenvalue. We simply compute any column of the adjugate matrix of $[K(R) - I_4]$, or solve the equivalent linear equations of the form

$$(K(R) - 1 * I_4) \cdot \begin{bmatrix} 1 \\ v_1 \\ v_2 \\ v_3 \end{bmatrix} = 0 \quad q = r_{\text{opt}} = \text{normalize} \begin{bmatrix} 1 \\ v_1 \\ v_2 \\ v_3 \end{bmatrix}. \quad (70)$$

As always, one may need to check for degenerate special cases.

Non-ideal cases. It is important to note, as emphasized by Bar-Itzhack, that if there are *significant errors* in the numerical matrix R , then the actual non-unit maximal eigenvalue of $K(R)$ can be computed numerically or algebraically as usual, and then that eigenvalue's eigenvector determines the *closest* normalized quaternion to the errorful rotation matrix, which can be very useful since such a quaternion always produces a valid rotation matrix.

In any case, *up to an overall sign*, r_{opt} is the desired numerical quaternion q corresponding to the target numerical rotation matrix $\hat{R} = R(q)$. In some circumstances, one is looking for a uniform statistical distribution of quaternions, in which case the overall sign of q should be chosen *randomly*.

The Bar-Itzhack approach solves the problem of extracting the quaternion of an arbitrary numerical 3D rotation matrix in a fashion that involves no singularities and only trivial testing for special cases, thus essentially making the traditional methods obsolete. The extension of Bar-Itzhack’s method to the case of 4D rotations is provided in the Supplementary Material.

D On Defining the Quaternion Barycenter

The notion of a *Riemannian Barycenter* is generally associated with the work of [Grove et al., 1974], and may also be referred to as the *Karcher mean* [Karcher, 1977], defined as the point that minimizes the sum of squared geodesic distances from the elements of a collection of fixed points on a manifold. The general class of such optimization problems has also been studied, e.g., by [Manton, 2004]. We are interested here in the case of quaternions, which we know are points on the spherical 3-manifold \mathbf{S}^3 defined by the unit-quaternion subspace of \mathbb{R}^4 restricted to $q \cdot q = 1$ for any point q in \mathbb{R}^4 . This subject has been investigated by a number of authors, with Brown and Worsley [Brown and Worsley, 1992] discussing the problems with this computation in 1992, and Buss and Fillmore [Buss and Fillmore, 2001] proposing a solution applicable to computer graphics 3D orientation interpolation problems in 2001, inspired to some extent by Shoemake’s 1985 introduction of the quaternion *slerp* as a way to perform geodesic orientation interpolations in 3D using Eq. (5) for $R(q)$. There are a variety of methods and studies related to the quaternion barycenter problem. In 2002, Moahker published a rigorous account on averaging in the group of rotations [Moahker, 2002], while subsequent treatments included the 2007 work by Markley et al. [Markley et al., 2007], focusing on aerospace and astronomy applications, and the comprehensive review in 2013 by Hartley et al. [Hartley et al., 2013], aimed in particular at the machine vision and robotics community, with additional attention to conjugate rotation averaging (the “hand-eye calibration” problem in robotics), and multiple rotation averaging. While we have focused on measures starting from sums of squares that lead to closed form optimization problems, [Hartley et al., 2011] have carefully studied the utility of the corresponding L_1 norm and the iterative Weiszfeld algorithm for finding its optimal solution numerically.

The task at hand is basically to extend the Bars-Itzhack algorithm to an entire collection of frames instead of a single rotation. We need to find an optimal rotation matrix $R(q)$ that corresponds to the quaternion point closest to the geodesic center of an *unordered* set of reference data. We already know that the case of the “barycenter” of a single orientation frame is solved by the Bars-Itzhack algorithm of Appendix C, which finds the quaternion closest to a single item of rotation matrix data (the quaternion barycenter of a single rotation is itself). For two items of data, $R_1 = R(q_1)$ and $R_2 = R(q_2)$, the quaternion barycenter is determined by the *slerp* interpolator to be

$$q(q_1, q_2)_{\text{barycenter}} = q_1 \star (\bar{q}_1 \star q_2)^{1/2} = \text{slerp} \left(q_1, q_2, \frac{1}{2} \right).$$

For three or more items, no closed form is currently known.

We start with a data set of N rotation matrices $R(p_k)$ that are represented by the quaternions p_k , and we want $R(q)$ to be as close as possible to the set of $R(p_k)$. That rotation matrix, or its associated quaternion point, are the orientation frame analogs of the Euclidean barycenter for a set of Euclidean points. As before, it is clear that the mathematically most justifiable measure employs the *geodesic arclength* on the quaternion sphere; but to the best of anyone’s knowledge,

there is no way to apply linear algebra to find the corresponding $R(q_{\text{opt}})$. Achieving a numerical solution to that problem is the task solved by Buss and Fillmore [Buss and Fillmore, 2001], as well as a number of others, including, e.g., [Moakher, 2002, Markley et al., 2007, Hartley et al., 2013]. The problem that we can understand algebraically is, once again, the approximate *chord measure*, which we can immediately formulate in a sign-insensitive fashion using the Fröbenius measure $\|M\|^2 = \text{tr}(M \cdot M^t)$, giving us the following starting point:

$$\left. \begin{aligned} \mathbf{S}_{\text{barycenter}}(q) &= \sum_{k=1}^N \|R(q) - R(p_k)\|^2 \\ &= \sum_{k=1}^N \text{tr}([R(q) - R(p_k)] \cdot [R^t(q) - R^t(p_k)]) \\ &= \sum_{k=1}^N \text{tr}(2I_4 - 2R(q) \cdot R^t(p_k)) \\ &= \sum_{k=1}^N (8 - 2\text{tr} R(q) \cdot R(\bar{p}_k)) \end{aligned} \right\}. \quad (71)$$

Dropping the constants and converting as usual to maximize over the cross-term instead of minimizing the distance measure, we define a tentative spherical barycenter as the maximum of the variation over the quaternion q of the following:

$$\left. \begin{aligned} \Delta_{\text{trial barycenter}}(q) &= \frac{1}{4} \sum_{k=1}^N \text{tr}(R(q) \cdot R(\bar{p}_k)) \\ &= \sum_{k=1}^N q \cdot K_k(p) \cdot q \end{aligned} \right\}, \quad (72)$$

where for each $k = 1, \dots, N$, our first guess at the profile matrix is

$$K_k(p)_{\text{trial}} = \frac{1}{4} \begin{bmatrix} 3p_0^2 - p_1^2 - p_2^2 - p_3^2 & 4p_0p_1 & 4p_0p_2 & 4p_0p_3 \\ 4p_0p_1 & -p_0^2 + 3p_1^2 - p_2^2 - p_3^2 & 4p_1p_2 & 4p_1p_3 \\ 4p_0p_2 & 4p_1p_2 & -p_0^2 - p_1^2 + 3p_2^2 - p_3^2 & 4p_2p_3 \\ 4p_0p_3 & 4p_1p_3 & 4p_2p_3 & -p_0^2 - p_1^2 - p_2^2 + 3p_3^2 \end{bmatrix} \quad (73)$$

But if, as pointed out by [Markley et al., 2007], we simply add one copy of the identity matrix in the form $(1/4)I_4 = (1/4)(p_0^2 + p_1^2 + p_2^2 + p_3^2)I_4$ to the matrix $K(p)$, we get a much simpler matrix that we can use instead because constants do not affect the optimization process. Our partial profile matrix for each $k = 1, \dots, N$ is now

$$K_k(p) = \begin{bmatrix} p_0^2 & p_0p_1 & p_0p_2 & p_0p_3 \\ p_0p_1 & p_1^2 & p_1p_2 & p_1p_3 \\ p_0p_2 & p_1p_2 & p_2^2 & p_2p_3 \\ p_0p_3 & p_1p_3 & p_2p_3 & p_3^2 \end{bmatrix}, \quad (74)$$

or to be precise, after the sum over k , the profile matrix in terms of the quaternion columns $[p_k]$ becomes of \mathbf{P}

$$K(\mathbf{P})_{ab} = \sum_{k=1}^N [p_k]_a [p_k]_b = [\mathbf{P} \cdot \mathbf{P}^t]_{ab} \quad (75)$$

with quaternion indices (a, b) ranging from 0 to 3. Finally, we can write the expression for the chord-based barycentric measure to be optimized to get q_{opt} as

$$\Delta_{\text{barycenter}}(q) = q \cdot K(\mathbf{P}) \cdot q. \quad (76)$$

We also have another option: if, for some reason, we only have numerical 3×3 rotation matrices R_k and not their associated quaternions p_k , we can recast Eq. (72) in terms of Eq. (63) for each matrix R_k , and use the sum over k of *those* numerical matrices to extract our optimal quaternion. This is nontrivial because the simple eigensystem form of the profile matrix K for the Bar-Itzhack task was valid only for *one* rotation data matrix, and as soon as we start summing over additional matrices, all of that simplicity disappears, though the eigensystem problem remains intact.

The optimizing the approximate chord-measure for the “average rotation,” the “quaternion average,” or the spherical barycenter of the quaternion orientation frame data set $\{p_k\}$ (or $\{R_k\}$) now just reduces, as before, to finding the (normalized) eigenvector corresponding to the largest eigenvalue of K . It is also significant that the initial K_{trial} matrix in Eq. (73) is *traceless*, and so the traceless algebraic eigenvalue methods would apply, while the simpler K matrix in Eq. (75) is *not traceless*, and thus, in order to apply the algebraic eigenvalue method, we would have to use the generalization presented in the Supplementary Material that includes an arbitrary trace term.

Acknowledgments

We thank Sonya M. Hanson for reacquainting us with this problem, providing much useful information and advice, and for motivating us to pursue this challenging investigation to its conclusion. We also express our appreciation to the referees for suggestions that added significantly to the completeness and scope of the paper and to Randall Bramley, Roger Germundsson, B. K. P. Horn, and Michael Trott for their valuable input.

References

- [Abramowitz and Stegun, 1970] Abramowitz, M. and Stegun, I. (1970). *Handbook of mathematical functions*. Dover Publications Inc., New York. Pages 17–18.
- [Arun et al., 1987] Arun, K. S., Huang, T. S., and Blostein, S. D. (1987). Least-squares fitting of two 3D point sets. *IEEE Trans. Pattern Anal. Machine Intell.*, PAMI-9(5):698–700.
- [Bar-Itzhack, 2000] Bar-Itzhack, I. Y. (2000). New method for extracting the quaternion from a rotation matrix. *Journal of Guidance, Control, and Dynamics*, 23(6):1085–1087.
- [Bell, 2008] Bell, J. (1733(2008)). A conjecture on the forms of the roots of equations. *An English translation of Euler’s De formis radicum aequationum cujusque ordinis conjectatio*.
- [Boyer and Merzbach, 1991] Boyer, C. B. and Merzbach, U. C. (1991). *A History of Mathematics*. Wiley, New York, 2nd edition.
- [Brown and Worsey, 1992] Brown, J. and Worsey, A. (1992). Problems with defining barycentric coordinates for the sphere. *Mathematical Modelling and Numerical analysis*, 26:37–49.
- [Buchholz and Sommer, 2005] Buchholz, S. and Sommer, G. (2005). On averaging in clifford groups. *Computer Algebra and Geometric Algebra With Applications*, pages 229–238.

- [Buss and Fillmore, 2001] Buss, S. R. and Fillmore, J. P. (2001). Spherical averages and applications to spherical splines and interpolation. *ACM Transactions on Graphics (TOG)*, 20(2):95–126.
- [Cliff, 1966] Cliff, N. (1966). Orthogonal rotation to congruence. *Psychometrika*, 31:33–42.
- [Coutsias et al., 2004] Coutsiias, E., Seok, C., and Dill, K. (2004). Using quaternions to calculate RMSD. *J Comput Chem.*, 25(15):1849–1857.
- [Coutsias and Wester, 2019] Coutsiias, E. and Wester, M. (2019). Rmsd and symmetry. *J Comput Chem.*, 40(15):1496–1508.
- [Davenport, 1968] Davenport, P. (1968). A vector approach to the algebra of rotations with applications. Technical Report TN D-4696, NASA: Goddard Space Flight Center, Greenbelt, Maryland.
- [Denton et al., 2019] Denton, P. B., Park, S. J., Tao, T., and Zhang, X. (2019). Eigenvectors from eigenvalues: A survey of a basic identity in linear algebra.
- [Descartes, 1954] Descartes, R. (1637(1954)). *Book III: On the construction of solid and supersolid problems, The Geometry of René Descartes*. Dover, facsimile of the first edition.
- [Diamond, 1988] Diamond, R. (1988). A note on the rotational superposition problem. *Acta Crystallogr.*, A44:211–216.
- [Euler, 1733] Euler, L. (1733). De formis radicum aequationum cujusque ordinis conjectatio. *Commentarii academiae scientiarum imperialis Petropolitanae*, 6:216–231.
- [Faugeras and Hebert, 1983] Faugeras, O. and Hebert, M. (1983). A 3D recognition and positioning algorithm using geometrical constraints between primitive surfaces. In *Proc. 8th Joint Conf. on Artificial Intell.*, IJCAI’83, pages 996–1002. Morgan Kaufmann.
- [Faugeras and Hebert, 1986] Faugeras, O. and Hebert, M. (1986). The representation, recognition, and locating of 3D objects. *International Journal of Robotic Research (IJRR)*, 5:27–52.
- [Flower, 1999] Flower, D. (1999). Rotational superposition: a review of methods. *J. Mol. Graph. Model.*, 17:238–244.
- [Fogolari et al., 2016] Fogolari, F., Fomthum, C. J. D., Fortuna, S., Soler, M. A., Corazza, A., and Esposito, G. (2016). Accurate estimation of the entropy of rotationtranslation probability distributions. *Journal of Chemical Theory and Computation*, 12(1):1–8. PMID: 26605696.
- [Gibson, 1960] Gibson, W. (1960). Orthogonal from oblique transformations. *Educational and Psychological Measurement*, 20(4):713–721.
- [Golub and van Loan, 1983] Golub, G. and van Loan, C. (1983). *Matrix Computations*. Johns Hopkins University Press, Baltimore, MD, 1st edition. Sec 12.4.
- [Green, 1952] Green, B. F. (1952). The orthogonal approximation of an oblique structure in factor analysis. *Psychometrika*, 17:429–440.
- [Grove et al., 1974] Grove, K., Karcher, H., and Ruh, E. A. (1974). Jacobi fields and Finsler metrics on compact Lie groups with an application to differentiable pinching problem. *Math. Ann.*, 211:7–21.

- [Hanson, 2006] Hanson, A. J. (2006). *Visualizing Quaternions*. Morgan-Kaufmann/Elsevier.
- [Hanson and Thakur, 2012] Hanson, A. J. and Thakur, S. (2012). Quaternion maps of global protein structure. *Jour. Molec. Graphics and Modelling*, 38:256–278.
- [Hartley et al., 2011] Hartley, R., Aftab, K., and Trumpf, J. (2011). L1 rotation averaging using the Weiszfeld algorithm. In *Proceedings of the IEEE Computer Society Conference on Computer Vision and Pattern Recognition*, pages 3041–3048.
- [Hartley et al., 2013] Hartley, R., Trumpf, J., Dai, Y., and Li, H. (2013). Rotation averaging. *Int. J. Comput. Vis.*, 103(3):267–305.
- [Havel and Najfeld, 1994] Havel, T. and Najfeld, I. (1994). Applications of geometric algebra to the theory of molecular conformation. Part 1. The optimum alignment problem. *J. Mol. Struct.*, 308:241–262.
- [Hebert, 1983] Hebert, M. (1983). Reconnaissance de formes tridimensionnelles. Ph. D. thesis, University of Paris South. Available as INRIA Tech. Rep. ISBN 2-7261-0379-0.
- [Horn et al., 1988] Horn, B. K., Hilden, H. M., and Negahdaripour, S. (1988). Closed-form solution of absolute orientation using orthonormal matrices. *J. Opt. Soc. Am. A*, 5(7):1127–1136.
- [Horn, 1987] Horn, B. K. P. (1987). Closed-form solution of absolute orientation using unit quaternions. *J. Opt. Soc. Am. A*, 4:629–642.
- [Huang et al., 1986] Huang, T. S., Blostein, S. D., and Margerum, E. A. (1986). Least-squares estimation of motion parameters from 3D point correspondences. In *Proc. IEEE Conf. Computer Vision and Pattern Recognition*, pages 24–26. IEEE Computer Society.
- [Huggins, 2014a] Huggins, D. J. (2014a). Comparing distance metrics for rotation using the k-nearest neighbors algorithm for entropy estimation. *J. Comput. Chem.*, 35:377–385. His eq (14) is $\sqrt{2}$ theta, Eq (15) is just theta.
- [Huggins, 2014b] Huggins, D. J. (2014b). Estimating translational and orientational entropies using the k-nearest neighbors algorithm. *J. Chem. Theory Comput.*, 10:3617–3625.
- [Huynh, 2009] Huynh, D. Q. (2009). Metrics for 3d rotations: Comparison and analysis. *J. Math. Imaging Vis.*, 35(2):155–164.
- [Jupp and Kent, 1987] Jupp, P. and Kent, J. (1987). Fitting smooth paths to spherical data. *Appl. Statist.*, 36:34–46.
- [Kabsch, 1976] Kabsch, W. (1976). A solution for the best rotation to relate two sets of vectors. *Acta Crystallogr.*, A32:922–923.
- [Kabsch, 1978] Kabsch, W. (1978). A discussion of the solution for the best rotation to relate two sets of vectors. *Acta Crystallogr.*, A34:827–828.
- [Karcher, 1977] Karcher, H. (1977). Riemannian center of mass and mollifier smoothing. *Comm. on Pure and Applied Mathematics*, 30(5):509–541.

- [Kearsley, 1990] Kearsley, S. (1990). An algorithm for the simultaneous superposition of a structural series. *J. Comput. Chem.*, 11:1187–1192.
- [Kearsley, 1989] Kearsley, S. K. (1989). On the orthogonal transformation used for structural comparisons. *Acta Crystallogr.*, A45(2):208–210.
- [Kneller, 1991] Kneller, G. R. (1991). Superposition of molecular structures using quaternions. *Molecular Simulation*, 7(1–2):113–119.
- [Lesk, 1986] Lesk, A. (1986). A toolkit for computational molecular biology 2. On the optimal superposition of 2 sets of coordinates. *Acta Cryst.*, A42:110–113.
- [Liu et al., 2010] Liu, P., Agrafiotis, D. K., and Theobald, D. L. (2010). Fast determination of the optimal rotational matrix for macromolecular superpositions. *J. Comput. Chem.*, 31:1561–1563.
- [MacLachlan, 1982] MacLachlan, A. (1982). Rapid comparison of protein structures. *Acta Crystallogr.*, A38:871–873.
- [Manton, 2004] Manton, J. (2004). A globally convergent numerical algorithm for computing the centre of mass on compact Lie groups. In *Proc. 8th Intern. Conf. on Control, Automation, Robotics, and Vision*, pages 2211–2216, Kunming, China.
- [Markley, 1988] Markley, F. L. (1988). Attitude determination using vector observations and the singular value decomposition. *Journal of the Astronautical Sciences*, 38(2):245–258.
- [Markley et al., 2007] Markley, F. L., Cheng, Y., Crassidis, J. L., and Oshman, Y. (2007). Averaging quaternions. *J. Guidance, Control, & Dynamics*, 30(4):1193–1197.
- [Markley and Mortari, 2000] Markley, F. L. and Mortari, D. (2000). Quaternion attitude estimation using vector observations. *Journal of the Astronautical Sciences*, 48(2):359–380.
- [Moakher, 2002] Moakher, M. (2002). Means and averaging in the group of rotations. *SIAM J. Matrix Anal. Appl.*, 24(1):1–16.
- [Nickalls, 1993] Nickalls, R. (1993). A new approach to solving the cubic: Cardan’s solution revealed. *The Mathematical Gazette*, 77:354–359.
- [Nickalls, 2009] Nickalls, R. (2009). The quartic equation: invariants and Euler’s solution revealed. *The Mathematical Gazette*, 93:66–75.
- [Park and Ravani, 1997] Park, F. C. and Ravani, B. (1997). Smooth invariant interpolation of rotations. *ACM Trans. Graph.*, 16(3):277–295.
- [Sarlette and Sepulchre, 2009] Sarlette, A. and Sepulchre, R. (2009). Consensus optimization on manifolds. *SIAM Journal on Control and Optimization*, 48(1):56–76.
- [Schönemann, 1966] Schönemann, P. (1966). A generalized solution of the orthogonal procrustes problem. *Psychometrika*, 31:1–10.
- [Shepperd, 1978] Shepperd, S. W. (1978). Quaternion from rotation matrix. *Journal of Guidance and Control*, 1(3):223–224.

- [Shoemake, 1985] Shoemake, K. (1985). Animating rotation with quaternion curves. In *Computer Graphics*, volume 19, pages 245–254. Proceedings of SIGGRAPH 1985.
- [Shuster and Natanson, 1993] Shuster, M. D. and Natanson, G. A. (1993). Quaternion computation from a geometric point of view. *The Journal of the Astronautical Sciences*, 41(4):545–556.
- [Theobald, 2005] Theobald, D. (2005). Rapid calculation of RMSDs using a quaternion-based characteristic polynomial. *Acta Crystallogr.*, A61:478–480.
- [Umeyama, 1991] Umeyama, S. (1991). Least-squares estimation of transformation parameters between two point patterns. *IEEE Trans. Pattern Anal. Machine Intell.*, 13(4):376–380.
- [Wahba, 1965] Wahba, G. (1965). Problem 65-1, A least squares estimate of spacecraft attitude. *SIAM Review*, 7(3):409.
- [Weisstein, 2019a] Weisstein, E. W. (2019a). Cubic formula. <http://mathworld.wolfram.com/CubicFormula.html>. [Online; accessed 12-May-2019].
- [Weisstein, 2019b] Weisstein, E. W. (2019b). Quartic equation. <http://mathworld.wolfram.com/QuarticEquation.html>. [Online; accessed 12-May-2019].
- [Wikipedia:Cardano, 2019] Wikipedia:Cardano (2019). Ars Magna (Gerolamo Cardano) — Wikipedia, the free encyclopedia. [http://en.wikipedia.org/w/index.php?title=Ars%20Magna%20\(Gerolamo%20Cardano\)&oldid=873028064](http://en.wikipedia.org/w/index.php?title=Ars%20Magna%20(Gerolamo%20Cardano)&oldid=873028064). [Online; accessed 15-May-2019].
- [Wikipedia:Kabsch, 2018] Wikipedia:Kabsch (2018). Kabsch algorithm — Wikipedia, the free encyclopedia. <http://en.wikipedia.org/w/index.php?title=Kabsch%20algorithm&oldid=838166818>. [Online; accessed 22-August-2018].
- [Wikipedia:Wahba, 2018] Wikipedia:Wahba (2018). Wahba’s problem — Wikipedia, the free encyclopedia. <http://en.wikipedia.org/w/index.php?title=Wahba's%20problem&oldid=854401910>. [Online; accessed 22-August-2018].
- [Zhang, 2000] Zhang, Z. (2000). A flexible new technique for camera calibration. *IEEE Transactions on Pattern Analysis and Machine Intelligence*, 22:13301334.

Supplementary Material: The Quaternion-Based Spatial Coordinate and Orientation Frame Alignment Problems

Andrew J. Hanson
Luddy School of Informatics, Computing, and Engineering
Indiana University, Bloomington, Indiana, 47405, USA

Abstract

Supplementary material for the paper *The Quaternion-Based Spatial Coordinate and Orientation Frame Alignment Problems* is presented here. The most significant additional result is the extension of the 3D treatment in the main text to four dimensions. Following a review of quaternion properties now including the representation of 4D rotations using quaternion pairs, we give a detailed study of the 4D quaternion-based spatial alignment problem, which is significantly different from the 3D problem in the main text. Next, we use the 4D quaternion rotation method to extend our treatment to 4D orientation-frame alignment. The 3D Bar-Itzhak profile-matrix method for extracting a quaternion from a 3D numerical rotation matrix is extended to 4D numerical rotation matrices, followed by a look at the algebraic solutions of 2D alignment problems, whose deceptive simplicity does not carry over to the 3D and 4D cases. Finally, we supplement the 3D orientation alignment section of the main text with careful studies of the properties, limitations, and features of our 3D orientation frame alignment methods, followed by an extended exposition and analysis of the strengths and weaknesses of the 6DOF combined spatial and orientation frame alignment techniques. The Appendix provides a comprehensive study of the quartic equation solutions to eigenvalue problems, focusing on applications to the eigensystems of real symmetric matrices.

1 Foundations of Quaternions for 3D and 4D Problems

We begin with a review of quaternion properties used in the 3D analysis, folding in some additional details, and then systematically add the extensions that are exploited to handle the 4D case. The treatment here is designed to be self-contained, repeating any relevant material from the main paper, thus avoiding any confusion involving cross-references to the main paper for equations and conceptual background.

Quaternions for 3D Analysis. We take a quaternion to be a point $q = (q_0, q_1, q_2, q_3) = (q_0, \mathbf{q})$ in 4D Euclidean space with unit norm, $q \cdot q = 1$ (see, e.g., [Hanson, 2006] for further details about quaternions). The last three terms, \mathbf{q} , play the role of a generalized imaginary number, so the conjugation operation is $\bar{q} = (q_0, -\mathbf{q})$. Quaternions obey a multiplication operation denoted by \star

and defined as follows:

$$q \star p = Q(q) \cdot p = \begin{bmatrix} q_0 & -q_1 & -q_2 & -q_3 \\ q_1 & q_0 & -q_3 & q_2 \\ q_2 & q_3 & q_0 & -q_1 \\ q_3 & -q_2 & q_1 & q_0 \end{bmatrix} \cdot \begin{bmatrix} p_0 \\ p_1 \\ p_2 \\ p_3 \end{bmatrix} = (q_0 p_0 - \mathbf{q} \cdot \mathbf{p}, q_0 \mathbf{p} + p_0 \mathbf{q} + \mathbf{q} \times \mathbf{p}), \quad (1)$$

where the orthonormal matrix $Q(q)$ is an alternative form of quaternion multiplication that explicitly demonstrates that the action of q on p by quaternion multiplication *literally* rotates the quaternion unit vector p in 4D Euclidean space. Another non-trivial matrix form of quaternion multiplication that is useful in some calculations is the left-acting matrix \tilde{Q} producing a *right* multiplication,

$$q \star p = \tilde{Q}(p) \cdot q = \begin{bmatrix} p_0 & -p_1 & -p_2 & -p_3 \\ p_1 & p_0 & p_3 & -p_2 \\ p_2 & -p_3 & p_0 & p_1 \\ p_3 & p_2 & -p_1 & p_0 \end{bmatrix} \cdot \begin{bmatrix} q_0 \\ q_1 \\ q_2 \\ q_3 \end{bmatrix}. \quad (2)$$

Choosing exactly one of the three imaginary components in both q and p to be nonzero gives back the classic complex algebra $(q_0 + iq_1)(p_0 + ip_1) = (q_0 p_0 - q_1 p_1) + i(q_0 p_1 + p_0 q_1)$, so there are three copies of the complex numbers embedded in the quaternion algebra; the difference is that in general the final term $\mathbf{q} \times \mathbf{p}$ changes sign if one reverses the order, making the quaternion product order-dependent, unlike the complex product. Quaternions also satisfy the nontrivial “multiplicative norm” relation

$$\|q\| \|p\| = \|q \star p\|, \quad (3)$$

where $\|q\|^2 = q \cdot q = \Re(q \star \bar{q})$, that uniquely characterizes the real, complex, quaternion, and octonion number systems comprising the Hurwitz algebras. Quaternions also obey a number of interesting scalar triple-product identities,

$$r \cdot (q \star p) = q \cdot (r \star \bar{p}) = \bar{r} \cdot (\bar{p} \star \bar{q}), \quad (4)$$

where the complex conjugate entries are the natural consequences of the sign changes occurring only in the (imaginary) 3D part.

Conjugating a vector $\mathbf{x} = (x, y, z)$ written as a purely “imaginary” quaternion $(0, \mathbf{x})$ by quaternion multiplication is isomorphic to the construction of a 3D Euclidean rotation $R(q)$ generating all possible elements of the special orthogonal group $\mathbf{SO}(3)$. If we compute

$$q \star (c, x, y, z) \star \bar{q} = (c, R_3(q) \cdot \mathbf{x}), \quad (5)$$

we see that only the purely imaginary part is affected, whether or not the arbitrary real constant $c = 0$. Collecting coefficients gives this fundamental form of an arbitrary 3D rotation expressed in terms of quaternions,

$$R_{ij}(q) = \left. \begin{aligned} & \delta_{ij} (q_0^2 - \mathbf{q}^2) + 2q_i q_j - 2\epsilon_{ijk} q_0 q_k \\ & \left[\begin{array}{ccc} q_0^2 + q_1^2 - q_2^2 - q_3^2 & 2q_1 q_2 - 2q_0 q_3 & 2q_1 q_3 + 2q_0 q_2 \\ 2q_1 q_2 + 2q_0 q_3 & q_0^2 - q_1^2 + q_2^2 - q_3^2 & 2q_2 q_3 - 2q_0 q_1 \\ 2q_1 q_3 - 2q_0 q_2 & 2q_2 q_3 + 2q_0 q_1 & q_0^2 - q_1^2 - q_2^2 + q_3^2 \end{array} \right] \end{aligned} \right\}, \quad (6)$$

where the mapping from q to $R_3(q)$ is two-to-one because $R_3(q) = R_3(-q)$. Note that $R(q)$ is a *proper* rotation, with determinant $\det R(q) = (q \cdot q)^3 = +1$, and that the identity quaternion $q_{\text{ID}} = (1, 0, 0, 0) \equiv q \star \bar{q}$ corresponds to the identity rotation matrix, as does $-q_{\text{ID}} = (-1, 0, 0, 0)$. The *columns* of $R(q)$ are exactly the needed quaternion representation of the *frame triad* describing the orientation of a body in 3D space, i.e., the columns are the vectors of the frame's local x , y , and z axes relative to an initial identity frame. Choosing the following parameterization preserving $q \cdot q = 1$ (with $\hat{\mathbf{n}} \cdot \hat{\mathbf{n}} = 1$),

$$q = (\cos(\theta/2), \hat{n}_1 \sin(\theta/2), \hat{n}_2 \sin(\theta/2), \hat{n}_3 \sin(\theta/2)) , \quad (7)$$

gives the ‘‘axis-angle’’ form of the rotation matrix,

$$R_3(q) = R_3(\theta, \hat{\mathbf{n}}) = \begin{bmatrix} \cos \theta + (1 - \cos \theta) \hat{n}_1^2 & (1 - \cos \theta) \hat{n}_1 \hat{n}_2 - \sin \theta \hat{n}_3 & (1 - \cos \theta) \hat{n}_1 \hat{n}_3 + \sin \theta \hat{n}_2 \\ (1 - \cos \theta) \hat{n}_1 \hat{n}_2 + \sin \theta \hat{n}_3 & \cos \theta + (1 - \cos \theta) \hat{n}_2^2 & (1 - \cos \theta) \hat{n}_2 \hat{n}_3 - \sin \theta \hat{n}_1 \\ (1 - \cos \theta) \hat{n}_1 \hat{n}_3 - \sin \theta \hat{n}_2 & (1 - \cos \theta) \hat{n}_2 \hat{n}_3 + \sin \theta \hat{n}_1 & \cos \theta + (1 - \cos \theta) \hat{n}_3^2 \end{bmatrix} . \quad (8)$$

This form of the 3D rotation exposes the fact that the direction $\hat{\mathbf{n}}$ is fixed, so $\hat{\mathbf{n}}$ is the lone real eigenvector of R_3 . Multiplying a quaternion p by the quaternion q to get a new quaternion $p' = q \star p$ simply *rotates* the 3Dframe corresponding to p by the matrix Eq. (6) written in terms of q , so

$$R_3(q \star p) = R_3(q) \cdot R_3(p) , \quad (9)$$

and this collapse of repeated rotation matrices into a single rotation matrix with a quaternion-product argument can be continued indefinitely.

Remark: *Eigensystem and properties of R_3 :* One of our themes is constructing and understanding eigensystems of interesting matrices, so here, as an aside, we expand the content of the previous paragraph to include some additional details. First, note that we have two ways of writing the 3D rotation, as $R_3(\theta, \hat{\mathbf{n}})$ and as $R_3(q)$. Thus there are two ways to write the eigenvalues, which we can compute to be

$$\left\{ \begin{array}{c} 1 \\ e^{i\theta} \\ e^{-i\theta} \end{array} \right\} \quad \left\{ \begin{array}{c} 1 \\ (q_0^2 - q_1^2 - q_2^2 - q_3^2 + 2iq_0 \sqrt{q_1^2 + q_2^2 + q_3^2}) \\ (q_0^2 - q_1^2 - q_2^2 - q_3^2 - 2iq_0 \sqrt{q_1^2 + q_2^2 + q_3^2}) \end{array} \right\} , \quad (10)$$

respectively, where the two columns are of course identical, but we have chosen expressions in q (along with an implicit choice of square root sign determining $\sin(\theta/2)$) that match exactly with the $R_3(q)$ eigenvectors. Those eigenvectors (unnormalized for notational clarity) can be written as:

$$\left\{ \begin{array}{l} \left[\begin{array}{c} n_1 \\ n_2 \\ n_3 \end{array} \right] \quad \left[\begin{array}{c} -in_2 - n_1n_3 \\ in_1 - n_2n_3 \\ n_1^2 + n_2^2 \end{array} \right] \quad \left[\begin{array}{c} +in_2 - n_1n_3 \\ -in_1 - n_2n_3 \\ n_1^2 + n_2^2 \end{array} \right] \\ \left[\begin{array}{c} q_1 \\ q_2 \\ q_3 \end{array} \right] \quad \left[\begin{array}{c} -q_1q_3 - iq_2\sqrt{q_1^2 + q_2^2 + q_3^2} \\ -q_2q_3 + iq_1\sqrt{q_1^2 + q_2^2 + q_3^2} \\ q_1^2 + q_2^2 \end{array} \right] \quad \left[\begin{array}{c} -q_1q_3 + iq_2\sqrt{q_1^2 + q_2^2 + q_3^2} \\ -q_2q_3 - iq_1\sqrt{q_1^2 + q_2^2 + q_3^2} \\ q_1^2 + q_2^2 \end{array} \right] \end{array} \right\} \quad (11)$$

where $\det R_4(p, q) = (p \cdot p)^2 (q \cdot q)^2$ and $\text{tr } R_4(p, q) = 4p_0q_0$. Since this is a quadratic form in p and q , the rotation is unchanged under $(p, q) \rightarrow (-p, -q)$, and the quaternions are again a double covering. If we set $p = q$, we recover a matrix that leaves the w component invariant, and is just the rotation Eq. (6) for the $\mathbf{x}_3 = (x, y, z)$ component. If we set $p = q_{\text{ID}}$, we find the interesting result that $R_4(q, q_{\text{ID}}) = Q(q)$ from Eq. (1), and $R_4(q_{\text{ID}}, \bar{p}) = \tilde{Q}(p)$ from Eq. (2).

Rotations in 4D can be composed in quaternion form parallel to the 3D case, with

$$R_4(p, q) \cdot R_4(p', q') = R_4(p \star p', q \star q') .$$

We observe that the 4D columns of Eq. (15) can be used to define 4D Euclidean orientation frames in the same fashion as the 3D columns of Eq. (6), and we will exploit this to treat the 4D orientation-frame alignment problem below.

Remark: Eigensystem and properties of R_4 : We can also compute the eigenvalues of our 4D rotation matrix $R_4(p, q)$ from Eq. (15). The 3D form of $R_3(q)$ in terms of explicit fixed axes that we used does not have an exact analog in 4D because 4D rotations leave a *plane* invariant, not an axis. Nevertheless, we can still find very compact form for the 4D eigenvalues. Our exact 4D analog of Eq. (10), after applying the transformations $q_1^2 + q_2^2 + q_3^2 \rightarrow 1 - q_0^2$ for q and p to simplify the expression, is just

$$\left\{ \begin{array}{l} p_0q_0 - \sigma(p_0, q_0) \left(+\sqrt{(1-p_0^2)(1-q_0^2)} + i\sqrt{(1-p_0^2)q_0^2} + i\sqrt{p_0^2(1-q_0^2)} \right) \\ p_0q_0 - \sigma(p_0, q_0) \left(+\sqrt{(1-p_0^2)(1-q_0^2)} - i\sqrt{(1-p_0^2)q_0^2} - i\sqrt{p_0^2(1-q_0^2)} \right) \\ p_0q_0 - \sigma(p_0, q_0) \left(-\sqrt{(1-p_0^2)(1-q_0^2)} + i\sqrt{(1-p_0^2)q_0^2} - i\sqrt{p_0^2(1-q_0^2)} \right) \\ p_0q_0 - \sigma(p_0, q_0) \left(-\sqrt{(1-p_0^2)(1-q_0^2)} - i\sqrt{(1-p_0^2)q_0^2} + i\sqrt{p_0^2(1-q_0^2)} \right) \end{array} \right\} , \quad (16)$$

where the overall sign in the right-hand terms depends on the sign of $p_0q_0 = (1/4) \text{tr } R_4(p, q)$,

$$\sigma(p_0, q_0) = \text{sign}(p_0q_0) .$$

This feature is subtle, and arises in the process of removing a spurious apparent asymmetry between p_0 and q_0 in the eigenvalue expressions associated with the appearance of $\sqrt{q_0^2}$ and $\sqrt{p_0^2}$; incorrect signs arise in removing the square roots without $\sigma(p_0, q_0)$, which is required to make the determinant equal to the products of the eigenvalues. The eigenvectors can be computed in the usual way, but we know of no informative simple algebraic form. Interestingly, the eigensystem of the *profile matrix* of $R_4(p, q)$, discussed later in Section 4, is much simpler.

2 Double-Quaternion Approach to the 4D RMSD Problem

Here we present the nontrivial steps needed to understand and solve the 4D spatial and orientation-frame RMSD optimization problems in the quaternion framework. We extend our solutions for 4×4 symmetric, traceless profile matrices M_3 arising from 3D Euclidean data to the case of unconstrained 4×4 profile matrices M_4 , which arise naturally for 4D Euclidean data.

While we might expect the quaternion eigensystem of the 4D profile matrix to allow us to solve the 4D RMSD problem in exactly the same fashion as in 3D, this is, interestingly, false. We will need several stages of analysis to actually find the correct way to exploit quaternions in the 4D RMSD optimization context. In this Section, we study the problem by itself, in a way that can be easily solved using a quaternion approach with the *numerical* methods traditional in the 3D problem. We devote the Appendix to a detailed treatment of the alternative *algebraic* solutions to the eigensystems of the 4×4 symmetric real matrices that are relevant to our quaternion-based spatial and orientation-frame alignment problems in 3D and 4D.

2.1 Review of the Notation for the RMSD Problem

Our starting point for all alignment analysis is the minimization of the difference measure quantifying the rotational alignment of a D -dimensional set of point test data $\{x_k\}$ relative to a reference data set $\{y_k\}$,

$$\mathbf{S}_D = \sum_{k=1}^N \|R_D \cdot x_k - y_k\|^2, \quad (17)$$

which we replace by a maximization of its cross-term

$$\Delta_D = \sum_{k=1}^N (R_D \cdot x_k) \cdot y_k = \sum_{a=1, b=1}^D R_D^{ba} E_{ab} = \text{tr } R_D \cdot E, \quad (18)$$

where E is the cross-covariance matrix

$$E_{ab} = \sum_{k=1}^N [x_k]_a [y_k]_b = [\mathbf{X} \cdot \mathbf{Y}^t]_{ab}, \quad (19)$$

and $[x_k]$ denotes the k th column of \mathbf{X} .

For 3D data, we convert this to a quaternion matrix problem by applying Eq. (6) to get

$$\Delta(q) = \text{tr } R(q) \cdot E = (q_0, q_1, q_2, q_3) \cdot M_3(E) \cdot (q_0, q_1, q_2, q_3)^t \equiv q \cdot M_3(E) \cdot q, \quad (20)$$

Choosing the traditional 3D indexing $\{x, y, z\}$ for (a, b) , the traceless, symmetric profile matrix takes the form

$$M_3(E) = \begin{bmatrix} E_{xx} + E_{yy} + E_{zz} & E_{yz} - E_{zy} & E_{zx} - E_{xz} & E_{xy} - E_{yx} \\ E_{yz} - E_{zy} & E_{xx} - E_{yy} - E_{zz} & E_{xy} + E_{yx} & E_{zx} + E_{xz} \\ E_{zx} - E_{xz} & E_{xy} + E_{yx} & -E_{xx} + E_{yy} - E_{zz} & E_{yz} + E_{zy} \\ E_{xy} - E_{yx} & E_{zx} + E_{xz} & E_{yz} + E_{zy} & -E_{xx} - E_{yy} + E_{zz} \end{bmatrix}. \quad (21)$$

The maximal measure is given by the eigensystem of the maximal eigenvalue ϵ_{opt} of M_3 and the corresponding quaternion eigenvector q_{opt} , with the result

$$\left. \begin{aligned} \Delta_{\text{opt}} &= \text{tr}[R_3(q_{\text{opt}}) \cdot E] \\ &= q_{\text{opt}} \cdot M_3 \cdot q_{\text{opt}} \\ &= q_{\text{opt}} \cdot (\epsilon_{\text{opt}} q_{\text{opt}}) \\ &= \epsilon_{\text{opt}} \end{aligned} \right\}. \quad (22)$$

2.2 Starting Point for the 4D RMSD Problem.

The 4D double quaternion matrix Eq. (15) provides the most general quaternion context that we know of for expressing an RMSD problem. We start with the RMSD minimization problem for 4D Euclidean point data expressed as the maximization problem for the by-now-familiar cross-term expression

$$\Delta_4 = \sum_{k=1}^N (R_4 \cdot x_k) \cdot y_k = \sum_{a=0, b=0}^3 R_4^{ba} E_{4:ab} = \text{tr } R_4 \cdot E_4, \quad (23)$$

where

$$E_{4:ab} = \sum_{k=1}^N [x_k]_a [y_k]_b = [\mathbf{X} \cdot \mathbf{Y}^t]_{ab} \quad (24)$$

is the cross-covariance matrix whose (a, b) indices we will usually write as (w, x, y, z) in the manner of Eq. (21).

Using Eq. (15) in Eq. (23) to perform the 4D version of the rearrangement of the similarity function, we can rewrite our measure as

$$\Delta_4 = \text{tr } R_4(p, q) \cdot E_4 = (p_0, p_1, p_2, p_3) \cdot M_4(E_4) \cdot (q_0, q_1, q_2, q_3)^t \equiv p \cdot M_4(E_4) \cdot q, \quad (25)$$

where the profile matrix for the 4D data now becomes

$$M_4(E_4) = \begin{bmatrix} E_{ww} + E_{xx} + E_{yy} + E_{zz} & E_{yz} - E_{zy} - E_{wx} + E_{xw} & E_{zx} - E_{xz} - E_{wy} + E_{yw} & E_{xy} - E_{yx} - E_{wz} + E_{zw} \\ E_{yz} - E_{zy} + E_{wx} - E_{xw} & E_{ww} + E_{xx} - E_{yy} - E_{zz} & E_{xy} + E_{yx} - E_{wz} - E_{zw} & E_{zx} + E_{xz} + E_{wy} + E_{yw} \\ E_{zx} - E_{xz} + E_{wy} - E_{yw} & E_{xy} + E_{yx} + E_{wz} + E_{zw} & E_{ww} - E_{xx} + E_{yy} - E_{zz} & E_{yz} + E_{zy} - E_{wx} - E_{xw} \\ E_{xy} - E_{yx} + E_{wz} - E_{zw} & E_{zx} + E_{xz} - E_{wy} - E_{yw} & E_{yz} + E_{zy} + E_{wx} + E_{xw} & E_{ww} - E_{xx} - E_{yy} + E_{zz} \end{bmatrix} \quad (26)$$

and we note that, in contrast to $M_3(E_3)$, $M_4(E_4)$ is *neither* traceless nor symmetric.

2.3 A Tentative 4D Eigensystem

Our task is now to find an algorithm that allows us to successfully compute the quaternion pair $(p_{\text{opt}}, q_{\text{opt}})$, or, equivalently, the global rotation $R_4(p_{\text{opt}}, q_{\text{opt}})$, that maximizes the measure

$$\Delta_4 = \text{tr } R_4(p, q) \cdot E_4 = p \cdot M_4(E_4) \cdot q, \quad (27)$$

with $M_4(E_4)$ a general real matrix with a generic trace and no symmetry conditions. Note that now we can have *both* left and right eigenvectors p and q for a single eigenvalue of the profile matrix M_4 : q would correspond to the eigenvectors of M_4 , and p would correspond to the eigenvectors of the transpose M_4^t . *Warning*: The eigensystem of M_4 typically has some complex eigenvalues and is furthermore *insufficient* by itself to solve the 4D RMSD optimization problem, so additional refinements will be necessary. We now explore a path to an optimal solution amenable to quaternion-based numerical evaluation, with applicable algebraic approaches elaborated in the Appendix.

For some types of calculations, we may find it useful to decompose M_4 in a way that isolates particular features using the form

$$M_4(w, x, y, z, \dots) = \begin{bmatrix} w + x + y + z & a - a_w & b - b_w & c - c_w \\ a + a_w & w + x - y - z & C - C_w & B + B_w \\ b + b_w & C + C_w & w - x + y - z & A - A_w \\ c + c_w & B - B_w & A + A_w & w - x - y + z \end{bmatrix}, \quad (28)$$

where $(w, x, y, z) = (E_{ww}, E_{xx}, E_{yy}, E_{zz})$, $a = E_{yz} - E_{zy}$, cyclic, $A = E_{yz} + E_{zy}$, cyclic, $a_w = E_{wx} - E_{xw}$, cyclic, $A_w = E_{wx} + E_{xw}$, cyclic, and $\text{tr}(M_4) = 4w$. This effectively exposes the structural symmetries of M_4 .

We next review the properties of the eigenvalue equation $\det[M_4 - eI_4] = 0$, where e is the variable we solve for to obtain the four eigenvalues ϵ_k , and I_4 denotes the 4D identity matrix; transposing M_4 does not change the eigenvalues but does interchange the distinct left and right eigenvectors. While M_4 itself has new properties, the corresponding expressions in terms of e and ϵ_k , along with the outcome of eliminating e [Abramowitz and Stegun, 1970], are by now familiar:

$$\det[M_4 - eI_4] = e^4 + e^3 p_1 + e^2 p_2 + e p_3 + p_4 = 0 \quad (29)$$

$$(e - \epsilon_1)(e - \epsilon_2)(e - \epsilon_3)(e - \epsilon_4) = 0 \quad (30)$$

$$\left. \begin{aligned} p_1 &= (-\epsilon_1 - \epsilon_2 - \epsilon_3 - \epsilon_4) \\ p_2 &= (\epsilon_1 \epsilon_2 + \epsilon_1 \epsilon_3 + \epsilon_2 \epsilon_3 + \epsilon_1 \epsilon_4 + \epsilon_2 \epsilon_4 + \epsilon_3 \epsilon_4) \\ p_3 &= (-\epsilon_1 \epsilon_2 \epsilon_3 - \epsilon_1 \epsilon_2 \epsilon_4 - \epsilon_1 \epsilon_3 \epsilon_4 - \epsilon_2 \epsilon_3 \epsilon_4) \\ p_4 &= \epsilon_1 \epsilon_2 \epsilon_3 \epsilon_4 \end{aligned} \right\} . \quad (31)$$

We make no assumptions about M_4 , so its structure includes a trace term $4w = -p_1$ as well as the possible antisymmetric components shown in Eq. (28), yielding the following expressions for the $p_k(E_4)$ following from the expansion of $\det[M_4 - eI_4]$:

$$p_1(E_4) = -\text{tr}[M_4] = -4w \quad (32)$$

$$\begin{aligned} p_2(E_4) &= \frac{1}{2} (\text{tr}[M_4])^2 - \frac{1}{2} \text{tr}[M_4 \cdot M_4] \\ &= 6w^2 - 2(x^2 + y^2 + z^2) - A^2 - a^2 - B^2 - b^2 - C^2 - c^2 \\ &\quad + A_w^2 + a_w^2 + B_w^2 + b_w^2 + C_w^2 + c_w^2 \end{aligned} \quad (33)$$

$$\begin{aligned} p_3(E_4) &= -\frac{1}{6} (\text{tr}[M_4])^3 + \frac{1}{2} \text{tr}[M_4 \cdot M_4] \text{tr}[M_4] - \frac{1}{3} \text{tr}[M_4 \cdot M_4 \cdot M_4] \\ &= -8xyz + 4w(x^2 + y^2 + z^2) \\ &\quad - 2ABC - 2Abc - 2aBc - 2abC \\ &\quad + 2A^2x - 2a^2x + 2B^2y - 2b^2y + 2C^2z - 2c^2z \\ &\quad - 2AB_wC_w + 2Ab_wc_w - 2aB_wc_w + 2ab_wC_w \\ &\quad - 2A_wBC_w + 2a_wBc_w - 2a_wbC_w + 2A_wbc_w \\ &\quad - 2A_wB_wC + 2a_wb_wC - 2A_wb_wc + 2a_wB_wc \\ &\quad + 2a^2w + 2A^2w - 2A_w^2w - 2A_w^2x - 2a_w^2w + 2a_w^2x \\ &\quad + 2b^2w + 2B^2w - 2B_w^2w - 2B_w^2y - 2b_w^2w + 2b_w^2y \\ &\quad + 2c^2w + 2C^2w - 2C_w^2w - 2C_w^2z - 2c_w^2w + 2c_w^2z \end{aligned} \quad (34)$$

$$p_4(E_4) = \det[M_4] . \quad (35)$$

2.4 Issues with the Naive 4D Approach

We previously found that we could maximize $\Delta_3 = \text{tr}(R_3 \cdot E_3)$ over the 3D rotation matrices R_3 by mapping E_3 to the profile matrix M_3 , with $\Delta_3 = q \cdot M_3 \cdot q$, solving for the maximal eigenvalue ϵ_{opt}

of the symmetric matrix M_3 , and choosing $R_{\text{opt}} = R_3(q_{\text{opt}})$ with q_{opt} the normalized quaternion eigenvector corresponding to $\Delta_3(\text{opt}) = \epsilon_{\text{opt}}$. The obvious 4D extension of the 3D quaternion RMSD problem would be to examine $\Delta_4 = \text{tr}(R_4 \cdot E_4) = q_\lambda \cdot M_4 \cdot q_\rho$. This is defined over the 4D rotation matrices R_4 , where M_4 in Eq. (26) turns out no longer to be symmetric, so we must split the eigenvector space into a separate left-quaternion q_λ and right-quaternion q_ρ . We might guess that as in the 3D case, M_4 would have a maximal eigenvalue ϵ_{opt} (already a problem – it may be complex), and we could use the “optimal” left and right eigenvectors $q_{\lambda:\text{opt}}$ and $q_{\rho:\text{opt}}$ that could be obtained as the corresponding eigenvectors of M_4 and M_4^t . Then the solution to the 4D optimization problem would look like this:

$$\Delta_4(\text{opt}) \stackrel{?}{=} q_{\lambda:\text{opt}} \cdot M_4 \cdot q_{\rho:\text{opt}} = (q_{\lambda:\text{opt}} \cdot q_{\rho:\text{opt}}) \epsilon_{\text{opt}} . \quad (36)$$

Unfortunately, this is wrong. First, even when this result is real, Eq. (36) is typically smaller than the actual maximum of $\text{tr}(R_4(q_\lambda, q_\rho) \cdot E_4)$ over the space of 4D rotation matrices (or their equivalent representations in terms of a search through q_λ and q_ρ). Even a simple *slerp* through q_{ID} and just beyond the apparent optimal eigenvectors $q_{\lambda:\text{opt}}$ and $q_{\rho:\text{opt}}$ from an eigenvalue of M_4 can yield *larger* values of Δ_4 ! And, to add insult to injury, starting with those eigenvectors $q_{\lambda:\text{opt}}$ and $q_{\rho:\text{opt}}$, one does not in general even find a *basis* for some normalized linear combination that yields the true optimal result. What is going wrong, and what is the path to our hoped-for quaternionic solution to the 4D RMSD problem, which seems so close to the 3D RMSD problem, but then fails so spectacularly to correspond to the obvious hypothesis?

2.5 Insights from the Singular Value Decomposition

We know that the 3D version of Eq. (36) is certainly correct with ϵ_{opt} the maximal eigenvalue of $M_3(E_3)$, and we know also that there is *some* rotation matrix $R_4(q_\lambda, q_\rho)$ that maximizes $\text{tr}(R_4(q_\lambda, q_\rho) \cdot E_4)$, and therefore the 4D expression Eq. (36) must describe $\Delta_4(\text{opt})$ for *some* non-trivial pair of quaternions (q_λ, q_ρ) . The crucial issue is that the 3D RMSD problem and the 4D RMSD problem differ, with 3D being a special case due to the symmetry of the 4×4 profile matrix. We know also that the SVD form of the optimal rotation matrix is valid in *any* dimension, so we conjecture that the key is to look at the commonality of the SVD solutions in 3D and 4D, and work backwards to see how those non-quaternion-driven equations might relate to what we know is *in principle* a quaternion approach to the 4D problem that looks like Eq. (36).

Therefore, we first look at the general singular-value decomposition for the spatial alignment problem [Schönemann, 1966, Golub and van Loan, 1983] and then analyze the 3D and 4D problems to understand how we can recover a quaternion-based construction of the 4D spatial RMSD solution. For 3D and 4D, the basic SVD construction of the optimal rotation for a cross-covariance matrix E takes the form

$$\{U, S, V\} = \text{SingularValueDecomposition}(E) \quad (37)$$

where

$$E(U, S, V) = U \cdot S \cdot V^t \quad (38)$$

$$R_{\text{opt}}(U, D, V) = V \cdot D \cdot U^t \quad (39)$$

$$D_3 = \text{Diagonal}(1, 1, \text{sign det}(V \cdot U^t)) \quad (40)$$

$$D_4 = \text{Diagonal}(1, 1, 1, \text{sign det}(V \cdot U^t)) . \quad (41)$$

Here U and V are orthogonal matrices that are usually ordinary rotations, while D is usually the identity matrix but can be nontrivial in more situations than one might think. A critical component for this analysis is the diagonal matrix S , whose elements are the all-positive square roots of the eigenvalues of the symmetric matrix $E_4^t \cdot E_4$ (the trace of this matrix is the squared Fröbenius norm of E). The first key fact is that in any dimension the RMSD cross-term obeys the following sequence of transformations following from the SVD relations of Eqs. (38)–(41):

$$\left. \begin{aligned} \Delta(\text{opt}) = \text{tr}(R_{\text{opt}} \cdot E) &= \text{tr}(R_{\text{opt}} \cdot [U \cdot S \cdot V^t]) \\ &= \text{tr}([V \cdot D \cdot U^t] \cdot [U \cdot S \cdot V^t]) \\ &= \text{tr}(D \cdot S) \end{aligned} \right\} . \quad (42)$$

Note the appearance of D in the SVD formula for the optimal measure; we found in numerical experiments that including this term is absolutely essential to guaranteeing agreement with brute force verification of the optimization results, particularly in 4D.

3D Context. Thus an alternative to considering the 3D optimization of $\text{tr}(R \cdot E)$ in the context of E alone is to look at the 3×3 matrices

$$\left. \begin{aligned} F &= E^t \cdot E \\ F' &= E \cdot E^t \end{aligned} \right\} \quad (43)$$

and to note that, although E itself will not in general be symmetric, F and F' are intrinsically symmetric. Thus they have the same eigenvalues, and like all nonsingular matrices of this form, and unlike E itself, will have real positive eigenvalues [Golub and van Loan, 1983] that we can write as $(\gamma_1, \gamma_2, \gamma_3)$. From Eq. (38), we can show that $\text{tr} F = \text{tr} F' = \text{tr}(S \cdot S)$, and since the trace is the sum of the eigenvalues, the eigensystem of F or F' determines S . The diagonal elements that enter naturally into the SVD are therefore just the square roots

$$S(E) = \text{Diagonal}(\sqrt{\gamma_1}, \sqrt{\gamma_2}, \sqrt{\gamma_3}) . \quad (44)$$

So far, this has no obvious connection to the quaternion system. For our next step, let us now examine how the 3D SVD system relates to the profile matrix $M_3(E_3)$ derived from the quaternion decomposition to give the form in Eq. (21). We define the analogs of Eq. (43) for a profile matrix as

$$\left. \begin{aligned} G &= M^t \cdot M \\ G' &= M \cdot M^t \end{aligned} \right\} , \quad (45)$$

where we recall that in 3D, ϵ_{opt} is just the maximal eigenvalue of $M_3(E)$. Thus if we arrange the eigenvalues of $M_3(E)$ in descending order as $(\epsilon_1, \epsilon_2, \epsilon_3, \epsilon_4)$, we obviously have

$$\text{Eigenvalues}(G) = \text{Eigenvalues}(G') = (\alpha_1, \alpha_2, \alpha_3, \alpha_4) = (\epsilon_1^2, \epsilon_2^2, \epsilon_3^2, \epsilon_4^2) . \quad (46)$$

Therefore, since we already know that $\epsilon_1(M) = \Delta(\text{opt})$, we have precisely the sought-for connection,

$$\sqrt{\text{Max Eigenvalue}(G)} = \sqrt{\alpha_1} = \text{tr}(D \cdot S) = \Delta(\text{opt}) = \epsilon_1(M) . \quad (47)$$

That is, given E , compute $M(E)$ from the quaternion decomposition, and, instead of examining the eigensystem of $M(E)$ itself, take the square root of the maximal eigenvalue of the manifestly

symmetric, positive-definite real matrix $G = M^t \cdot M$. This is the quaternion-based translation of the 3D application of the SVD method to obtaining the optimal rotation: numerical methods in particular do not care whether you are computing the maximal eigenvalue of a symmetric quaternion-motivated matrix M_3 or of the associated symmetric matrix $M_3^t \cdot M_3$.

Note: In 3D, we can compute *all four* of the eigenvalues of G from the *three* elements of S [Coutsias et al., 2004]: defining

$$\text{Diagonal}(D \cdot S) = (\lambda_1, \lambda_2, \lambda_3) , \quad (48)$$

then we can write

$$\begin{bmatrix} \alpha_1 \\ \alpha_2 \\ \alpha_3 \\ \alpha_4 \end{bmatrix} = \begin{bmatrix} (+\lambda_1 + \lambda_2 + \lambda_3)^2 \\ (-\lambda_1 - \lambda_2 + \lambda_3)^2 \\ (-\lambda_1 + \lambda_2 - \lambda_3)^2 \\ (+\lambda_1 - \lambda_2 - \lambda_3)^2 \end{bmatrix} , \quad (49)$$

where obviously $\sqrt{\alpha_1} = \text{tr}(D \cdot S)$ is maximal.

The final step is to connect $R_3(\text{opt})$ to a quaternion via $R_3(q_{\text{opt}})$ without requiring prior knowledge of the SVD solution Eq. (39). We know that the square root of the maximal eigenvalue of $G = M^t \cdot M$, which depends only on the quaternion decomposition, gives us $\text{tr}(D \cdot S) = \Delta(\text{opt})$ without using the SVD, and we know that in 3D the profile matrix M is symmetric, so G and G' share a single maximal eigenvector v corresponding to $\alpha_1 = (\text{tr}(D \cdot S))^2 = (\Delta(\text{opt}))^2$. Using this eigenvector we thus have

$$v \cdot G \cdot v = (M \cdot v)^t \cdot (M \cdot v) = v \cdot ((\text{tr}(D \cdot S))^2 \cdot v) = (\Delta(\text{opt}))^2 ,$$

so in this case $v = q_{\text{opt}}$ is itself the optimal eigenvector determining $R_3(q_{\text{opt}})$.

4D Context. The 4D case, as we are now aware, cannot be solved using the non-symmetric profile matrix $M_4(E_4)$ directly. But now we can see a more general way to exploit the 4D quaternion decomposition of Eq. (26) by constructing the *manifestly symmetric products*

$$\left. \begin{aligned} G &= M_4^t \cdot M_4 \\ G' &= M_4 \cdot M_4^t \end{aligned} \right\} . \quad (50)$$

Although this superficially extends Eq. (45) to 4D, it is quite different because M_4 is not itself symmetric (as M_3 was), and so, while G and G' have the same eigenvalues, they have *distinct eigenvectors* q_ρ and q_λ , respectively. If we use the maximal eigenvalue α_1 to solve for q_ρ and q_λ as follows, these in fact will produce the optimal quaternion system. First we solve these equations using the maximal eigenvalue α_1 of G ,

$$\left. \begin{aligned} G \cdot q_\rho &= \alpha_1 q_\rho = (\text{tr}(D \cdot S))^2 q_\rho \\ G' \cdot q_\lambda &= \alpha_1 q_\lambda = (\text{tr}(D \cdot S))^2 q_\lambda \end{aligned} \right\} . \quad (51)$$

At this point, the *signs* of the eigenvectors have to be checked for a correction, since the eigenvector is still correct whatever its sign or scale. But we know that the value of $q_\lambda \cdot M_4(E_4) \cdot q_\rho$ must be positive, so we simply check that sign, and change, say, $q_\lambda \rightarrow -q_\lambda$ if needed to make the sign

positive. There is still an *overall* sign ambiguity, but that is natural and an intrinsic part of the rotation $R_4(q_\lambda, q_\rho)$, so now we can use these eigenvectors to generate the optimal measure for the 4D translational RMSD problem using *only* the quaternion-based data, giving finally the whole spectrum of ways to write $\Delta_4(\text{opt})$:

$$\Delta_4(\text{opt}) = \text{tr}(R_{4,\text{opt}}(q_\lambda, q_\rho) \cdot E_4) = q_\lambda \cdot M_4(E_4) \cdot q_\rho = \sqrt{\alpha_1} . \quad (52)$$

Note: In 4D, we can compute all the eigenvalues of G from the *four* elements of S : defining

$$\text{Diagonal}(D \cdot S) = (\lambda_1, \lambda_2, \lambda_3, \lambda_4) , \quad (53)$$

then we can write

$$\begin{bmatrix} \alpha_1 \\ \alpha_2 \\ \alpha_3 \\ \alpha_4 \end{bmatrix} = \begin{bmatrix} (+\lambda_1 + \lambda_2 + \lambda_3 + \lambda_4)^2 \\ (+\lambda_1 + \lambda_2 - \lambda_3 - \lambda_4)^2 \\ (+\lambda_1 - \lambda_2 + \lambda_3 - \lambda_4)^2 \\ (+\lambda_1 - \lambda_2 - \lambda_3 + \lambda_4)^2 \end{bmatrix} , \quad (54)$$

where again $\sqrt{\alpha_1} = \text{tr}(D \cdot S)$ is maximal.

Summary: Now we have the entire algorithm for solving the RMSD spatial alignment problem in 4D by exploiting the quaternion decomposition of Eq. (25) and Eq. (26), based on Eq. (15), inspired by, but in no way dependent upon knowing, the SVD solution to the problem:

- **Compute the profile matrix.** Using the quaternion decomposition Eq. (15) of the general 4D rotation matrix $R_4(p, q)$, extract the 4D profile matrix $M_4(E_4)$ of Eq. (26) from the initial proximity measure

$$\Delta_4 = \text{tr}(R_4(p, q) \cdot E_4) = p \cdot M_4(E_4) \cdot q . \quad (55)$$

So far all we know is the numerical value of M_4 and the fact the Δ_4 can be maximized by exploring the entire space of the quaternion pair (p, q) .

- **Construct the symmetric matrices and extract the optimal eigenvalue.** The maximal eigenvalue α_1 of the 4×4 symmetric matrix $G = M_4^t \cdot M_4$ is itself easily obtained by numerical means, just as one has done traditionally for M_3 . If all we need is the optimal value of the proximity measure for comparison, we are done:

$$\Delta_4(\text{opt}) = \sqrt{\text{Max Eigenvalue} \left(G = M_4^t \cdot M_4 \right)} = \sqrt{\alpha_1} . \quad (56)$$

The alternative algebraic methods for computing the eigenvalues are discussed in the Appendix.

- **If needed, compute the left and right eigenvectors of G :** Our two distinct symmetric matrices, $G = M_4^t \cdot M_4$ and $G' = M_4 \cdot M_4^t$ have their own distinct maximal eigenvectors, both corresponding to the maximal eigenvalue α_1 shared by G and G' , so we can easily use this common maximal numerical eigenvalue to solve

$$\left. \begin{aligned} (G - \alpha_1 I_4) \cdot q_{\text{opt}:\rho} &= 0 \\ (G' - \alpha_1 I_4) \cdot q_{\text{opt}:\lambda} &= 0 \end{aligned} \right\} \quad (57)$$

for the numerical values of $q_{\text{opt}:\lambda}$ and $q_{\text{opt}:\rho}$. We correct the signs so that $q_{\text{opt}:\lambda} \cdot M_4(E_4) \cdot q_{\text{opt}:\rho} > 0$, and then these in turn yield the required 4D rotation matrix

$$R_{4:\text{opt}}(q_{\text{opt}:\lambda}, q_{\text{opt}:\rho})$$

from Eq. (15).

If everything is in order, all of the following ways of expressing $\Delta_4(\text{opt})$ should now be equivalent,

$$\Delta_4(\text{opt}) = \text{tr}(R_{4:\text{opt}}(q_{\text{opt}:\lambda}, q_{\text{opt}:\rho}) \cdot E_4) = q_{\text{opt}:\lambda} \cdot M_4(E_4) \cdot q_{\text{opt}:\rho} = \sqrt{\alpha_1} \quad , \quad (58)$$

independently of the fact that one knows from the SVD decomposition of E_4 that $\Delta_4(\text{opt}) = \text{tr}(D \cdot S) = \sqrt{\alpha_1}$.

3 4D Orientation-Frame Alignment

In this section, we review and slightly expand the details of the 3D orientation-frame in the main text. Then we extend that treatment to handle the case of 4D orientation-frame alignment to complete the picture we started in Section 2 on the 4D spatial frame alignment problem. A detailed evaluation of the accuracy of the 3D chord measure compared to the arc-length measure, along with other questions, is given separately in Section 6.

3.1 Details of the 3D Orientation-Frame alignment Problem

We first review the basic structure of our 3D orientation-frame method and then proceed to present some additional details.

Review of Orientation Frames in 3D. The ideal optimization problem for 3D orientation frames requires a measure constructed from the geodesic arc lengths on the quaternion hypersphere. Starting with the bare angle between two quaternions on \mathbf{S}^3 , $\alpha = \arccos(q_1 \cdot q_2)$, where we recall that $\alpha \geq 0$, we define a *pseudometric* [Huynh, 2009] for the geodesic arc-length distance as

$$d_{\text{geodesic}}(q_1, q_2) = \min(\alpha, \pi - \alpha) : 0 \leq d_{\text{geodesic}}(q_1, q_2) \leq \frac{\pi}{2} \quad , \quad (59)$$

as illustrated in Fig. (1). An efficient implementation of this is to take

$$d_{\text{geodesic}}(q_1, q_2) = \arccos(|q_1 \cdot q_2|) \quad , \quad (60)$$

which we now exploit to construct a measure from geodesic arc-lengths on the quaternion hypersphere instead of Euclidean distances in space. Thus to compare a test quaternion-frame data set $\{p_k\}$ to a reference data set $\{r_k\}$, we employ the geodesic-based least squares measure

$$\mathbf{S}_{\text{geodesic}} = \sum_{k=1}^N (\arccos |(q \star p_k) \cdot r_k|)^2 = \sum_{k=1}^N (\arccos |q \cdot (r_k \star \bar{p}_k)|)^2 \quad , \quad (61)$$

where the alternative second form follows from Eq. (4).

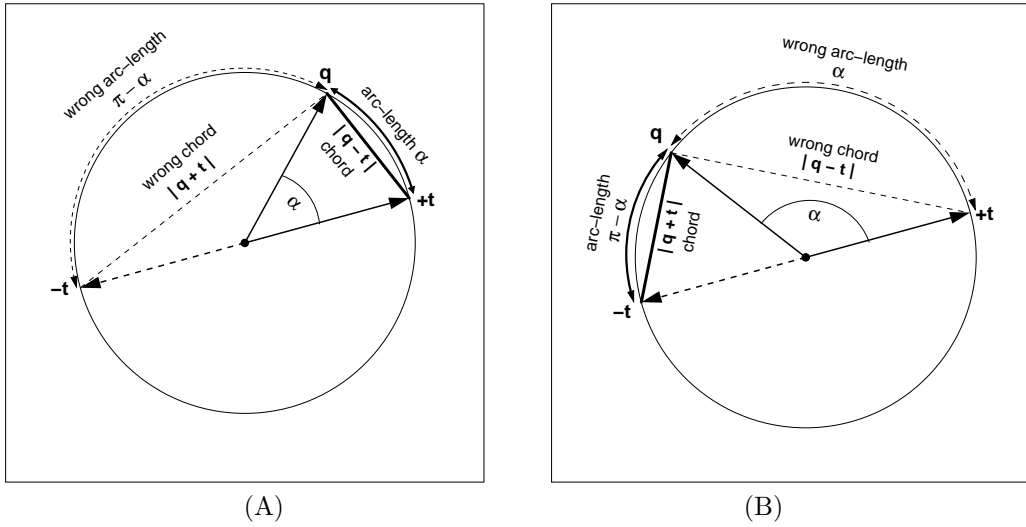


Figure 1: Geometric context involved in choosing a *quaternion distance* that will result in the correct *average rotation matrix* when the quaternion measures are optimized. Because the quaternion vectors represented by t and $-t$ give the same rotation matrix, one must choose $|\cos \alpha|$ or the *minima*, that is $\min(\alpha, \pi - \alpha)$ or $\min(\|q - t\|, \|q + t\|)$, of the alternative distance measures to get the *correct* items in the arc-length or chord measure summations. (A) and (B) represent the cases when the first or second choice should be made, respectively.

Since this does not easily fit into a linear algebra approach to construct optimal solutions to the orientation-frame alignment problem, we choose to approximate the measure of Eq. (61) by the linearizable *chord distance* measure, which does, under certain conditions, permit a valid closed form solution. We take as our approximate measure the chordal pseudometric [Huynh, 2009, Hartley et al., 2013],

$$d_{\text{chord}}(q_1, q_2) = \min(\|q_1 - q_2\|, \|q_1 + q_2\|) : 0 \leq d_{\text{chord}}(q_1, q_2) \leq \sqrt{2}. \quad (62)$$

We compare the geometric origins for Eq. (60) and Eq. (62) in Fig. (1). Note that the crossover point between the two expressions in Eq. (62) is at $\pi/2$, so the hypotenuse of the right isosceles triangle at that point has length $\sqrt{2}$.

The solvable approximate optimization function analogous to $\|R \cdot x - y\|^2$ that we will now explore for the quaternion-frame alignment problem will thus take the form that must be minimized as

$$\mathbf{S}_{\text{chord}} = \sum_{k=1}^N (\min(\|(q \star p_k) - r_k\|, \|(q \star p_k) + r_k\|))^2. \quad (63)$$

We can convert the sign ambiguity in Eq. (63) to a deterministic form like Eq. (60) by observing, with the help of Fig. (1), that

$$\|q_1 - q_2\|^2 = 2 - 2q_1 \cdot q_2, \quad \|q_1 + q_2\|^2 = 2 + 2q_1 \cdot q_2. \quad (64)$$

Clearly $(2 - 2|q_1 \cdot q_2|)$ is always the smallest of the two values. Thus minimizing Eq. (63) amounts to maximizing the now-familiar cross-term form, which we can write as

$$\left. \begin{aligned} \Delta_{\text{chord}}(q) &= \sum_{k=1}^N |(q \star p_k) \cdot r_k| \\ &= \sum_{k=1}^N |q \cdot (r_k \star \bar{p}_k)| \\ &= \sum_{k=1}^N |q \cdot t_k| \end{aligned} \right\}. \quad (65)$$

Here we have used the identity $(q \star p) \cdot r = q \cdot (r \star \bar{p})$ from Eq. (4) and defined the quaternion displacement or "attitude error" [Markley et al., 2007]

$$t_k = r_k \star \bar{p}_k. \quad (66)$$

Note that we could have derived the same result using Eq. (3) to show that $\|q \star p - r\| = \|q \star p - r\| \|p\| = \|q - r \star \bar{p}\|$.

The final step is to choose the samples of q that include our expected optimal quaternion, and adjust the sign of each data value t_k to \tilde{t}_k by the transformation

$$\tilde{t}_k = t_k \text{sign}(q \cdot t_k) \rightarrow |q \cdot t_k| = q \cdot \tilde{t}_k. \quad (67)$$

The neighborhood of q matters because, as argued by [Hartley et al., 2013], even though the allowed range of 3D rotation angles is $\theta \in (-\pi, \pi)$ (or quaternion sphere angles $\alpha \in (-\pi/2, \pi/2)$), convexity of the optimization problem cannot be guaranteed for collections outside local regions centered on some θ_0 of size $\theta_0 \in (-\pi/2, \pi/2)$ (or $\alpha_0 \in (-\pi/4, \pi/4)$): beyond this range, local basins may exist that allow the mapping Eq. (67) to produce distinct local variations in the assignments of the $\{\tilde{t}_k\}$

and in the solutions for q_{opt} . Within considerations of such constraints, Eq. (67) now allows us to take the summation outside the absolute value, and write the quaternion-frame optimization problem in terms of maximizing the cross-term expression

$$\left. \begin{aligned} \Delta_{\text{chord}}(q) &= \sum_{k=1}^N q \cdot \tilde{t}_k \\ &= q \cdot V(t) \end{aligned} \right\} \quad (68)$$

where $V = \sum_{k=1}^N \tilde{t}_k$ is the analog of the Euclidean RMSD profile matrix M . However, since this is *linear* in q , we have the remarkable result that, as noted in the treatment of [Hartley et al., 2013] regarding the quaternion L_2 chordal-distance norm, the solution is immediate. We have simply

$$q_{\text{opt}} = \frac{V}{\|V\|} , \quad (69)$$

since that immediately maximizes the value of $\Delta_{\text{chord}}(q)$ in Eq. (68). This gives the maximal value of the measure as

$$\Delta_{\text{chord}}(q_{\text{opt}}) = \|V\| , \quad (70)$$

and thus $\|V\|$ is the exact orientation frame analog of the spatial RMSD maximal eigenvalue ϵ_{opt} , except it is far easier to compute.

Alternative chord-measure approach parallel to the Euclidean case. Having understood the chordal distance approach for the orientation-alignment problem in terms of the pseudometric Eq. (62) and the measure Eq. (65) transformed into the form Eq. (68) involving the corrected quaternion displacements $\{\tilde{t}_k\}$, we now observe that we can also express the problem in a form much closer to our Euclidean RMSD optimization problem. Returning to the form

$$\mathbf{S}_{\text{chord}} = \sum_{k=1}^N \|q \star p_k - r_k\|^2 . \quad (71)$$

we see that we can effectively transform the sign of *only* $p_k \rightarrow \tilde{p}_k$ using the same test as Eq. (67) to make Eq. (71) valid as it stands; we then proceed, in the same fashion as the spatial alignment problem but with the modification required by Eq. (65), to convert to a cross-term form as follows:

$$\begin{aligned} \Delta_{\text{chord}}(q) &= \sum_{k=1}^N |(q \star p_k) \cdot r_k| = \sum_{k=1}^N (q \star \tilde{p}_k) \cdot r_k \\ &= \sum_{a=0, b=0}^3 Q(q)_{ba} \sum_{k=1}^N [\tilde{p}_k]_a [r_k]_b \\ &= \text{tr } Q(q) \cdot W . \end{aligned} \quad (72)$$

Here W is essentially a cross-covariance matrix in the quaternion data elements and $Q(q)$ is the quaternion matrix of Eq. (1). Since $Q(q)$ is linear in q , we can simply pull out their coefficients, yielding

$$\Delta_{\text{chord}}(q) = q \cdot V(W) , \quad (73)$$

where V is a four-vector corresponding to the profile matrix in the spatial problem:

$$V(W) = \begin{bmatrix} +W_{00} + W_{11} + W_{22} + W_{33} \\ +W_{01} - W_{10} + W_{23} - W_{32} \\ +W_{02} - W_{20} + W_{31} - W_{13} \\ +W_{03} - W_{30} + W_{12} - W_{21} \end{bmatrix}. \quad (74)$$

This is of course exactly the same as the quaternion difference transformation Eq. (66), expressed as a profile matrix transformation, and Eq. (73) leads, assuming consistent data localization, to the same optimal unit quaternion

$$q_{\text{opt}} = \frac{V}{\|V\|}, \quad (75)$$

that maximizes the value of Δ_{chord} in Eq. (68), and the maximal value of the measure is again $\Delta_{\text{chord}}(q_{\text{opt}}) = \|V\|$.

Matrix Form of the Linear Vector Chord Distance. While Eq. (68) (or Eq. (73)) does not immediately fit into the eigensystem-based RMSD matrix method used in the spatial problem, it can in fact be easily transformed from a system linear in q to an equivalent matrix system *quadratic* in q . Since any power of the optimization measure will yield the same extremal solution, we can simply *square* the right-hand side of Eq. (68) and write the result in the form

$$\begin{aligned} \Delta_{\text{chord-sq}} &= (q \cdot V)(q \cdot V) \\ &= \sum_{a=0, b=0}^3 q_a V_a V_b q_b \\ &= q \cdot \Omega \cdot q, \end{aligned} \quad (76)$$

where $\Omega_{ab} = V_a V_b$ is a 4×4 symmetric matrix with $\det \Omega = 0$, and $\text{tr} \Omega = \sum_a V_a^2 \neq 0$. The eigensystem of Ω is just defined by the eigenvalue $\|V\|^2$, and combination with the spatial eigensystem can be achieved either numerically or algebraically using the trace $\neq 0$ case of our quartic solution. The process differs dramatically from what we did with Δ_{chord} , but the forms of the eigenvectors are necessarily *identical*. Thus it is in fact possible to merge the QFA system for Δ_{chord} into the matrix method of the spatial RMSD using Eq. (76).

Fixing Sign Problem with Quadratic Rotation Matrix Chord Distance. However, there is another approach that has a very natural way to incorporate manifestly *sign-independent* quaternion chord distances into our general context, and which has a very interesting close relationship to Δ_{chord} . The method begins with the observation that full 3D rotation matrices like Eq. (6) can be arranged to rotate the set of frames of the $\{p_k\}$ to be as close as possible to the reference frame $\{r_k\}$ by employing a measure that is a particular product of rotation matrices. The essence is to notice that the trace of any 3D rotation matrix expressed in axis-angle form (rotation about a fixed axis $\hat{\mathbf{n}}$ by θ) can be expressed in two equivalent forms:

$$\text{tr} R(\theta, \hat{\mathbf{n}}) = 1 + 2 \cos \theta \quad (77)$$

$$\text{tr} R(q) = 3q_0^2 - q_1^2 - q_2^2 - q_3^2 = 4q_0^2 - 1, \quad (78)$$

and therefore traces of rotation matrices can be turned into maximizable functions of the angles appearing in the trace. Noting that the squared Fröbenius norm of a matrix M is the trace $\text{tr } M \cdot M^t$, we begin with the goal of minimizing a Fröbenius norm of the form

$$\|R(q) \cdot R(p_k) - R(r_k)\|_{\text{Frob.}}^2 ,$$

and then convert from a minimization problem in this norm to a maximization of the cross-term as usual. The result is, remarkably, an explicitly symmetric and traceless profile matrix in the quaternions. We thus begin with this form of the orientation-frame measure (see, e.g., [Huynh, 2009, Moakher, 2002, Hartley et al., 2013]),

$$\begin{aligned} \Delta_{\text{RRR}} &= \sum_{k=1}^N \text{tr} [R(q) \cdot R(p_k) \cdot R^{-1}(r_k)] = \sum_{k=1}^N \text{tr} [R(q \star p_k \star \bar{r}_k)] \\ &= \sum_{k=1}^N \text{tr} [R(q) \cdot R(p_k \star \bar{r}_k)] = \sum_{k=1}^N \text{tr} [R(q) \cdot R^{-1}(r_k \star \bar{p}_k)] , \end{aligned} \quad (79)$$

where \bar{r} denotes the complex conjugate or inverse quaternion. We note that due to the correspondence of Δ_{RRR} with a cosine measure (via Eq. (77)), this must be *maximized* to find the optimal q , so both Δ_{chord} and Δ_{RRR} correspond naturally to the cross-term measure we used for Euclidean point data, which we will later refer to as Δ_x when necessary to distinguish it.

We next observe that the formulas for Δ_{RRR} and the pre-summation arguments of Δ_{chord} are related as follows:

$$\sum_{k=1}^N \text{tr} [R(q) \cdot R(p_k) \cdot R(\bar{r}_k)] = \sum_{k=1}^N \left(4((q \star p_k) \cdot r_k)^2 - (q \cdot q)(p_k \cdot p_k)(r_k \cdot r_k) \right) , \quad (80)$$

where of course the last term reduces to a constant since we apply the unit-length constraint to all the quaternions, but is algebraically essential to the construction. The odd form of Eq. (80) is not a typographical error: the conjugate \bar{r} of the reference data must be used in the $R \cdot R \cdot R$ expression, and the ordinary r must be used in both terms on the right-hand. We conclude that using the $R \cdot R \cdot R$ measure and replacing the argument of Δ_{chord} by its square *before* summing over k are equivalent maximizing measures that eliminate the quaternion sign dependence. Now using the quaternion triple-term identity $(q \star p) \cdot r = q \cdot (r \star \bar{p})$ of Eq. (4), we see that each term of Δ_{RRR} reduces to a quaternion product that is a quaternion difference, or a “quaternion displacement” $t_k = r_k \star \bar{p}_k$, i.e., the rotation mapping each individual test frame to its corresponding reference frame,

$$\left. \begin{aligned} \Delta_{\text{RRR}} &= \sum_{k=1}^N \text{tr} [R(q) \cdot R(p_k) \cdot R(\bar{r}_k)] = \sum_{k=1}^N \left(4((q \star p_k) \cdot r_k)^2 - (q \cdot q)(p_k \cdot p_k)(r_k \cdot r_k) \right) \\ &= \sum_{k=1}^N \left(4(q \cdot (r_k \star \bar{p}_k))^2 - 1 \right) \\ &= 4 \sum_{a,b} q_a \left(\sum_{k=1}^N [t_k]_a [t_k]_b \right) q_b - N \\ &= 4q \cdot A(t) \cdot q - N . \end{aligned} \right\} \quad (81)$$

Here the 4×4 matrix $A(t)_{ab} = \sum_{k=1}^N [t_k]_a [t_k]_b$ is the alternative (equivalent) profile matrix that was introduced by [Markley et al., 2007, Hartley et al., 2013] for the chord-based *quaternion-averaging* problem. We can therefore use either the measure Δ_{RRR} or

$$\Delta_A = q \cdot A(t) \cdot q \quad (82)$$

as our rotation-matrix-based sign-insensitive chord-distance optimization measure. Exactly like our usual spatial measure, these measures must be *maximized* to find the optimal q . It is, however, important to emphasize that the optimal quaternion will *differ* for the Δ_{chord} , $\Delta_{\text{chord-sq}}$, and $\Delta_{\text{RRR}} \sim \Delta_A$ measures, though they will normally be very similar. More details are explored in Section 6.

Details of Rotation Matrix Form. We now recognize that the sign-insensitive measures are all very closely related to our original spatial RMSD problem, and all can be solved by finding the optimal quaternion eigenvector q_{opt} of a 4×4 matrix. The procedure for $\Delta_{\text{chord-sq}}$ and Δ_A follows immediately, but it is useful to work out the options for Δ_{RRR} in a little more detail.

Choosing Eq. (79) has the remarkable feature of producing, via Eq. (6) for $R(q)$, an expression *quadratic* in q , with a symmetric, traceless profile matrix $U(p, r)$ that is *quartic* in the quaternion elements p_k and r_k . This variant of the chord-based QFA problem thus falls into the same category as the standard RMSD problem, and permits the application of the same exact solution (or, indeed, the traditional numerical solution method if that is more efficient). The profile matrix equation is unwieldy to write down explicitly in terms of the quaternion elements quartic in $\{p, r\}$, but we actually have several options for expressing the content in a simpler form. One is to write the matrices in abstract canonical 3×3 form, e.g.,

$$R(p) = [P] = \begin{bmatrix} p_{xx} & p_{xy} & p_{xz} \\ p_{yx} & p_{yy} & p_{yz} \\ p_{zx} & p_{zy} & p_{zz} \end{bmatrix}, \quad (83)$$

where the *columns* of this matrix are just the three axes of each data element's frame triad. This is often exactly what our original data look like, for example, if the residue orientation frames of a protein are computed from cross-products of atom-atom vectors [Hanson and Thakur, 2012]. Then we can define for each data element the 3×3 matrix

$$[T_k] = R(p_k) \cdot R(\bar{r}_k) = R(p_k \star \bar{r}_k) = R^{-1}(t_k),$$

so we can write T either in terms of a 3×3 matrix like Eq. (83) derived from the actual frame-column data, or in terms of Eq. (6) and the quaternion frame data $t_k = r_k \star \bar{p}_k$. We then may write the frame measure in general as

$$\Delta_{\text{RRR}} = \sum_{k=1}^N \text{tr}(R(q) \cdot T_k) = \sum_{a=1, b=1}^3 R_{ba}(q) T_{ab}, \quad (84)$$

where the frame-based cross-covariance matrix is simply $T_{ab} = \sum_{k=1}^N [T_k]_{ab}$. As before, we can easily expand $R(q)$ using Eq. (6) to convert the measure to a 4D linear algebra problem of the form

$$\Delta_{\text{RRR}} = \sum_{a=0, b=0}^3 q_a \cdot U_{ab}(p, r) \cdot q_b = q \cdot U(p, r) \cdot q. \quad (85)$$

Here $U(p, r) = U(T)$ has the same relation to T as $M(E)$ does to E in Eq. (21). We may choose to write the profile matrix $U = \sum_k U_k$ appearing in Δ_{RRR} either in terms of the individual k -th components of the numerical 3D rotation matrix $T = R^{-1}(t)$ or using the composite quaternion $t = r \star \bar{p}$:

$$\begin{aligned}
U_k(T) &\equiv U(t_k) \\
&= \begin{bmatrix} T_{xx} + T_{yy} + T_{zz} & T_{yz} - T_{zy} & T_{zx} - T_{xz} & T_{xy} - T_{yx} \\ T_{yz} - T_{zy} & T_{xx} - T_{yy} - T_{zz} & T_{xy} + T_{yx} & T_{xz} + T_{zx} \\ T_{zx} - T_{xz} & T_{xy} + T_{yx} & -T_{xx} + T_{yy} - T_{zz} & T_{yz} + T_{zy} \\ T_{xy} - T_{yx} & T_{xz} + T_{zx} & T_{yz} + T_{zy} & -T_{xx} - T_{yy} + T_{zz} \end{bmatrix}_k \quad (86) \\
&= \begin{bmatrix} 3t_0^2 - t_1^2 - t_2^2 - t_3^2 & 4t_0t_1 & 4t_0t_2 & 4t_0t_3 \\ 4t_0t_1 & -t_0^2 + 3t_1^2 - t_2^2 - t_3^2 & 4t_1t_2 & 4t_1t_3 \\ 4t_0t_2 & 4t_1t_2 & -t_0^2 - t_1^2 + 3t_2^2 - t_3^2 & 4t_2t_3 \\ 4t_0t_3 & 4t_1t_3 & 4t_2t_3 & -t_0^2 - t_1^2 - t_2^2 + 3t_3^2 \end{bmatrix}_k \quad (87)
\end{aligned}$$

Both Eq. (86) and Eq. (87) are *quartic* (and identical) when expanded in terms of the quaternion data $\{p_k, r_k\}$. To compute the necessary 4×4 numerical profile matrix U , one need only substitute the appropriate 3D frame triads or their corresponding quaternions for the k th frame pair and sum over k . Since the orientation-frame profile matrix U is symmetric and traceless just like the Euclidean profile matrix M , the same solution methods for the optimal quaternion rotation q_{opt} will work without alteration in this case, which is probably the preferable method for the general problem.

Evaluation. The details of evaluating the properties of our quaternion-frame alignment algorithms, and especially comparing the chord approximation to the arc-length measure, are tedious and are available separately in Section 6. The top-level result is that, even for quite large rotational differences, the mean differences between the arc-length measure's numerical optimal angle and the various chord approximations are on the order of a few thousandths of a degree.

3.2 The 4D Orientation-Frame alignment Problem

Orientation frames in four dimensions have axes that are the columns of a 4D rotation matrix taking the identity frame to the new orientation frame. Therefore, in parallel with the 3D case, such frames can be represented either as 4D rotation matrices (the action on a 4D identity frame to get a new set of 4 orthogonal axes), or as the pair of quaternions (q, q') used in Eq. (15) to define $R_4(q, q')$. As in the 3D frame case, we will take advantage of the chord-distance linearization of the geodesic angular measure, and we shall present two alternative approaches to the optimization measure.

Quadratic Form. In 3D, with Eq. (68) having a single quaternion involved in the rotation, we were able to write down Δ_{chord} in terms of a simple expression linear in the quaternion q and the cumulative data V , and we observed that a quadratic expression $(q \cdot V)^2$ would also produce the same optimal eigenvector $q = V/\|V\|$. The optimal frame problem in 4D, in contrast, already requires a pair of quaternions, and one strategy is to split the analogs of the 3D quadratic expression

into two parts, yielding

$$\Delta_{4:\text{chord-sq}}(q, q') = (q \cdot V) (q' \cdot V') = q_a (V_a V'_b) q'_b = q \cdot \Omega_4 \cdot q' \quad (88)$$

as the generalization from 3D to 4D. Here, each 4D test frame consists of frames denoted by the quaternion pair (p, p') , and each reference frame employs a pair (r, r') , so we build the data coefficients starting from

$$\left. \begin{aligned} V &= \sum_{k=1}^N (r_k \star \bar{p}_k) = \sum_{k=1}^N t_k \\ V' &= \sum_{k=1}^N (r'_k \star \bar{p}'_k) = \sum_{k=1}^N t'_k \end{aligned} \right\} \quad (89)$$

and then applying the transformation

$$\left. \begin{aligned} t_k &\rightarrow \tilde{t}_k = t_k \text{sign}(q \cdot t_k) \\ t'_k &\rightarrow \tilde{t}'_k = t'_k \text{sign}(q \cdot t'_k) \end{aligned} \right\} \quad (90)$$

to achieve consistent (local) signs. According to Eq. (74), V could also be constructed from $W_{ab} = \sum_{k=1}^N [\tilde{p}_k]_a [r_k]_b$, and V' from $W'_{ab} = \sum_{k=1}^N [\tilde{p}'_k]_a [r'_k]_b$, noting that here p is transformed by the “tilde” of Eq. (90). Now, for the 4D frame pairs, the solution for the optimal quaternions must achieve the maximum for *both* elements of the pair, and so we obtain as a solution maximizing Eq. (88)

$$\left. \begin{aligned} q_{\text{opt}} &= \frac{V}{\|V\|} \\ q'_{\text{opt}} &= \frac{V'}{\|V'\|} \\ \Delta_{4:\text{chord-sq}}(\text{opt}) &= \|V\| \|V'\| \end{aligned} \right\} \quad (91)$$

Remark: There is a particular reason to prefer Eq. (88) for the 4D orientation frame problem: in the next section, we will see that the separate *pre-summation* arguments for V and V' , gathered together, are *exactly* equal to the joint summand of the 4D triple rotation pre-summation arguments, following the pattern seen in Eq. (80) for the 3D orientation-frame analysis.

Quartic Triple Rotation Form. One can also eliminate the sign choice step altogether by defining a 4D frame similarity measure that is the exact analog of Eq. (79) in 3D as follows:

$$\Delta_{\text{RRR4}} = \sum_{k=1}^N \text{tr} [R(q, q') \cdot R(p_k, p'_k) \cdot R^{-1}(r_k, r'_k)] \quad (92)$$

$$= \sum_{k=1}^N \text{tr} [R(q, q') \cdot R(p_k \star \bar{r}_k, p'_k \star \bar{r}'_k)] \quad (93)$$

$$= \sum_{k=1}^N \text{tr} [R(q, q') \cdot R^{-1}(t_k, t'_k)] \quad (94)$$

$$= q \cdot U(p, p'; r, r') \cdot q' \quad (95)$$

Remarkably, there is a 4D version of the 3D identity Eq. (80) relating the triple rotation measure to the quadratic realizations of the linear quaternion rotation measures, namely

$$\left. \begin{aligned}
\sum_{k=1}^N \text{tr} [R(q, q') \cdot R(p_k, p'_k) \cdot R(\bar{r}_k, \bar{r}'_k)] &= 4 \sum_{k=1}^N ((q \star p_k) \cdot r_k) ((q' \star p'_k) \cdot r'_k) \\
&= 4 \sum_{k=1}^N (q \cdot (r_k \star \bar{p}_k)) (q' \cdot (r'_k \star \bar{p}'_k)) \\
&= 4 \sum_{k=1}^N (q \cdot t_k) (q' \cdot t'_k) \\
&= 4 \sum_{a,b} q_a \left(\sum_{k=1}^N [t_k]_a [t'_k]_b \right) q'_b \\
&= 4 q \cdot A(t = r \star \bar{p}, t' = r' \star \bar{p}') \cdot q'
\end{aligned} \right\}, \quad (96)$$

Thus the pre-summation version of the arguments in the $(q \cdot V)(q' \cdot V')$ version of the 4D chord measure turns out to be *exactly* the same as the triple-matrix product measure summand without the additional trace term that is present in 3D. Furthermore, as long as one follows the rules of changing *both* the primed and unprimed signs together (the condition for $R_4(q, q')$'s invariance), this measure is sign-independent. The 4×4 matrix $A(t, t')$ is the 4D profile matrix equivalent to that of [Markley et al., 2007, Hartley et al., 2013] for the 3D chord-based quaternion-averaging problem. We can therefore use either the measure Δ_{RRR4} or

$$\Delta_{\text{A4}} = q \cdot A(t, t') \cdot q' \quad (97)$$

with $A(t, t')_{ab} = \sum_{k=1}^N [t_k]_a [t'_k]_b$ as our rotation-matrix-based sign-insensitive chord-distance optimization measure.

To get an expression in terms of R , we now use Eq. (15) for $R(q, q')$ to decompose the measure Eq. (93) into the rotation-averaging form

$$\Delta_{\text{RRR4}} = \text{tr} [R(q, q') \cdot T(p, p'; r, r')] \quad (98)$$

$$= q \cdot U(T) \cdot q', \quad (99)$$

where $T(p, p'; r, r') = \sum_{k=1}^N R^{-1}(t_k, t'_k)$ and $U(T)$ has the same relationship to T as the 4D profile matrix $M(E)$ in Eq. (26) does to the cross-correlation matrix E . In the next section, we will see that the singleton version of this map is unusually degenerate, with rank one, though that feature does not persist for data sets with $N > 1$.

Now, as in the 4D spatial RMSD analysis, we might naturally assume that we could follow the 3D case by determining the maximal eigenvalue ϵ_0 of U and its left and right eigenvectors q_λ and q_ρ , which would give

$$\Delta_{\text{RRR4}} \stackrel{?}{=} q_\lambda \cdot U \cdot q_\rho = (q_\lambda \cdot q_\rho) \epsilon_0 .$$

As before, this is not a maximal value for the measure Δ_{RRR4} over the possible range of $R(q, q')$. To solve the optimization correctly, we must again be very careful, and work with the maximal eigenvalue $\alpha(\text{RRR4:opt})$ of $G = U^t \cdot U$ and $G' = U \cdot U^t$, which we can get numerically as usual, or algebraically from the quartic solution for the eigenvalues for symmetric 4×4 matrices with a trace, yielding

$$\Delta_{\text{RRR4}}(\text{opt}) = \sqrt{\max \text{eigenvalue} (U^t \cdot U)} = \sqrt{\alpha(\text{RRR4:opt})} .$$

If we need the actual optimal rotation matrix solving

$$\Delta_{\text{RRR4}}(\text{opt}) = \text{tr} \left(R_4(q_{\text{opt}}, q'_{\text{opt}}) \cdot S \right) = q_{\text{opt}} \cdot U \cdot q'_{\text{opt}} = \sqrt{\alpha(\text{RRR4:opt})} ,$$

then we just use our optimal eigenvalue to solve

$$\begin{aligned} (G - \alpha(\text{RRR4:opt})I_4) \cdot q &= 0 \\ (G' - \alpha(\text{RRR4:opt})I_4) \cdot q' &= 0 \end{aligned}$$

for q_{opt} and q'_{opt} , or use the equivalent adjugate-column method to extract the eigenvectors. That gives the desired 4D rotation matrix $R_4(q_{\text{opt}}, q'_{\text{opt}})$ explicitly via Eq. (15). The same approach applies to the solution of $\Delta_{A4} = q \cdot A(t, t') \cdot q'$, Note that this can all be accomplished numerically, directly as above or with Singular Value Decomposition, or using the quaternion eigenvalue decomposition on the symmetric matrices either numerically or algebraically,

4 On Obtaining Quaternions and Quaternion Pairs from 3D and 4D Rotation Matrices

4.1 Extracting a Quaternion from 3D Rotation Matrices

The quaternion RMSD profile matrix method can be used to implement a singularity-free algorithm to obtain the (sign-ambiguous) quaternions corresponding to numerical 3D and 4D rotation matrices. There are many existing approaches to the 3D problem in the literature (see, e.g., [Shepperd, 1978], [Shuster and Natanson, 1993], or Section 16.1 of [Hanson, 2006]). In contrast to these approaches, Bar-Itzhack [Bar-Itzhack, 2000] has observed, in essence, that if we simply replace the data matrix E_{ab} by a numerical 3D orthogonal rotation matrix R , the numerical quaternion q that corresponds to $R_{\text{numeric}} = R(q)$, as defined by Eq. (6), can be found by solving our familiar maximal quaternion eigenvalue problem. The initially unknown optimal matrix (technically its quaternion) computed by maximizing the similarity measure turns out to be computable as a single-element quaternion barycenter problem. To see this, take $S(r)$ to be the sought-for optimal rotation matrix, with its own quaternion r , that must maximize the Bar-Itzhack measure. We start with the Fröbenius measure describing the match of two rotation matrices corresponding to the quaternion r for the unknown quaternion and the numeric matrix R containing the known 3×3 rotation matrix data:

$$\begin{aligned} \mathbf{S}_{\text{BI}} &= \|S(r) - R\|_{\text{Frob}}^2 = \text{tr} ([S(r) - R] \cdot [S^t(r) - R^t]) \\ &= \text{tr} (I_3 + I_3 - 2(S(r) \cdot R^t)) \\ &= \text{const} - 2 \text{tr} S(r) \cdot R^t . \end{aligned}$$

Pulling out the cross-term as usual and converting to a maximization problem over the unknown quaternion r , we arrive at

$$\Delta_{\text{BI}} = \text{tr} S(r) \cdot R^t = r \cdot K(R) \cdot r , \tag{100}$$

where R is (approximately) an orthogonal matrix of numerical data, and $K(R)$ is analogous to the profile matrix $M(E)$. Since both S and R are $\text{SO}(3)$ rotation matrices, so is their product

$T = S \cdot R^t$, and thus that product itself corresponds to some axis $\hat{\mathbf{n}}$ and angle θ , where

$$\text{tr } S(r) \cdot R^t(q) = \text{tr } T(r \star \bar{q}) = \text{tr } T(\theta, \hat{\mathbf{n}}) = 1 + 2 \cos \theta .$$

The maximum is obviously close to the ideal value $\theta = 0$, which corresponds to $S \approx R$. Thus if we find the maximal quaternion eigenvalue ϵ_{opt} of the profile matrix $K(R)$ in Eq. (100), our closest solution is well-represented by the corresponding normalized quaternion eigenvector r_{opt} ,

$$q = r_{\text{opt}} . \quad (101)$$

This numerical solution for q will correspond to the targeted numerical rotation matrix, solving the problem. To complete the details of the computation, we replace the elements E_{ab} in Eq. (21) by a general orthonormal rotation matrix with columns $\mathbf{X} = (x_1, x_2, x_3)$, \mathbf{Y} , and \mathbf{Z} , scaling by $1/3$, thus obtaining the special 4×4 profile matrix K whose elements in terms of a known numerical matrix $R = [\mathbf{X}|\mathbf{Y}|\mathbf{Z}]$ (transposed in the algebraic expression for K due to the R^t in Δ_{BI}) are

$$K(R) = \frac{1}{3} \begin{bmatrix} x_1 + y_2 + z_3 & y_3 - z_2 & z_1 - x_3 & x_2 - y_1 \\ y_3 - z_2 & x_1 - y_2 - z_3 & x_2 + y_1 & x_3 + z_1 \\ z_1 - x_3 & x_2 + y_1 & -x_1 + y_2 - z_3 & y_3 + z_2 \\ x_2 - y_1 & x_3 + z_1 & y_3 + z_2 & -x_1 - y_2 + z_3 \end{bmatrix} . \quad (102)$$

Determining the algebraic eigensystem of Eq. (102) is a nontrivial task. However, as we know, any orthogonal 3D rotation matrix $R(q)$, or equivalently, $R^t(q) = R(\bar{q})$, can also be ideally expressed in terms of quaternions via Eq. (6), and this yields an alternate useful algebraic form

$$K(q) = \frac{1}{3} \begin{bmatrix} 3q_0^2 - q_1^2 - q_2^2 - q_3^2 & 4q_0q_1 & 4q_0q_2 & 4q_0q_3 \\ 4q_0q_1 & -q_0^2 + 3q_1^2 - q_2^2 - q_3^2 & 4q_1q_2 & 4q_1q_3 \\ 4q_0q_2 & 4q_1q_2 & -q_0^2 - q_1^2 + 3q_2^2 - q_3^2 & 4q_2q_3 \\ 4q_0q_3 & 4q_1q_3 & 4q_2q_3 & -q_0^2 - q_1^2 - q_2^2 + 3q_3^2 \end{bmatrix} \quad (103)$$

This equation then allows us to quickly prove that K has the correct properties to solve for the appropriate quaternion corresponding to R . First we note that the coefficients p_n of the eigensystem are simply constants,

$$p_1 = 0 \quad p_2 = -\frac{2}{3} \quad p_3 = -\frac{8}{27} \quad p_4 = -\frac{1}{27} .$$

Computing the eigenvalues and eigenvectors using the symbolic quaternion form, we see that the eigenvalues are constant, with maximal eigenvalue exactly one, and the eigenvectors are almost trivial, with the maximal eigenvector being the inverse of the quaternion q that corresponds to the (numerical) rotation matrix:

$$\epsilon = \left\{ 1, -\frac{1}{3}, -\frac{1}{3}, -\frac{1}{3} \right\} \quad (104)$$

$$r = \left\{ \begin{bmatrix} q_0 \\ q_1 \\ q_2 \\ q_3 \end{bmatrix}, \begin{bmatrix} -q_1 \\ q_0 \\ 0 \\ 0 \end{bmatrix}, \begin{bmatrix} -q_2 \\ 0 \\ q_0 \\ 0 \end{bmatrix}, \begin{bmatrix} -q_3 \\ 0 \\ 0 \\ q_0 \end{bmatrix} \right\} . \quad (105)$$

The first column is the quaternion r_{opt} , with $\Delta_{\text{BI}}(r_{\text{opt}}) = 1$. (This would be 3 if we had not divided by 3 in the definition of K .)

Alternate version. From the quaternion barycenter work of Markley et al. [Markley et al., 2007], we know that Eq. (103) actually has a much simpler form with the same unit eigenvalue and natural quaternion eigenvector. (This form appears naturally below in the 4D extension of the Bar-Itzhack algorithm.) If we simply take Eq. (103) multiplied by 3, add the constant term $I_4 = (q_0^2 + q_1^2 + q_2^2 + q_3^2)I_4$, and divide by 4, we get a more compact quaternion form of the matrix, namely

$$K'(q) = \begin{bmatrix} q_0^2 & q_0q_1 & q_0q_2 & q_0q_3 \\ q_0q_1 & q_1^2 & q_1q_2 & q_1q_3 \\ q_0q_2 & q_1q_2 & q_2^2 & q_2q_3 \\ q_0q_3 & q_1q_3 & q_2q_3 & q_3^2 \end{bmatrix}. \quad (106)$$

This has vanishing determinant and trace $\text{tr } K' = 1 = -p_1$, with all other p_k coefficients vanishing, and eigensystem with eigenvalues identical to Eq. (103):

$$\epsilon = \{1, 0, 0, 0\} \quad (107)$$

$$r = \left\{ \begin{bmatrix} q_0 \\ q_1 \\ q_2 \\ q_3 \end{bmatrix}, \begin{bmatrix} -q_1 \\ q_0 \\ 0 \\ 0 \end{bmatrix}, \begin{bmatrix} -q_2 \\ 0 \\ q_0 \\ 0 \end{bmatrix}, \begin{bmatrix} -q_3 \\ 0 \\ 0 \\ q_0 \end{bmatrix} \right\}. \quad (108)$$

As elegant as this is, in practice, our numerical input data are from the 3×3 matrix R itself, and not the quaternions, so we will almost always just use those numbers in Eq. (102) to solve the problem.

Completing the solution. In typical applications, *the solution is immediate, requiring only trivial algebra.* The maximal eigenvalue is always known in advance to be unity for any valid rotation matrix, so we need only to compute the eigenvector from the numerical matrix Eq. (102) with unit eigenvalue. We simply compute any column of the adjugate matrix of $K(R) - I_4$, or solve the equivalent linear equations of the form

$$(K(R) - 1 * I_4) \cdot \begin{bmatrix} 1 \\ v_1 \\ v_2 \\ v_3 \end{bmatrix} = 0 \quad q = r_{\text{opt}} = \text{normalize} \begin{bmatrix} 1 \\ v_1 \\ v_2 \\ v_3 \end{bmatrix}. \quad (109)$$

As always, one may need to check for degenerate special cases.

Non-ideal cases. It is important to note, as emphasized by Bar-Itzhack, that if there are *significant errors* in the numerical matrix R , then the actual non-unit maximal eigenvalue of $K(R)$ can be computed numerically or algebraically as usual, and then that eigenvalue's eigenvector determines the *closest* normalized quaternion to the errorful rotation matrix, which can be very useful since such a quaternion always produces a valid rotation matrix.

In any case, *up to an overall sign*, r_{opt} is the desired numerical quaternion q corresponding to the target numerical rotation matrix $R = R(q)$. In some circumstances, one is looking for a

uniform statistical distribution of quaternions, in which case the overall sign of q should be chosen *randomly*.

The Bar-Itzhack approach solves the problem of extracting the quaternion of an arbitrary numerical 3D rotation matrix in a fashion that involves no singularities and only trivial testing for special cases, thus essentially making the traditional methods obsolete.

4.2 Extracting Quaternion Pairs from 4D Rotation Matrices

We know from Eq. (15) that any 4D orthogonal matrix $R_4(p, q)$ can be expressed as a quadratic form in two independent unit quaternions. This is a consequence of the fact that the 6-parameter orthogonal group $\mathbf{SO}(4)$ is double covered by the composition of two smaller 3-parameter unitary groups, that is $\mathbf{SU}(2) \times \mathbf{SU}(2)$; the group $\mathbf{SU}(2)$ has essentially the same properties as a single quaternion, so it is not surprising that $\mathbf{SO}(4)$ should be related to a pair of quaternions.

We begin our treatment of the 4D case by extending Eq. (100) to 4D with a numerical $\mathbf{SO}(4)$ matrix R_4 , giving us a Bar-Itzhack measure to maximize of the form

$$\Delta_{4:\text{BI}} = \text{tr } S(\ell, r) \cdot R_4^t = \ell \cdot K_4(R_4) \cdot r = \ell \cdot K_4(p, q) \cdot r. \quad (110)$$

Here (ℓ, r) are the left and right quaternions over which we are varying the measure, and $K_4(R_4)$ is the 4D generalization of Eq. (102). To compute $K_4(R_4)$, we define a general 4D orthonormal rotation matrix with columns $\mathbf{W} = (w_0, w_1, w_2, w_3)$, etc., so the matrix takes the form $R_4 = [\mathbf{W}|\mathbf{X}|\mathbf{Y}|\mathbf{Z}]$, producing a numerical profile matrix of the form (taking into account the transpose in Eq. (110))

$$K_4(R_4) = \frac{1}{4} \begin{bmatrix} w_0 + x_1 + y_2 + z_3 & -w_1 + x_0 + y_3 - z_2 & -w_2 - x_3 + y_0 + z_1 & -w_3 + x_2 - y_1 + z_0 \\ w_1 - x_0 + y_3 - z_2 & w_0 + x_1 - y_2 - z_3 & -w_3 + x_2 + y_1 - z_0 & w_2 + x_3 + y_0 + z_1 \\ w_2 - x_3 - y_0 + z_1 & w_3 + x_2 + y_1 + z_0 & w_0 - x_1 + y_2 - z_3 & -w_1 - x_0 + y_3 + z_2 \\ w_3 + x_2 - y_1 - z_0 & -w_2 + x_3 - y_0 + z_1 & w_1 + x_0 + y_3 + z_2 & w_0 - x_1 - y_2 + z_3 \end{bmatrix}. \quad (111)$$

Now, from Eq. (15), we know that we also have an analog to Eq. (103), and for $R_4(p, q)$ this takes the remarkably compact algebraic form

$$K_4(p, q) = \begin{bmatrix} p_0q_0 & p_0q_1 & p_0q_2 & p_0q_3 \\ p_1q_0 & p_1q_1 & p_1q_2 & p_1q_3 \\ p_2q_0 & p_2q_1 & p_2q_2 & p_2q_3 \\ p_3q_0 & p_3q_1 & p_3q_2 & p_3q_3 \end{bmatrix}. \quad (112)$$

This matrix is exactly the outer product of p and q , with vanishing determinant, rank 1, and trace $(p \cdot q)$, which makes it extremely simple. The eigensystem is

$$\epsilon = \{p \cdot q, 0, 0, 0\} \quad (113)$$

$$r_{\text{right}} = \left\{ \begin{bmatrix} p_0 \\ p_1 \\ p_2 \\ p_3 \end{bmatrix}, \begin{bmatrix} -q_1 \\ q_0 \\ 0 \\ 0 \end{bmatrix}, \begin{bmatrix} -q_2 \\ 0 \\ q_0 \\ 0 \end{bmatrix}, \begin{bmatrix} -q_3 \\ 0 \\ 0 \\ q_0 \end{bmatrix} \right\} \quad (114)$$

$$\ell_{\text{left}} = \left\{ \begin{bmatrix} q_0 \\ q_1 \\ q_2 \\ q_3 \end{bmatrix}, \begin{bmatrix} -p_1 \\ p_0 \\ 0 \\ 0 \end{bmatrix}, \begin{bmatrix} -p_2 \\ 0 \\ p_0 \\ 0 \end{bmatrix}, \begin{bmatrix} -p_3 \\ 0 \\ 0 \\ p_0 \end{bmatrix} \right\}, \quad (115)$$

with an interesting swap between p and q in the zero eigenvectors, and the sole non-vanishing eigenvalue is just $\epsilon = \text{tr } K_4(p, q) = p \cdot q$, which is a convenient function of the numerical data. Thus the left and right eigenvectors can be easily computed from the numerical data in Eq. (111) using the eigenvalue extracted from the trace. Again, if a statistical distribution in the double quaternion space is desired, the signs can be chosen randomly, consistent with the sign of $\text{tr } K_4(R_4)$.

Once again, we can simply take the *numerical* value of the eigenvalue of $K_4(R_4)$, which is just the trace, and solve for the *right* eigenvector r_{right} , which will be the *left* quaternion p , and for the *left* eigenvector ℓ_{left} (the eigenvector of the transpose of $K_4(R_4)$), which will be the *right* quaternion q . We can either use any (normalized) adjugate column or just solve some permutation of the following linear equations directly for the eigenvectors. *No further computation is required.*

$$(K(R) - \text{tr } K(R) * I_4) \cdot \begin{bmatrix} 1 \\ v_1 \\ v_2 \\ v_3 \end{bmatrix} = 0 \quad p = r_{\text{opt}} = \text{normalize} \begin{bmatrix} 1 \\ v_1 \\ v_2 \\ v_3 \end{bmatrix} \quad (116)$$

$$((K(R))^t - \text{tr } K(R) * I_4) \cdot \begin{bmatrix} 1 \\ v'_1 \\ v'_2 \\ v'_3 \end{bmatrix} = 0 \quad q = \ell_{\text{opt}} = \text{normalize} \begin{bmatrix} 1 \\ v'_1 \\ v'_2 \\ v'_3 \end{bmatrix} \quad (117)$$

The solution to our problem is thus $R_4(p, q) = R_4(r_{\text{opt}}, \ell_{\text{opt}})$. As in 3D, if the numerical matrix R_4 has some moderate errors and the maximum eigenvalue *differs* significantly from $\text{tr } K(R)$, we can solve for the actual maximal eigenvalue and insert that into Eqs. (116) and (117) to find the left and right eigenvectors numerically.

There is one important caveat: the 3D quaternion rotation $R_3(q)$ does not care what the sign of q is, but the 4D quaternion rotation $R_4(p, q)$ is only invariant under *both* $p \rightarrow -p$ and $q \rightarrow -q$ in tandem. To ensure that $R_4(p, q)$ is the same matrix, the signs of the quaternions must be adjusted after the initial computation so that the sign of $(\ell \cdot r)$ matches the sign of the numerical input value of $R_{4(1,1)} = \text{tr } K_4(R_4) = p \cdot q$. That guarantees that the solution describes the same matrix that we used as input, and not its negative.

5 Two-Dimensional Limit of 3D Problem

All rotations of the type we have been trying to optimize reduce to a rotation in a 2D plane, which in 3D is defined by the plane perpendicular to the eigenvector $\hat{\mathbf{n}}$ of the rotation matrix Eq. (6). Data sets that are highly linear, determining a robust straight line from least squares, can even circumvent the RMSD problem entirely: a very good rotation matrix can be calculated from the direction $\hat{\mathbf{x}}$ determined by the line fitted to the data set $\{x_i\}$, and the similar direction $\hat{\mathbf{y}}$ corresponding to the reference data set $\{y_i\}$. An optimal rotation matrix in 3D is then simply

$$R(\theta, \hat{\mathbf{n}}) = R(\arccos(\hat{\mathbf{x}} \cdot \hat{\mathbf{y}}), \widehat{\hat{\mathbf{x}} \times \hat{\mathbf{y}}}), \quad (118)$$

which is easily generalized to any dimension by isolating just the projections of vectors to the plane determined by $\hat{\mathbf{x}}$ and $\hat{\mathbf{y}}$, and rotating in that 2D basis. Thus we conclude that, in general, if we had access to a prescient preconditioning rotation of the proper form, the entire RMSD problem would reduce to a very simple rotation in some 2D plane parameterized by a single angle. We can simulate

this, giving a massively simpler set of expressions, by assuming the data are coplanar, all having $z = 0$ (or more conditions in higher dimensions) and thus lying in the canonical $\{\hat{\mathbf{x}}, \hat{\mathbf{y}}\}$ plane, for example. This reduces our fundamental RMSD profile matrix Eq. (21) for M to

$$M_{z=0} = \begin{bmatrix} x+y & 0 & 0 & c \\ 0 & x-y & C & 0 \\ 0 & C & -x+y & 0 \\ c & 0 & 0 & -x-y \end{bmatrix}, \quad (119)$$

where $x = E_{xx}$, $y = E_{yy}$, $c = E_{xy} - E_{yx}$, and $C = E_{xy} + E_{yx}$. Then $p_2 = -c^2 - C^2 - 2(x^2 + y^2)$, $p_3 = 0$, and $p_4 = (c^2 + (x+y)^2)(C^2 + (x-y)^2)$, and similarly for the other cyclic cases, $x = 0$ and $y = 0$. The p_2 and p_4 are obviously functions of only two variables, $u = c^2 + (x+y)^2$ and $v = C^2 + (x-y)^2$, so we can write in general $p_2 = -u - v$ and $p_4 = uv$. The eigenvalue equation $\det[M - eI_4] = e^4 + e^3 p_1 + e^2 p_2 + e p_3 + p_4 = 0$ reduces to $e^4 + e^2 p_2 + p_4 = 0$ and the eigenvalues become $\epsilon = (\sqrt{u}, \sqrt{v}, -\sqrt{v}, -\sqrt{u})$, while the normalized (quaternion) eigenvectors become

$$q = \left\{ \left[\begin{array}{c} \frac{x+y+\sqrt{u}}{\sqrt{c^2+(x+y+\sqrt{u})^2}} \\ 0 \\ 0 \\ \frac{c}{\sqrt{c^2+(x+y+\sqrt{u})^2}} \end{array} \right], \left[\begin{array}{c} 0 \\ \frac{x-y+\sqrt{v}}{\sqrt{C^2+(x-y+\sqrt{v})^2}} \\ \frac{C}{\sqrt{C^2+(x-y+\sqrt{v})^2}} \\ 0 \end{array} \right], \left[\begin{array}{c} 0 \\ \frac{x-y-\sqrt{v}}{\sqrt{C^2+(x-y-\sqrt{v})^2}} \\ \frac{C}{\sqrt{C^2+(x-y-\sqrt{v})^2}} \\ 0 \end{array} \right], \left[\begin{array}{c} \frac{x+y-\sqrt{u}}{\sqrt{c^2+(x+y-\sqrt{u})^2}} \\ 0 \\ 0 \\ \frac{c}{\sqrt{c^2+(x+y-\sqrt{u})^2}} \end{array} \right] \right\}. \quad (120)$$

The leading eigenvalue and its eigenvector produce this optimal rotation in the $\{\hat{\mathbf{x}}, \hat{\mathbf{y}}\}$ plane:

$$R_{2D} = \begin{bmatrix} \frac{(x+y+\sqrt{u})^2 - c^2}{c^2 + (x+y+\sqrt{u})^2} & -\frac{2c(x+y+\sqrt{u})}{c^2 + (x+y+\sqrt{u})^2} \\ \frac{2c(x+y+\sqrt{u})}{c^2 + (x+y+\sqrt{u})^2} & \frac{(x+y+\sqrt{u})^2 - c^2}{c^2 + (x+y+\sqrt{u})^2} \end{bmatrix}. \quad (121)$$

Yet Another Form. However, we have neglected something. How does this look if we simply go back to the data matrices for 2D? Let us first write down the 2D version of Eq. (17), taking $E_{ab} = \sum_{k=1}^N [x_k]_a [y_k]_b$ for $a, b = \{1, 2\}$, so the raw form for the spatial RMSD task is to find the rotation matrix

$$R_2(\theta) = \begin{bmatrix} \cos \theta & -\sin \theta \\ \sin \theta & \cos \theta \end{bmatrix}$$

maximizing

$$\Delta_2 = \sum_{k=1}^N (R_2 \cdot x_k) \cdot y_k = \sum_{a=1, b=1}^2 R_2^{ba} E_{ab} = (E_{xx} + E_{yy}) \cos \theta + (E_{xy} - E_{yx}) \sin \theta. \quad (122)$$

We can either differentiate with respect to θ and set $\Delta_2'(\theta) = 0$, or simply observe directly that $\Delta_2(\theta)$ is largest when the vector $(\cos \theta, \sin \theta)$ is parallel to its coefficients; both arguments lead to the solution

$$\tan \theta = \frac{E_{xy} - E_{yx}}{E_{xx} + E_{yy}} = \frac{N}{M} \quad (123)$$

$$(\cos \theta, \sin \theta) = \left(\frac{M}{\sqrt{M^2 + N^2}}, \frac{N}{\sqrt{M^2 + N^2}} \right). \quad (124)$$

Now we can see that

$$\begin{aligned} x + y &= E_{xx} + E_{yy} &= M \\ c &= E_{xy} - E_{yx} &= N \\ u &= (E_{xx} + E_{yy})^2 + (E_{xy} - E_{yx})^2 &= M^2 + N^2 \\ \epsilon &= \lambda &= \pm \sqrt{M^2 + N^2}, \end{aligned} \quad (125)$$

and $c^2 + (x + y + \sqrt{u})^2 = 2\lambda(M + \lambda)$. Thus in fact the profile matrix becomes

$$\mathbf{M}_2 = \begin{bmatrix} M & N \\ N & -M \end{bmatrix} \quad (126)$$

and this has eigenvalues exactly $\epsilon = \pm\sqrt{u} = \pm\sqrt{M^2 + N^2}$. The eigenvectors are the first and last columns of Eq. (120) expressed in terms of Eq. (125), so the maximal eigenvector is (a, b) , where

$$\begin{aligned} a &= \cos(\theta/2) = \frac{\lambda + M}{\sqrt{2\lambda(\lambda + M)}} = \sqrt{\frac{\lambda + M}{2\lambda}} \\ b &= \sin(\theta/2) = \frac{N}{\sqrt{2\lambda(\lambda + M)}} = \text{sign } N \sqrt{\frac{\lambda - M}{2\lambda}}. \end{aligned} \quad (127)$$

(Note the crucial $(\text{sign } N)$ factor.) Going back to our original 2D rotation matrix in Eq. (121) and substituting Eq. (125), we recover our optimal result, namely

$$R_2(\theta) = \begin{bmatrix} \frac{M}{\sqrt{M^2 + N^2}} & -\frac{N}{\sqrt{M^2 + N^2}} \\ \frac{N}{\sqrt{M^2 + N^2}} & \frac{M}{\sqrt{M^2 + N^2}} \end{bmatrix} \quad (128)$$

$$= \begin{bmatrix} \cos \theta & -\sin \theta \\ \sin \theta & \cos \theta \end{bmatrix}. \quad (129)$$

These results are interesting to study because, despite the complexity of the general solution, the intrinsic algebraic structure of any RMSD problem is entirely characterized by a planar rotation such as that described by Eq. (121) and Eq. (128).

6 Evaluating the 3D Orientation Frame Solution.

The validity of our approximate chord-measures for determining the optimal global frame rotation can be evaluated by comparing their outcomes to the precise geodesic arc-length measure of Eq. (61). The latter is tricky to optimize, but choosing appropriate techniques, e.g., in the Mathematica `FindMinimum[]` utility, it is possible to determine good numerical solutions without writing custom code; in our experiments, fluctuations due to numerical precision limitations were noticeable, but presumably conventional conditioning techniques, which we have not attempted to explore, could improve that significantly. We employed a collection of 1000 simulated quaternion data sets of

length 100 for the reference cases, then imposed a normal distribution of random noise on the reference data, followed by a global rotation of all those noisy data points distributed around 45° to produce a corresponding collection of corresponding quaternion test data sets to be aligned. (Observe that we do *not* expect the optimal rotation angles to match the exact global rotations, though they will be nearby.)

We then collected the optimal quaternions for the following cases:

- (a) **Arc-Length (numerical).** This is the “gold standard,” modulo the occasional data pair that seems to challenge the numerical stability of the computation (which was to be expected). We obtained the data set (a) of quaternions that numerically minimized the nonlinear geodesic arc-length-squared measure of Eq. (61); this is in principle the best estimate one can possibly get for the optimal quaternion rotations to align a set of 3D test-frame triads with a corresponding set of reference-frame triads. There is no known way to find this set of optimal quaternions using our linear algebra methods.
- (b) **Chord-Length (numerical and algebraic).** This approach, designated as the data set (b), is based on the approximation to Eq. (17) illustrated in Fig 1, replacing the arc-length by the chord-length, which amounts to removing the arccosine and using the effective maximal cosines ($t \rightarrow \tilde{t}$) to define the measure. The form given in Eq. (71) is a minimization problem that is exactly the quaternion analog of the RMSD problem definition in Eq. (17) for spatial data, with the additional constraint that all the spatial data must be unit-length 4-vectors (which have only 3 degrees of freedom) instead of arbitrary 3-vectors. In addition, the convergence condition for clustering of the data within ball should in principle be satisfied for the optimal solution of Eq. (71) to be global; our data simulation pushes these limits, but in practice the convergence is typically satisfied. Just as Eq. (17) and its cross-term form Eq. (18) give exactly the same results for spatial data when the measures are minimized and maximized, respectively, the orientation-problem equations Eq. (71) and Eq. (72) do the same for the quaternion measure. Finally, the two cross-term forms Eq. (73) and Eq. (76) give the same optimal quaternions, with the interesting fact that Eq. (73) yields the optimal quaternion from a linear equation, and Eq. (76) gives an identical result from a quadratic matrix equation that works the same way as the RMSD matrix optimization, except that the symmetric profile matrix is no longer traceless.

Thus there are in fact four ways of looking at the chord-length measure and obtaining exactly the same optimal quaternions, and we have checked these using two numerical optimizations and two algebraic optimizations. These options are:

- **Minimizing Euclidean Chord-Length Squared.** Here we write the chord-approximation to the QFA problem using Eq. (71), which is exactly parallel to the RMSD problem employing Eq. (17), modulo the sign ambiguity issue. We test this by performing a numerical minimization.
- **Maximizing Chord-Length Cross-Term.** Just as the RMSD cross-term maximization problem Eq. (18) is equivalent to the RMSD minimization problem of Eq. (17), we can use maximization of the quaternion cross-term Eq. (72) equivalently with the minimization of the chord-length Eq. (71). We test this by performing a numerical maximization.
- **Linear Reduction of Chord-Length Cross-Term.** Pulling out the linear coefficients of the each quaternion component in Eq. (72) generates Eq. (73), where the 4-vector

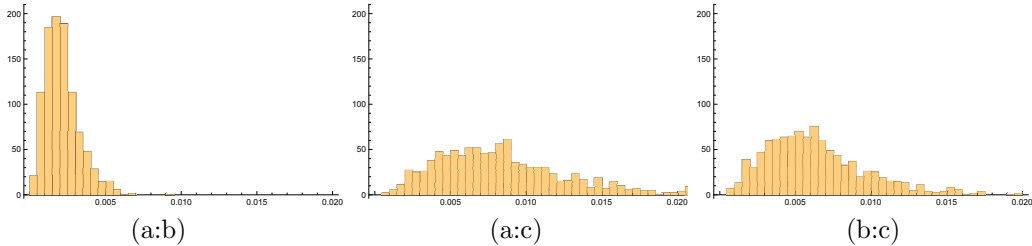


Figure 2: Spectrum in degrees of angular differences between optimal quaternion alignment rotations for quaternion frames. (a:b): (a) vs (b), true arc-length vs approximate quadratic chord-length measure. (a:c): (a) vs (c), true arc-length vs approximate quartic chord-length measure. (b:c): (b) vs (c), approximate quadratic vs approximate quartic chord-length measure.

$V_a(W)$ of Eq. (74) plays the role of the RMSD profile matrix $M_{ab}(E)$ in Eq. (20). Here we test the optimization by algebraically solving the linear expression Eq. (73).

- **Quadratic Equivalent Matrix Form of the Chord-Length Cross-Term.** Finally, there is in fact a maximal matrix eigenvalue problem Eq. (76) that works like Eq. (20) by squaring Eq. (73) to get a matrix problem $q \cdot \Omega \cdot q$ with $\Omega_{ab} = V_a V_b$. Despite the presence of a nonvanishing trace, the maximal quaternion eigenvectors are the same as the other three cases above. This produces the same optimal quaternion solutions as solving the (much, much simpler) linear problem of Eq. (73). This can also be checked algebraically.

- (c) **($\text{tr } \mathbf{R}(\mathbf{q}) \cdot \mathbf{R}(\mathbf{p}) \cdot \mathbf{R}(\bar{\mathbf{r}})$) Chord-Length (algebraic).** Finally, the most rigorous method if consistency of quaternion signs cannot be guaranteed is to use a measure in which algebraic squares occur throughout and enforce rigorous sign-independence. This is our (c) data set. Such measures must of necessity be *quartic* in the quaternion test and reference data, and thus are distinct from the measures of (b) that are *quadratic* in the data elements. This $(\text{tr } R(q) \cdot R(p) \cdot R(\bar{r}))$ measure is the form that is most easily integrated into the combined rotational-translational problem treated in the next section, because the combined matrices are both symmetric and traceless like the original RMSD profile matrices. Furthermore, it is obvious from Eq. (80) that this measure is exactly the same as the one obtained from Eq. (72) if we squared *each term in k* before summing the cross-term data elements in option (b). Thus, whichever actual formula we choose, we appear to have exhausted the options for quaternion-sign-independent quartic measures for the orientation data problem.

The task now is simply to evaluate how close the optimal quaternion solutions for the arc-length measure (a) are to the quadratic chord-length measures (b) and the quartic chord-length measures (c). In addition, we would like to know how close the fragile but very elegant quadratic measures (b) are to the rigorously sign-insensitive quartic measures (c); we expect them to be similar, but we do not expect them to be identical.

To quantify the closeness of the measures, we took the magnitude of the inner products between competing optimal quaternions for the same data set, which is essentially a cosine measure, took the arccosines, and converted to degrees. The results were histogrammed for 1000 random samples consisting of $N = 100$ data points, and are presented in Fig 2. The means and standard deviations

of the optimal total rotations relative to the identity frame for the three cases are:

Measure Type	Mean(deg)	Std Dev(deg)
(a) arc-length	44.8062	11.2307
(b) chord quadratic	44.8063	11.2308
(c) chord quartic	44.8065	11.2310

One can see that our simulated data set involved a large range of global rotations, and that all three methods produced a set of rotations back to the optimal alignment that are not significantly different statistically. We thus expect very little difference in the histograms of the case-by-case optimal quaternions produced by the three methods. The mean differences illustrated in the Figures are summarized as follows:

Figure:(Pair)	Mean(deg)	Std Dev(deg)
Figure 2 (a:b)	0.0021268	0.0011284
Figure 2 (a:c)	0.0084807	0.0044809
Figure 2 (b:c)	0.0063539	0.0033526

We emphasize that these numbers are in degrees for 1000 simulated samples with a distribution of global angles having a standard deviation of 11° . Thus we should have no issues using the chord approximation, though it does seem that the $q \cdot V$ measure is significantly better both in accuracy and simplicity of computation.

7 The 3D Combined Point+Frame Alignment Problem.

The 3D combined alignment problem for both spatial data and orientation-frame data involves a number of issues and subtleties that we were able to treat only superficially in the main text. In this section, we explore various options and evaluate their performance. This is necessary for anyone who might think of trying to attempt a combined alignment problem, so we have attempted to anticipate the questions and alternatives that might be explored and check their properties. The overall result is that it seems difficult to obtain significant additional information from the combined alignment strategies that we examined, so potential exploiters of this paradigm are forewarned.

From the main text, we are in possession of precise alignment procedures for both 3D spatial coordinates and 3D frame triad data (using the exact measure for the former and one of the approximate chord measures for the latter), and thus we can consider the full 6 degree-of-freedom alignment problem for combined data from a single structure. In fact this problem can also be solved in closed algebraic form given the our existing eigensystem formulation of the orientation alignment problem. While there are clearly appropriate domains of this type, e.g., any protein structure in the PDB database can be converted to a list of residue centers and their local frame triads [Hanson and Thakur, 2012], little is known at this time about the potential value of combined alignment. To establish the most complete possible picture, we now proceed to describe the details of our solution to the alignment problem for combined translational and rotational data.

In our treatment, we will assume the Δ_{RRR} measure since its profile matrix is traceless and manifestly independent of the quaternion signs, but there is no obstacle to using $\Delta_{\text{frame-sq}}$ if the data are properly prepared and one prefers the simpler measure. For notational simplicity, we will

let Δ_f stand for whatever orientation frame measure we have chosen, corresponding to Δ_x for the spatial measure, and thus we will denote the combined measure by Δ_{xf} .

The Combined Optimization Measure. A significant aspect of establishing a combined measure including the point measure Δ_x and the frame orientation measure Δ_f is the fact that the measures are *dimensionally incompatible*. We *cannot* directly combine the corresponding data minimization measures $\Delta_x(q_x) = \epsilon_{x:\max}$ and $\Delta_f(q_f) = \epsilon_{f:\max}$ because the spatial measure has dimensions of $(\text{length})^2$ and the frame measure is essentially a dimensionless trigonometric function (the arc-distance measure produces $(\text{radians})^2$, which is still incompatible).

While it should be obvious that a combined measure requires an arbitrary, problem-specific, interpolating constant with dimensions of length to produce a compatible measure, there has been some confusion in the molecular entropy literature, where such measures seem first to have been employed. These issues were resolved and dimensionful constants introduced, e.g., in the work of Fogolari, et al. [Fogolari et al., 2016, Huggins, 2014]. Our approach to defining a valid heuristic combined measure has three components:

- **Normalize the Profiles.** The numerical sizes of the maximal eigenvalues of the Δ_x and the Δ_f systems can easily differ by orders of magnitude. Since scaling the profile matrices changes the eigenvalues *but not the eigenvectors*, it is perfectly legitimate to start by dividing the profiles by their maximal eigenvalues before beginning the combined optimization, since this accomplishes the sensible effect of assigning maximal eigenvalues of exactly unity to both of our scaled profile matrices.
- **Interpolate between the Profiles.** To allow an arbitrary sensible weighting distinguishing between a location-dominated measure and an orientation-dominated measure, we simply incorporate a linear interpolation parameter $t \in [0, 1]$, with $t = 0$ singling out Δ_x and the pure (unit eigenvalue) location-based RMSD, and $t = 1$ singling out Δ_f and the pure orientation (unit eigenvalue) QFA solution.
- **Scale the Frame Profile.** Finally, we incorporate the mandatory dimensional scaling adjustment by incorporating one additional (nominally dimensional) parameter σ that scales the orientation parameter space described by Δ_f to be more or less important than the “canonical” spatial dimension component Δ_x , which we leave unscaled. That is, with $\sigma = 0$ only the spatial measure survives, with $\sigma = 1$, the normalized measures have equal contributions, and with $\sigma > 1$, the orientation measure dominates (this effectively undoes the original frame profile eigenvalue scaling).

We thus start with a combined spatial-rotational measure of the form

$$\begin{aligned}
\Delta_{\text{initial}} &= (1-t) \sum_{a=1,b=1}^3 R^{ba}(q) E_{ab} + t \sigma \sum_{a=1,b=1}^3 R^{ba}(q) S_{ab} \\
&= (1-t) \text{tr}(R(q) \cdot E) + t \sigma \text{tr}(R(q) \cdot S) \\
&= \sum_{a=0,b=0}^3 q_a [(1-t) M_{ab}(E) + t \sigma U_{ab}(S)] q_b \\
&= q \cdot [(1-t) M(E) + t \sigma U(S)] \cdot q,
\end{aligned} \tag{130}$$

Table 1: Offsets of sample data for the spatial vs orientation data used in exploring the properties of combined measures.

and then impose the unit-eigenvalue normalization on $M(E)$ and $U(S)$, giving our final measure as

$$\Delta_{xf}(t, \sigma) = q \cdot \left[(1-t) \frac{M(E)}{\epsilon_x} + t \sigma \frac{U(S)}{\epsilon_f} \right] \cdot q. \quad (131)$$

Because of the dimensional incompatibility of Δ_x and Δ_f , we have to treat the ratio

$$\lambda^2 = \frac{t\sigma}{1-t}$$

as a dimensional constant such as that adopted by Fogolari et al. [Fogolari et al., 2016] in their entropy calculations, so if t is dimensionless, then σ carries the dimensional scale information.

From the profile matrix of Eq. (131), we now extract our optimal rotation solution using the same equations as always, solving for the maximal eigenvalue and its eigenvector either numerically or algebraically, leading to the equivalent of Eq. (22), as we have solved the standard RMSD maximal eigenvalue problem. The result is a parameterized eigensystem

$$\left. \begin{array}{l} \epsilon_{\text{opt}}(t, \sigma) \\ q_{\text{opt}}(t, \sigma) \end{array} \right\} \quad (132)$$

yielding the optimal values $R(q_{\text{opt}}(t, \sigma))$, $\Delta_{xf} = \epsilon_{\text{opt}}(t, \sigma)$ based on the data $\{E, S\}$ no matter what we take as the values of the two variables (t, σ) .

Properties of the Combined Optimization. Substantially different features arise in the solutions depending on how close the optimal rotations were for the initial, separate, systems Δ_x and Δ_f . We now choose a selection of simulated data sets with the following choices of approximate initial global rotations of the test data sets relative to the reference data:

DATA ID	(Space, Orientation)	Measured Offset
Data Set 1	($22^\circ, -22^\circ$)	44.60
Data Set 2	($22^\circ, -11^\circ$)	21.98
Data Set 3	($22^\circ, 0^\circ$)	11.15
Data Set 4	($22^\circ, 11^\circ$)	11.15
Data Set 5	($22^\circ, 21^\circ$)	1.20

In Fig 3, we plot the trajectory of the maximal combined similarity measure for Data Set 1 as a function of t , showing the behavior for $\sigma = 1.0, 0.80$, and 1.15 . Figure 4 shows a more comprehensive representation of the continuous behavior with σ , and in both figures, we see that the true optima are *at the end points*, $t = 0, 1$, the locations associated with the pure profile eigenvector solutions $q_x(\text{opt})$ and $q_f(\text{opt})$. There is no *better* optimal eigenvector (i.e., global rotation) for any intermediate value of t . In some circumstances, however, it might be argued that it is appropriate to choose the *distinguished value* of t at the minimum of the curve $\Delta_{xf}(t, \sigma = 1)$. As we shall see in a moment, just as in Fig 3 for $\sigma = 1$, this point is generally within a few percent of $t = 0.5$. As the spatial and orientation optima get closer and closer, the curves in t become much flatter and less distinguished, while the variation in σ is qualitatively the same as in Fig 4.

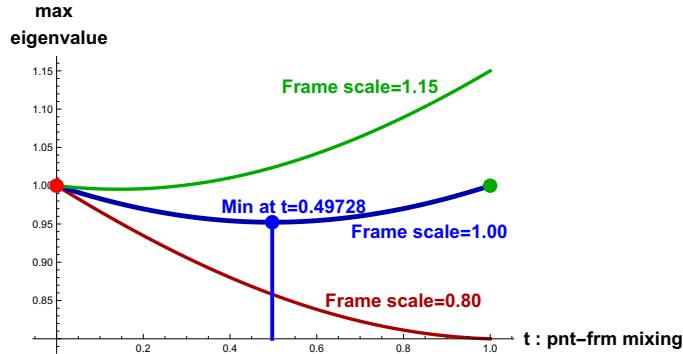


Figure 3: The blue curve is the path of the composite eigenvalue for Data Set 1 (the value of the similarity measure $\Delta_{xf}(t, 1)$) in the interpolation variable t with equally weighted space and orientation data, i.e., $\sigma = 1$. It has maxima only at the “pure” extremes at $t = 0, 1$, but there is a minimum that occurs, for these data, not at $t = 1/2$, but very nearby at $t = 0.49728$. Increasing the influence of the spatial data by taking $\sigma = 0.8$ gives the red curve, and increasing the influence of the orientation data by taking $\sigma = 1.15$ gives the green curve.

Finally, we examine one more amusing visualization of the properties of the composite solutions, restricting ourselves to $\sigma = 1$ for simplicity, and examining the “sideways warp” in the quaternion eigenvector $q_{\text{opt}}(t, \sigma = 1)$ in Eq. (132). We examine what happens to the combined similarity measure Eq. (131) if we smoothly interpolate from the identity matrix (that is, the quaternion $q_{\text{ID}} = (1, 0, 0, 0)$) through the optimal solution for each t and beyond the optimum by the same amount, using the *slerp* interpolation defined in Eq. (13), i.e., $q(s) = \text{slerp}(q_{\text{ID}}, q_{\text{opt}}(t, \sigma = 1), s)$. Figure 5 shows Data Set 1, with the largest relative spatial vs orientation angular differences, Figure 6 corresponds to the intervening Data Sets 2, 3, 4, and 5, with the Data Set parameters given above in Table 1. Data Set 5 in particular is perhaps the most realistic example, having nearly identical spatial and angular rotations, and we see negligible differences between the spatial and angular structures. These graphics also show how the local, non-optimal, neighboring quaternion values peak in s at the optimal ridge going from $t = 0$ to $t = 1$. The red dot is the maximum of Δ_x at $t = 0$, the green dot is the maximum of Δ_f at $t = 1$, and the blue dot, specific to each data set, is the distinguished point at the *minimum* of $\Delta_{xf}(t, \sigma = 1)$ in t , which for our data sets are always within 1% of $t = 0.5$. We observe that for equal and opposite rotations, the midpoint coincides almost exactly with the identity quaternion that occurs at the left and right boundaries of the plot. In other respects, the data in these figures show that we do not have *maxima* in the middle of the interpolation in t , but we do have a distinguished value, always very near $t = 0.5$, that could be used as a baseline for a hybrid translational-rotational rotation choice.

The Simple Approximation. Having now observed that it is possible to construct and solve a rigorous combined RMSD-QFA problem (with the chord-distance approximation in the angular measure), one might ask how that compares to the very simplest idea one might use to interpolate between the measures: what if we take the rigorous combined profile matrix defined by Eq. (131),

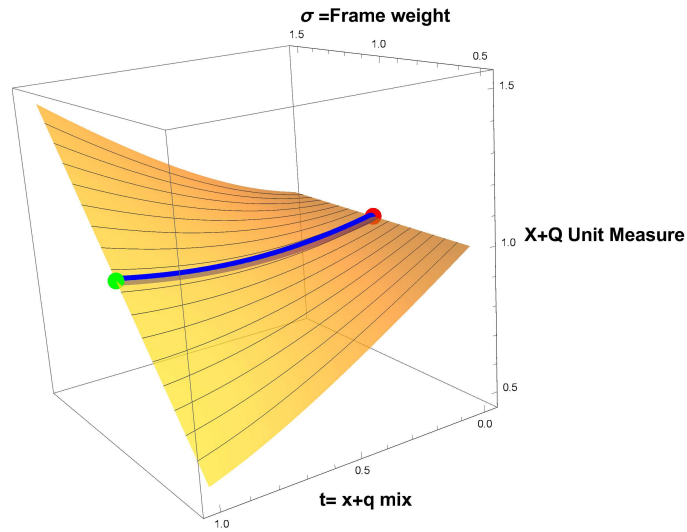


Figure 4: The $\Delta(t, \sigma)$ similarity-measure surface for Data Set 1 as a function of the interpolation parameter t and the relative scaling of the orientation term with σ , with the slightly concave curve at $\sigma = 1$ in the middle. The other data sets look very much like this one.

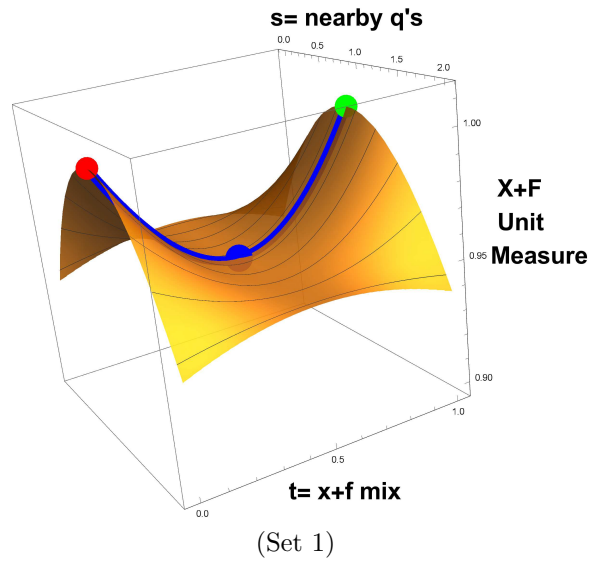


Figure 5: The $\Delta_{xf}(t, 1)$ similarity-measure surface for Data Set 1, x-angle 22° , f-angle -22° , and fixed $\sigma = 1$ showing the deviation with the quaternion varying perpendicularly around the solution $q(t)$, starting at the identity quaternion at $s = 0$, as a function of the interpolation parameter t . Since $q(t)$ is the maximal eigenvector, all variations in q peak there. Both have distinguished central points at $t \approx 0.5$.

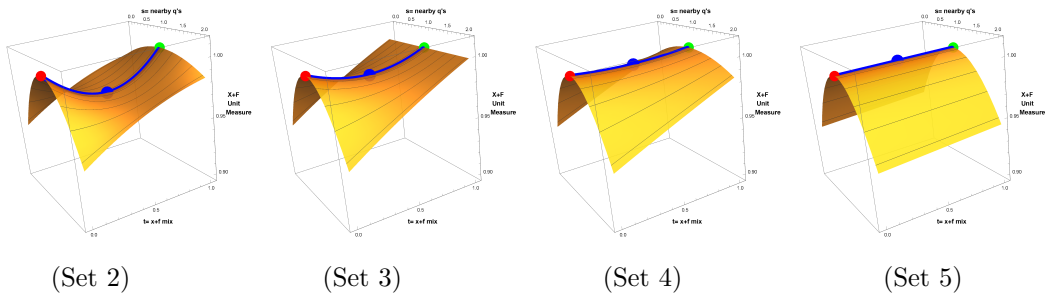


Figure 6: The $\Delta_{xf}(t, 1)$ similarity-measures with $q(s)$ interpolated from the identity through the optimum for Δ_{xf} and past to the identity-mirror point, for Data Sets 2, 3, 4, and 5, where Data Set 5 has the x-angle and the f-angle only one degree apart, as we might have for real experimental data.

Deviation of Slerp from Exact $\Delta(t)$

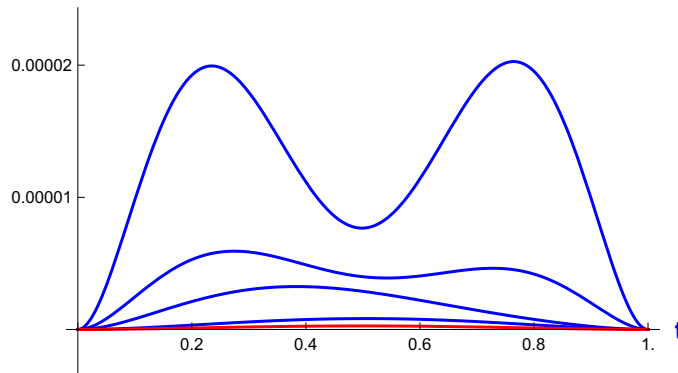


Figure 7: Here we see how close a simple $slerp(t)$ between the extremal optimal eigenvectors $q_{\text{opt}}(t = 0, \sigma = 1) = q_x(\text{opt})$ and $q_{\text{opt}}(t = 1, \sigma = 1) = q_f(\text{opt})$ is to the rigorous result where we optimized $q_{\text{opt}}(t, \sigma = 1)$ for all t . The differences are *relative to the unit eigenvalue*, and thus are of order thousandths of a percent, decreasing significantly as the global rotations applied to the space and orientation data approach one another. The largest deviation is for Data Set 1, which interestingly has a third minimum near the center in t ; for the highly similar data in Data Set 5, the difference shown in red had to be magnified by 100 even to show up on the graph.

compared to the *slerp* relating the two optimal eigenvectors of the independent spatial and orientation frame problems, that is

$$q(t) = \text{slerp}(q_{x:\text{opt}}, q_{f:\text{opt}}, t) . \quad (133)$$

Given the individual optimal eigenvectors, if we compare this simple $q(t)$ to Eq. (131) for any t (and $\sigma = 1$), we find that the differences are essentially negligible. In Fig 7, we plot the continuous differences of the similarity functions, which we recall are scaled to have a maximal eigenvalue equal to unity. These scaled differences are on the order of one thousandth of a percent or less as the global rotations applied to the spatial and rotational data become close to one another. We conclude that, for all practical purposes, we might as well use Eq. (133) to estimate the combined similarities.

A Details of the Algebraic Solutions to the Quartic Eigenvalue Problem

Given the data for the 3D or 4D test and reference structures, we can numerically solve for the maximal eigenvalue of $M_3(E_3)$ and its eigenvector in 3D, or the maximal eigenvalue of $G = M_4^t(E_4) \cdot M_4(E_4)$ and the left and right eigenvectors of G in 4D. Alternatively, we can apply the numerical SVD method directly to E_3 or E_4 to determine the optimal rotation matrix.

However, we can also work out the properties of the eigensystems of the various matrices that have come up in our treatment *algebraically*, using classic methods [Abramowitz and Stegun, 1970] for solving quartic polynomial equations for the eigenvalues, to provide deeper insights into the structure of the problem. We now study some features of these results in more detail, and in particular we consider real symmetric matrices, with and without a trace, since essentially every problem we have encountered reduces to finding the maximal eigenvalues of a matrix in that category.

The Eigenvalue Expansions. We begin by writing down the eigenvalue expansion of an arbitrary real 4D matrix M as

$$\det[M - eI_4] = 0 , \quad (134)$$

where e denotes a generic eigenvalue and I_4 is the 4D identity matrix. Our task is to express these eigenvalues, particularly the maximal eigenvalue, in terms of the elements of the matrix M , and also to find their eigenvectors.

By expanding Eq. (134) in powers of e , we see how the four eigenvalues $e = \epsilon_{k=1,\dots,4}$ depend on the known components of the matrix M and correspond to the solutions of the quartic equations that we can express in two useful forms,

$$e^4 + e^3 p_1 + e^2 p_2 + e p_3 + p_4 = 0 \quad (135)$$

$$(e - \epsilon_1)(e - \epsilon_2)(e - \epsilon_3)(e - \epsilon_4) = 0 . \quad (136)$$

Here the p_k are homogeneous polynomials of order k that can be expressed alternatively employing elements of M or elements of E for the 3D and 4D spatial data, or with the corresponding orientation-frame data. At this point we want to be as general as possible, and so we note the form valid for all 4×4 matrices M in the expansion of Eq. (134) and Eq. (135):

$$p_1(M) = -\text{tr}[M] \quad (137)$$

$$p_2(M) = -\frac{1}{2} \text{tr}[M \cdot M] + \frac{1}{2} (\text{tr}[M])^2 \quad (138)$$

$$p_3(M) = -\frac{1}{3} \text{tr}[M \cdot M \cdot M] + \frac{1}{2} \text{tr}[M \cdot M] \text{tr}[M] - \frac{1}{6} (\text{tr}[M])^3 \quad (139)$$

$$\begin{aligned} p_4(M) &= -\frac{1}{4} \text{tr}[M \cdot M \cdot M \cdot M] + \frac{1}{3} \text{tr}[M \cdot M \cdot M] \text{tr}[M] + \frac{1}{8} \text{tr}([M \cdot M])^2 - \frac{1}{4} \text{tr}[M \cdot M] (\text{tr}[M])^2 + \frac{1}{24} (\text{tr}[M])^4 \\ &= \det[M] . \end{aligned} \quad (140)$$

Remember that for our problem, M is just a real symmetric numerical matrix, and the four expressions $p_k(M)$ are also just a list of real numbers.

Matching the coefficients of powers of e in Eqs. (135) and (136), we can also eliminate e to express the the matrix data expressions p_k in terms of the symmetric polynomials of the eigenvalues ϵ_k as

[Abramowitz and Stegun, 1970]

$$\left. \begin{aligned} p_1 &= -\epsilon_1 - \epsilon_2 - \epsilon_3 - \epsilon_4 \\ p_2 &= \epsilon_1\epsilon_2 + \epsilon_1\epsilon_3 + \epsilon_2\epsilon_3 + \epsilon_1\epsilon_4 + \epsilon_2\epsilon_4 + \epsilon_3\epsilon_4 \\ p_3 &= -\epsilon_1\epsilon_2\epsilon_3 - \epsilon_1\epsilon_2\epsilon_4 - \epsilon_1\epsilon_3\epsilon_4 - \epsilon_2\epsilon_3\epsilon_4 \\ p_4 &= \epsilon_1\epsilon_2\epsilon_3\epsilon_4 \end{aligned} \right\}. \quad (141)$$

Both Eq. (135) and Eq. (141) can in principle be solved directly for the eigenvalues in terms of the matrix data using the solution of the quartic published by Cardano in 1545 and investigated further by Euler [Euler, 1733, Bell, 2008, Nickalls, 2009] (see also [Abramowitz and Stegun, 1970, Weisstein, 2019, Nickalls, 1993, Wikipedia:Cardano, 2019]). Applying, e.g., the Mathematica function

$$\text{Solve}[\text{myQuarticEqn}[e] == 0, e, \text{Quartics} \rightarrow \text{True}] \quad (142)$$

to Eq. (135) immediately returns a usable algebraic formula. However, applying `Solve[]` to Eq. (141) is in fact unsuccessful, although invoking `Reduce[pkofepsEqns, {\epsilon_1, \epsilon_2, \epsilon_3, \epsilon_4}, Quartics \rightarrow True, Cubics \rightarrow True]` can solve Eq. (141) iteratively and produces the same final answer that we obtain from Eq. (135), as does using a Gröbner basis based on Eq. (141).

In the main paper, we presented a robust algebraic solution that could be evaluated numerically for the quaternion eigenvalues in the special case of a symmetric traceless 4×4 profile matrix $M_3(E_3)$ based on the 3D cross-covariance matrix E_3 ; we will complete the steps deriving that solution below. But first we will study general 4×4 real matrices, and then specialize to symmetric matrices with and without a trace, as all of our cases of interest are of this type. We note [Golub and van Loan, 1983] that any nonsingular real matrix that can be written in the form $[S^t \cdot S]$ is itself symmetric and has only positive real eigenvalues; in general, the symmetric matrices $[S^t \cdot S]$ and $[S \cdot S^t]$ share one set of eigenvalues, but have distinct eigenvectors. Thus, even if we study only symmetric matrices, we can get significant information about *any* matrix S as long as we can recast our investigation to exploit the associated symmetric matrices $[S^t \cdot S]$ and $[S \cdot S^t]$.

The Basic Structure: Standard Algebraic Solutions for 4D Eigenvalues. When we solve Eq. (135) directly using the textbook quartic solution without explicitly imposing restrictions, we find that the general structure for the eigenvalues $e = \epsilon_k(p_1, p_2, p_3, p_4)$ takes the form

$$\left. \begin{aligned} \epsilon_1(p) &= -\frac{p_1}{4} + F(p) + G_+(p) & \epsilon_2(p) &= -\frac{p_1}{4} + F(p) - G_+(p) \\ \epsilon_3(p) &= -\frac{p_1}{4} - F(p) + G_-(p) & \epsilon_4(p) &= -\frac{p_1}{4} - F(p) - G_-(p) \end{aligned} \right\}. \quad (143)$$

Here $-p_1 = (\epsilon_1 + \epsilon_2 + \epsilon_3 + \epsilon_4)$ is the trace, and we can see that “canonical form” for the quartic Eq. (135), with a missing cubic term in e , results from simply changing variables from $e \rightarrow e + (\epsilon_1 + \epsilon_2 + \epsilon_3 + \epsilon_4)/4$ to effectively add $1/4$ of the trace to each eigenvalue. The other two types of

terms have the following explicit expressions in terms of the four independent coefficients p_k :

$$\left. \begin{aligned}
F(p_1, p_2, p_3, p_4) &= \sqrt{\frac{p_1^2}{16} - \frac{p_2}{6} + \frac{1}{12} \left(\sqrt[3]{a + \sqrt{-b^2}} + \frac{r^2}{\sqrt[3]{a + \sqrt{-b^2}}} \right)} \\
G_{\pm}(p_1, p_2, p_3, p_4) &= \sqrt{\frac{3p_1^2}{16} - \frac{p_2}{2} - F^2(p) \pm \frac{s(p)}{32 F(p)}} \\
&= \sqrt{\frac{p_1^2}{8} - \frac{p_2}{3} - \frac{1}{12} \left(\sqrt[3]{a + \sqrt{-b^2}} + \frac{r^2}{\sqrt[3]{a + \sqrt{-b^2}}} \right) \pm \frac{s(p)}{32 \sqrt{\frac{p_1^2}{16} - \frac{p_2}{6} + \frac{1}{12} \left(\sqrt[3]{a + \sqrt{-b^2}} + \frac{r^2}{\sqrt[3]{a + \sqrt{-b^2}}} \right)}}}
\end{aligned} \right\} \quad (144)$$

with

$$\left. \begin{aligned}
r^2(p_1, p_2, p_3, p_4) &= p_2^2 - 3p_1p_3 + 12p_4 = \sqrt[3]{a^2 + b^2} \\
a(p_1, p_2, p_3, p_4) &= p_2^3 + \frac{9}{2} (3p_3^2 + 3p_1^2p_4 - p_1p_2p_3 - 8p_2p_4) \\
b^2(p_1, p_2, p_3, p_4) &= r^6(p) - a^2(p) \\
s(p_1, p_2, p_3, p_4) &= 4p_1p_2 - p_1^3 - 8p_3
\end{aligned} \right\} . \quad (145)$$

For general real matrices, which may have complex conjugate pairs of eigenvalues, the sign of r^2 can play a critical role, so giving in to the temptation to write

$$\frac{r^2}{\sqrt[3]{a + \sqrt{-b^2}}} \rightarrow \sqrt[3]{a - \sqrt{-b^2}}$$

leads to anomalies; in addition, b^2 can take on any value, so evaluating this algebraic expression numerically while getting the phases of all the roots right can be problematic. So far as we can confirm, setting aside matrices with individual peculiarities, the formula Eq. (143) yields correct complex eigenvalues for all real matrices, though the numerical order of the eigenvalues can be irregular. When we restrict our attention to real symmetric matrices, a number of special constraints come into play that significantly improve the numerical behavior of the algebraic solutions, as well as allowing us to simplify the algebraic expression itself. The real symmetric matrices are all that concern us for any of the alignment problems.

Symmetric Matrices. We restrict our attention from here on to general symmetric 4×4 real matrices, for which the eigenvalues must be real, and so the roots of the matrix's quartic characteristic polynomial must be real. A critical piece of information comes from the fact that the quartic roots are based on an underlying cube root solution (a careful examination of how this works can be found, for example, in [Coutsias et al., 2004, Coutias and Wester, 2019, Nickalls, 2009]). As noted. e.g., in [Abramowitz and Stegun, 1970], the roots of this cubic are *real* provided that a particular discriminant is *negative*. This expression takes the form

$$q_{AS}^3 + r_{AS}^2 \leq 0 ,$$

where {AS} disambiguates the Abramowitz-Stegun variable names, and the relationship to our parameterization in terms of the eigenequation coefficients p_k is simply

$$q_{\text{AS}} = -\frac{1}{9} r^2(p_1, p_2, p_3, p_4), \quad r_{\text{AS}} = \frac{1}{27} a(p_1, p_2, p_3, p_4). \quad (146)$$

Thus we can see from Eq. (145) that

$$b^2(p_1, p_2, p_3, p_4) = r^6(p) - a^2(p) = -9^3 (q_{\text{AS}}^3 + r_{\text{AS}}^2), \quad (147)$$

and hence for symmetric real matrices we must have $b^2(p) \geq 0$. Therefore for this case we can always write

$$(a(p) + \sqrt{-b(p)^2}) \rightarrow (a + ib), \quad (148)$$

and then we can rephrase our general solution from Eqs. (143), (144), and (145) as

$$\left. \begin{aligned} F(p_1, p_2, p_3, p_4) &= \sqrt{\frac{p_1^2}{16} - \frac{p_2}{6} + \frac{1}{6} r(p) c(a, b)} \\ G_{\pm}(p_1, p_2, p_3, p_4) &= \sqrt{\frac{p_1^2}{8} - \frac{p_2}{3} - \frac{1}{6} r(p) c(a, b) \pm \frac{s(p)}{32 \sqrt{\frac{p_1^2}{16} - \frac{p_2}{6} + \frac{1}{6} r(p) c(a, b)}}} \\ &= \sqrt{\frac{3p_1^2}{16} - \frac{p_2}{2} - F^2(p) \pm \frac{s(p)}{32 F(p)}} \end{aligned} \right\}, \quad (149)$$

where the cube root terms can now be reduced to real-valued trigonometry:

$$\left. \begin{aligned} r(p) c(a, b) &= r(p) \cos\left(\frac{\arg(a + ib)}{3}\right) = \frac{1}{2} \left((a + ib)^{1/3} + (a - ib)^{1/3} \right) \\ r^2(p) &= p_2^2 - 3p_1 p_3 + 12p_4 = \sqrt[3]{a^2 + b^2} = (a + ib)^{1/3} (a - ib)^{1/3} \\ r^6(p) &= a^2(p) + b^2(p) \\ s(p) &= 4p_1 p_2 - p_1^3 - 8p_3 \end{aligned} \right\}. \quad (150)$$

Alternative Method: The Cube Root Triples Method and Its Properties. Our first general method above corresponds directly to [Abramowitz and Stegun, 1970], and consists of combinations of signs in two blocks of expressions. The second method that we are about to explore uses sums of three expressions in all four eigenvalues, with each term having a square root ambiguity; this is fundamentally Euler’s solution, discussed, for example, in [Coutsias et al., 2004, Coutias and Wester, 2019] and [Nickalls, 2009]. The correspondence between this triplet and the four expressions in Eq. (149) is delicate, but deterministic, and we will show the argument leading to the equations we introduced in the main text.

The “Cube Root Triple” method follows from the observation that if we break up the general form of the four quartic eigenvalues into a trace part and a sum of three identical parts whose signs are arranged to be traceless, we find an equation that can be easily solved, and which (under some conditions that we will remove) evaluates numerically to the same eigenvalues as Eq. (149), but can

be expressed in terms of a one-line formula for the eigenvalue system. The Ansatz that we start with is the following:

$$\left. \begin{aligned} \epsilon_1 &\stackrel{?}{=} -\frac{p_1}{4} + \sqrt{X} + \sqrt{Y} + \sqrt{Z} \\ \epsilon_2 &\stackrel{?}{=} -\frac{p_1}{4} + \sqrt{X} - \sqrt{Y} - \sqrt{Z} \\ \epsilon_3 &\stackrel{?}{=} -\frac{p_1}{4} - \sqrt{X} + \sqrt{Y} - \sqrt{Z} \\ \epsilon_4 &\stackrel{?}{=} -\frac{p_1}{4} - \sqrt{X} - \sqrt{Y} + \sqrt{Z} \end{aligned} \right\}. \quad (151)$$

If we now insert our expressions for $\epsilon_k(p_1, X, Y, Z)$ from Eq. (151) into Eq. (141), we see that the p_k equations are transformed into a quartic system of equations that can in principle be solved for the components of the eigenvalues,

$$\left. \begin{aligned} p_1 &= p_1 \\ p_2 &= \frac{3p_1^2}{8} - 2(X + Y + Z) \\ p_3 &= \frac{p_1^3}{16} - 8\sqrt{XYZ} - p_1(X + Y + Z) \\ p_4 &= \frac{p_1^4}{256} + X^2 + Y^2 + Z^2 - 2(YZ + ZX + XY) - p_1\sqrt{XYZ} - \frac{p_1^2}{8}(X + Y + Z) \end{aligned} \right\}. \quad (152)$$

While our original equation Eq. (141) does not respond to `Solve[... , { $\epsilon_1, \epsilon_2, \epsilon_3, \epsilon_4$ }, ...]`, and Eq. (152) with $X \rightarrow u^2, Y \rightarrow v^2, Z \rightarrow w^2$ does not respond to `Solve[... , { u, v, w }, ...]`, for some reason Eq. (152) with X, Y, Z as the free variables responds immediately to `Solve[pkEqnList , { X, Y, Z }, Quartics \rightarrow True]`, and produces a solution for $X(p), Y(p),$ and $Z(p)$ that we can manipulate into the following form,

$$F_f(p) = \frac{p_1^2}{16} - \frac{p_2}{6} - \frac{1}{12} \left(\phi(f) \left(a(p) + \sqrt{-b^2(p)} \right)^{1/3} + \frac{r^2(p)}{\phi(f) \left(a(p) + \sqrt{-b^2(p)} \right)^{1/3}} \right). \quad (153)$$

Here $F_f(p)$ with $f = (x, y, z)$ represents $X(p), Y(p),$ or $Z(p)$ corresponding to one of the three values of the cube roots $\phi(f)$ of (-1) given by

$$\phi(x) = -1, \quad \phi(y) = \frac{1}{2}(1 + i\sqrt{3}), \quad \phi(z) = \frac{1}{2}(1 - i\sqrt{3}), \quad (154)$$

and the utility functions are defined as above in Eq. (145). Once again, because we have symmetric real matrices with real eigenvalues, we know that the discriminant condition for real solutions requires $b^2(p) \geq 0$, so we can again apply Eq. (148) to transform each $\left(a(p) \pm \sqrt{-b^2(p)} \right)$ term into the form $(a(p) \pm ib(p))$. This time we get a slightly different formula because there is a different $\sqrt[3]{-1}$ phase incorporated into each of the X, Y, Z terms, and we obtain the following intermediate result:

$$F_f(p) = \frac{p_1^2}{16} - \frac{p_2}{6} - \frac{1}{12} \left(\phi(f) (a + ib)^{1/3} + r^2(p) \frac{1}{\phi(f) (a + ib)^{1/3}} \right)$$

$$= \frac{p_1^2}{16} - \frac{p_2}{6} - \frac{1}{6} \left(\phi(f)(a+ib)^{1/3} + \overline{\phi(f)}(a-ib)^{1/3} \right) \quad (155)$$

$$= \frac{p_1^2}{16} - \frac{p_2}{6} - \frac{1}{6} \left(\phi(f)(a+ib)^{1/3} + \overline{\phi(f)(a+ib)^{1/3}} \right) , \quad (156)$$

where $\overline{\phi(f)}$, etc., denotes the complex conjugate, and we took advantage of the relation $\sqrt[3]{a^2+b^2} = r^2(p)$. The cube root terms again reduce to real trigonometry, giving our final result (remember that $\phi(x) = -1$, changing the sign)

$$F_f(p_1, p_2, p_3, p_4) = \frac{p_1^2}{16} - \frac{p_2}{6} + \frac{1}{6} \left(r(p) \cos_f(p) \right) , \quad (157)$$

but now with the direct incorporation of the three phases of $\sqrt[3]{-1}$ from Eq. (154) (see, e.g., [Nickalls, 1993]), we get nothing but phase-shifted real cosines,

$$\cos_x(p) = \cos\left(\frac{\arg(a+ib)}{3}\right), \quad \cos_y(p) = \cos\left(\frac{\arg(a+ib)}{3} - \frac{2\pi}{3}\right), \quad \cos_z(p) = \cos\left(\frac{\arg(a+ib)}{3} + \frac{2\pi}{3}\right). \quad (158)$$

The needed subset of the utility functions now reduces to

$$\left. \begin{aligned} r^2(p_1, p_2, p_3, p_4) &= p_2^2 - 3p_1p_3 + 12p_4 = \sqrt[3]{a^2+b^2} = (a+ib)^{1/3}(a-ib)^{1/3} \\ a(p_1, p_2, p_3, p_4) &= p_2^3 + \frac{9}{2}(3p_3^2 + 3p_1^2p_4 - p_1p_2p_3 - 8p_2p_4) \\ b^2(p_1, p_2, p_3, p_4) &= r^6(p) - a^2(p) \end{aligned} \right\} . \quad (159)$$

Repairing Anomalies in the Cube Root Triple Form. We are not quite finished, as our X, Y, Z triplets acquire an ambiguity due to possible alternate sign choices when we take the square roots of X, Y, Z to construct the eigenvalues themselves using the Ansatz of Eq. (151). As long as all the terms of one part change sign together, the tracelessness of the X, Y, Z segment of the eigenvalue system is maintained, so there are a number of things that could happen with the signs without invalidating the general properties of Eq. (151). We can check that, with random symmetric matrix data, Eq. (151) with Eq. (157) will yield the correct eigenvalues about half the time, while Eq. (143) with Eq. (149) always works. Inspecting Eq. (149) and Eq. (157) with Eq. (158), we observe that $F(p_1, p_2, p_3, p_4) = \sqrt{F_x(p_1, p_2, p_3, p_4)} = \sqrt{X}$; we can also see that Eq. (149) suggests that a relation of the following form should hold,

$$G_{\pm}(p_1, p_2, p_3, p_4) \sim \sqrt{Y} \pm \sqrt{Z} ,$$

so we can immediately conjecture that something is going wrong with the sign choice of the root \sqrt{Z} . It turns out that $G_+(p)$ changes its algebraic structure to essentially that of $G_-(p)$ when the numerator $s(p) = (4p_1p_2 - p_1^3 - 8p_3)$ inside the square root in Eq. (149) changes sign. That tells us exactly where there is a discrepancy with the choice $\sqrt{Y} + \sqrt{Z}$. If we define the following sign test,

$$\sigma(p_1, p_2, p_3, p_4) = \text{sign}(4p_1p_2 - p_1^3 - 8p_3) , \quad (160)$$

we discover that we can make Eq. (151) agree exactly with the robust $G_{\pm}(p)$ from Eq. (149) for all the random symmetric numerical matrices we were able to test, provided we make the following

simple change to the final form of the X, Y, Z formula for the eigenvalue solutions:

$$\left. \begin{aligned} \epsilon_1 &= -\frac{p_1}{4} + \sqrt{X} + \sqrt{Y} + \sigma(p)\sqrt{Z} \\ \epsilon_2 &= -\frac{p_1}{4} + \sqrt{X} - \sqrt{Y} - \sigma(p)\sqrt{Z} \\ \epsilon_3 &= -\frac{p_1}{4} - \sqrt{X} + \sqrt{Y} - \sigma(p)\sqrt{Z} \\ \epsilon_4 &= -\frac{p_1}{4} - \sqrt{X} - \sqrt{Y} + \sigma(p)\sqrt{Z} \end{aligned} \right\}. \quad (161)$$

Algebraic Equivalence of Standard and Cube Root Triple Form. With the benefit of hindsight, we now complete the picture by working out the algebraic properties of Eq. (143) and Eq. (144) that confirm our heuristic derivation of Eq. (161). First, we look back at Eq. (152) and discover that, using the relations for p_2 and p_3 , we can incorporate $X + Y + Z = 3p_1^3/16 - p_2/2$ into p_3 to get a very suggestive form for our expression $s(p)$ from Eq. (145) in terms of the only square-root ambiguity in our original equations that we used to solve for $(X(p), Y(p), Z(p))$, which is

$$s(p_1, p_2, p_3, p_4) = 4p_1p_2 - p_1^3 - 8p_3 = 64\sqrt{X(p)Y(p)Z(p)}. \quad (162)$$

Already we see that this is potentially nontrivial because $s(p)$ does not have a deterministic sign, but $\sqrt{X(p)Y(p)Z(p)}$ will always be positive unless we have a deterministic reason to choose the negative root.

Next, using Eq. (153), we recast Eq. (144) in a form that uses $F(p) \equiv \sqrt{X(p)} \equiv \sqrt{F_x(p)}$, as well as Eq. (162), to give

$$\left. \begin{aligned} F(p_1, p_2, p_3, p_4) &= \sqrt{X(p_1, p_2, p_3, p_4)} \\ &= \sqrt{\frac{p_1^2}{16} - \frac{p_2}{6} + \frac{1}{12} \left(\sqrt[3]{a - \sqrt{-b^2}} + \sqrt[3]{a + \sqrt{-b^2}} \right)} \\ G_{\pm}(p_1, p_2, p_3, p_4) &= \sqrt{\frac{3p_1^2}{16} - \frac{p_2}{2} - F^2(p) \pm \frac{s(p)}{32 F(p)}} \\ &= \sqrt{A(p_1, p_2, p_3, p_4) \pm B(p_1, p_2, p_3, p_4)} \end{aligned} \right\} \quad (163)$$

where in fact we know a bit about how $B(p)$ should look:

$$B(p) = \frac{s(p)}{32 \sqrt{X(p)}}. \quad (164)$$

Now we solve the equations

$$\sqrt{A(p) \pm B(p)} = \sqrt{Y} \pm \sigma(p)\sqrt{Z} \quad (165)$$

for $A(p)$ and $B(p)$, to discover

$$\begin{aligned} A(p) &= Y(p) + \sigma^2 Z(p) \\ &= Y(p) + Z(p) \end{aligned} \quad (166)$$

$$B(p) = 2\sigma\sqrt{Y(p)Z(p)}, \quad (167)$$

where we note that these useful relations are nontrivial to discover *directly* from our original expressions for $F(p)$ and $G_{\pm}(p)$. Finally, using Eq. (164), we conclude that

$$s(p) = 64 \sigma(p) \sqrt{X(p)Y(p)Z(p)} , \quad (168)$$

which confirms that the appearance of

$$\sigma(p) = \text{sign}(s(p)) = \text{sign}(4p_1p_2 - p_1^3 - 8p_3) \quad (169)$$

in the (X, Y, Z) expression of Eq. (161) is rigorous and inevitable, as it can be deduced directly from its appearance in $B(p)$.

Alternative Reduction of the Quartic Solution. Perhaps a more explicit way to connect the (F, G_{\pm}) and (X, Y, Z) forms, and one we might have used from the beginning with further insight, is to observe that G_{\pm} is actually the square root of a perfect square,

$$\left. \begin{aligned} G_{\pm} &= \sqrt{\left(\sqrt{Y} \pm \sigma\sqrt{Z}\right)^2} \\ &= \sqrt{Y + Z \pm 2\sigma\sqrt{YZ}} \\ &= \sqrt{Y + Z \pm 2\sigma\frac{\sqrt{XYZ}}{\sqrt{X}}} \\ &= \sqrt{Y + Z \pm 2\sigma\frac{64\sqrt{XYZ}}{64\sqrt{X}}} \\ &= \sqrt{Y + Z \pm 2\sigma\frac{|s(p)|}{64\sqrt{X}}} \\ &= \sqrt{Y + Z \pm \frac{s(p)}{32\sqrt{X(p)}}} \end{aligned} \right\} , \quad (170)$$

where we used the fact that $\sigma(p)|s(p)| = s(p)$. As long as the sign with which G_{\pm} enters into the solution is consistent, the alternative overall signs of the radicals in Eq. (170) will be included correctly.

The Traceless Triple Form. The explicitly traceless X, Y, Z triplet form that corresponds to a set of eigenvalues in descending magnitude order that we introduced for the 3D RMSD problem in the main text is obtained by imposing the traceless condition, $p_1 = 0$, obeyed by the 3D profile matrix $M_3(E_3)$:

$$\left. \begin{aligned} \epsilon_1 &= +\sqrt{X} + \sqrt{Y} + \sigma(p)\sqrt{Z} \\ \epsilon_2 &= +\sqrt{X} - \sqrt{Y} - \sigma(p)\sqrt{Z} \\ \epsilon_3 &= -\sqrt{X} + \sqrt{Y} - \sigma(p)\sqrt{Z} \\ \epsilon_4 &= -\sqrt{X} - \sqrt{Y} + \sigma(p)\sqrt{Z} \end{aligned} \right\} . \quad (171)$$

Then Eq. (152) simplifies to

$$p_1 = 0 \quad (172)$$

$$p_2 = -2(X + Y + Z) \quad (173)$$

$$p_3 = -8\sigma(p)\sqrt{XYZ} \quad (174)$$

$$p_4 = X^2 + Y^2 + Z^2 - 2(YZ + ZX + XY) , \quad (175)$$

and the solutions for $X(p)$, $Y(p)$, and $Z(p)$ (and thus for $\epsilon_k(p)$) reduce to:

$$F_f(p_2, p_3, p_4) = +\frac{1}{6} \left(r(p) \cos_f(p) - p_2 \right) , \quad (176)$$

where the phased cosine terms retain their form

$$\cos_x(p) = \cos\left(\frac{\arg(a+ib)}{3}\right), \quad \cos_y(p) = \cos\left(\frac{\arg(a+ib)}{3} - \frac{2\pi}{3}\right), \quad \cos_z(p) = \cos\left(\frac{\arg(a+ib)}{3} + \frac{2\pi}{3}\right). \quad (177)$$

Here $F_f(p)$ with $f = (x, y, z)$ as always represents $X(p)$, $Y(p)$, or $Z(p)$ and the utility functions simplify to

$$\left. \begin{aligned} \sigma(p_3) &= \text{sign}(-p_3) \\ r^2(p_2, p_3, p_4) &= p_2^2 + 12p_4 = \sqrt[3]{a^2 + b^2} = (a+ib)^{1/3}(a-ib)^{1/3} \\ a(p_2, p_3, p_4) &= p_2^3 + \frac{9}{2}(3p_3^2 - 8p_2p_4) \\ b^2(p_2, p_3, p_4) &= r^6(p) - a^2(p) \\ &= \frac{27}{4}(16p_4p_2^4 - 4p_3^2p_2^3 - 128p_4^2p_2^2 + 144p_3^2p_4p_2 - 27p_3^4 + 256p_4^3) \end{aligned} \right\} . \quad (178)$$

Summary: We therefore have two alternate robust expressions, Eq. (143) with Eq. (149) and Eq. (161) with Eq. (157), for the entire eigenvalue spectrum of any real, symmetric 4×4 matrix M characterized by its four intrinsic eigenequation coefficients (p_1, p_2, p_3, p_4) . For the simpler traceless case, we can take advantage of Eq. (171) with Eq. (176).

References

- [Abramowitz and Stegun, 1970] Abramowitz, M. and Stegun, I. (1970). *Handbook of mathematical functions*. Dover Publications Inc., New York. Pages 17–18.
- [Bar-Itzhack, 2000] Bar-Itzhack, I. Y. (2000). New method for extracting the quaternion from a rotation matrix. *Journal of Guidance, Control, and Dynamics*, 23(6):1085–1087.
- [Bell, 2008] Bell, J. (1733(2008)). A conjecture on the forms of the roots of equations. *An English translation of Euler's De formis radicum aequationum cujusque ordinis conjectatio*.
- [Coutsias et al., 2004] Coutsiias, E., Seok, C., and Dill, K. (2004). Using quaternions to calculate RMSD. *J Comput Chem.*, 25(15):1849–1857.

- [Coutsias and Wester, 2019] Coutsiias, E. and Wester, M. (2019). Rmsd and symmetry. *J Comput Chem.*, 40(15):1496–1508.
- [Euler, 1733] Euler, L. (1733). De formis radicum aequationum cujusque ordinis conjectatio. *Commentarii academiae scientiarum imperialis Petropolitanae*, 6:216–231.
- [Fogolari et al., 2016] Fogolari, F., Fomthum, C. J. D., Fortuna, S., Soler, M. A., Corazza, A., and Esposito, G. (2016). Accurate estimation of the entropy of rotationtranslation probability distributions. *Journal of Chemical Theory and Computation*, 12(1):1–8. PMID: 26605696.
- [Golub and van Loan, 1983] Golub, G. and van Loan, C. (1983). *Matrix Computations*. Johns Hopkins University Press, Baltimore, MD, 1st edition. Sec 12.4.
- [Hanson, 2006] Hanson, A. J. (2006). *Visualizing Quaternions*. Morgan-Kaufmann/Elsevier.
- [Hanson and Thakur, 2012] Hanson, A. J. and Thakur, S. (2012). Quaternion maps of global protein structure. *Jour. Molec. Graphics and Modelling*, 38:256–278.
- [Hartley et al., 2013] Hartley, R., Trumpf, J., Dai, Y., and Li, H. (2013). Rotation averaging. *Int. J. Comput. Vis.*, 103(3):267–305.
- [Huggins, 2014] Huggins, D. J. (2014). Estimating translational and orientational entropies using the k-nearest neighbors algorithm. *J. Chem. Theory Comput.*, 10:3617–3625.
- [Huynh, 2009] Huynh, D. Q. (2009). Metrics for 3d rotations: Comparison and analysis. *J. Math. Imaging Vis.*, 35(2):155–164.
- [Jupp and Kent, 1987] Jupp, P. and Kent, J. (1987). Fitting smooth paths to spherical data. *Appl. Statist.*, 36:34–46.
- [Markley et al., 2007] Markley, F. L., Cheng, Y., Crassidis, J. L., and Oshman, Y. (2007). Averaging quaternions. *J. Guidance, Control, & Dynamics*, 30(4):1193–1197.
- [Moakher, 2002] Moakher, M. (2002). Means and averaging in the group of rotations. *SIAM J. Matrix Anal. Appl.*, 24(1):1–16.
- [Nickalls, 1993] Nickalls, R. (1993). A new approach to solving the cubic: Cardan’s solution revealed. *The Mathematical Gazette*, 77:354–359.
- [Nickalls, 2009] Nickalls, R. (2009). The quartic equation: invariants and Euler’s solution revealed. *The Mathematical Gazette*, 93:66–75.
- [Schönemann, 1966] Schönemann, P. (1966). A generalized solution of the orthogonal procrustes problem. *Psychometrika*, 31:1–10.
- [Shepperd, 1978] Shepperd, S. W. (1978). Quaternion from rotation matrix. *Journal of Guidance and Control*, 1(3):223–224.
- [Shoemake, 1985] Shoemake, K. (1985). Animating rotation with quaternion curves. In *Computer Graphics*, volume 19, pages 245–254. Proceedings of SIGGRAPH 1985.
- [Shuster and Natanson, 1993] Shuster, M. D. and Natanson, G. A. (1993). Quaternion computation from a geometric point of view. *The Journal of the Astronautical Sciences*, 41(4):545–556.

[Weisstein, 2019] Weisstein, E. W. (2019). Quartic equation. <http://mathworld.wolfram.com/QuarticEquation.html>. [Online; accessed 12-May-2019].

[Wikipedia:Cardano, 2019] Wikipedia:Cardano (2019). Ars Magna (Gerolamo Cardano) — Wikipedia, the free encyclopedia. [http://en.wikipedia.org/w/index.php?title=Ars%20Magna%20\(Gerolamo%20Cardano\)&oldid=873028064](http://en.wikipedia.org/w/index.php?title=Ars%20Magna%20(Gerolamo%20Cardano)&oldid=873028064). [Online; accessed 15-May-2019].